ABSTRACT

Title of Dissertation: INHIBITION IN THE CRAYFISH LATERAL GIANT CIRCUIT

Lucy Soda Venuti Winter, Doctor of Philosophy, 2020

Dissertation directed by: Associate Professor Dr. Jens Herberholz
Department of Psychology

Inhibition is critical for the proper functioning of neural circuits. Crayfish present a unique opportunity for the study of inhibition. Crustaceans have been used extensively as model organisms, and many important neuroscientific phenomena were originally described in crayfish or other crustaceans. Their escape responses, mediated by giant fibers, have received particular attention. The lateral giant system has been mapped out in great detail, and every synapse between the receptors that stimulate it to the muscles it recruits is known. Quite surprisingly, despite this extensive knowledge of the excitatory portions of the circuit, its inhibitors are still poorly understood. The lateral giant interneuron is a particularly good target in which to study inhibition, as it receives three unique types of inhibition. Its firing causes a rapid autoinhibition of the neuron, its general excitability is modulated by tonic inhibition, and its selectivity to sudden, phasic stimuli is partially mediated by sensory-evoked inhibition. While the existence and very basic characterization of these forms of inhibition have been described, the mechanisms and details of all three remain elusive. Here I present data which aids substantially in our understanding of these inhibitory systems. I show that the lateral giant's autoinhibition is

mediated by both GABA and glutamate, and that the axon of lateral giant neuron responds to these inhibitory neurotransmitters. I also pharmacologically characterize the inhibitory inputs evoked by its sensory afferents, and show that the neuron is sensitive to THIP, a compound which is selective for receptor subtypes that mediate tonic inhibition. In addition, I utilize alcohol exposure to uncover these mechanisms, allowing it to be used to interpret the recently discovered social modulation of alcohol's effect that is seen in crayfish, and aiding in our understanding of alcohol's interplay with cellular inhibition.

INHIBITION IN THE CRAYFISH LATERAL GIANT CIRCUIT

by

Lucy Soda Venuti Winter

Dissertation submitted to the Faculty of the Graduate School of the
University of Maryland, College Park in partial fulfillment
of the requirements for the degree of
Doctor of Philosophy
2020

Advisory committee:
Professor Jens Herberholz, chair
Professor Ricardo Araneda
Professor Catherine Carr
Professor Luiz Pessoa
Professor David Yager

Acknowledgements

I could not have completed this dissertation without the support of many people. I would first like to thank my wife, Annie. You have been a consistent source of calm during the stress and pressure that comes with graduate school, and with writing a dissertation. While this has been a difficult process, your support has made it easier. I would like to thank my parents, Steve and Kristin, as well as my grandparents, for encouraging my love of the intellectual things throughout my life.

I would also like to thank all of my committee members for their support throughout my education: Dr. Catherine Carr, who provided her laboratory equipment and knowledge whenever I needed it, Dr. Luiz Pessoa, who has been tremendously helpful with statistics, and Dr. David Yager, who has taught me all I know about teaching others. And of course, I would like to thank my advisor, Dr. Jens Herberholz, for his help and guidance throughout the entire process. Your support has made me a better scientist.

Table of Contents

List of Tables

List of Figures

1. Significance

Inhibition plays a critical role in producing appropriate neural function. It is important at many levels: without cellular inhibition, many small neural circuits cannot function, and the excitation/inhibition balance across the entire brain requires regulation to avoid disease states. Disruption of inhibitory systems are associated with epilepsy (Baulac et al., 2001), and are implicated in autism and schizophrenia (Foss-Feig et al., 2017; Tatti et al., 2017). Abnormalities in inhibition are associated with comatose state (Bagnato et al., 2012), and animal models of diseases such as Rett syndrome and fragile X show disturbances in the balance between excitation and inhibition (Tatti et al, 2017). Thus, a better understanding of inhibition will aid in understanding the healthy brain and in treating brain diseases.

Selection of behavior is vitally important for all motile creatures. Inhibition is involved in the selection between choices (Jocham et al., 2012), and learning requires inhibition to properly balance circuits undergoing excitatory plasticity (Froemke, 2015). Inhibition is also critical in the coordination of motor behavior, from timing in the crayfish tail-flip circuit (Edwards et al., 1999), to the well-studied relaxation of antagonistic muscles during the execution of mammalian reflexes (Hultborn et al., 1971). Due to its wide-ranging roles, a good understanding of inhibition is important for a complete analysis of almost any neural process. It is critical that inhibition is studied using a comparative approach, as the principles of such a basic phenomenon are likely applicable across clades.

Decapod crustaceans have been historically rich model organisms. Many discoveries in crayfish, lobsters, and crabs have turned out to be fundamental principles of neural functioning. The existence of gap junctions was first discovered in the crayfish escape circuit (Furshpan and Potter, 1957). The discovery that GABA has an inhibitory effect was made in crayfish, and later work in lobsters showed that it was released by neurons in response to stimulation (Florey, 1954; Otsuka et al., 1966). Despite the advantages that genetic tools provide in other organisms, crayfish remain a useful model due to their well-studied behaviors and easily accessible underlying neural circuits. This combination allows for unparalleled integration of studies at the behavioral, circuit, and neuronal level.

The extensive history of research in crayfish has led to circuits which are extensively described. The lateral giant circuit of the crayfish is particularly well understood (Edwards et al., 1999). It is located in the abdomen of the animal and subject to three distinct types of inhibition: self-evoked autoinhibition (Roberts, 1968), descending tonic inhibition from the brain (Vu & Krasne, 1992; Vu & Krasne, 1993; Vu et al., 1993), and sensory afferent-evoked post-excitatory inhibition (Vu et al., 1997), and thus represents a unique opportunity to study three separate types of inhibition in a single cell. Research in this area is aided by the high level of knowledge that many decades of study have provided on the circuit's excitatory components.

The studies of inhibition and alcohol are intimately related. A major target of alcohol is the GABAergic system (Lobo & Harris, 2008), which it may facilitate (Santhakumar et al., 2007) or attenuate (Yamakura & Harris, 2000). Alcohol also acts on

other inhibitory receptors, including glycine (Mihic et al., 1997). This interplay results in an extremely complex web of effects that is difficult to disentangle, despite ethanol's long history of use and abuse. Because inhibition is so heavily involved in the effects of alcohol, and inhibitory dysregulation is a major cause of disease, it is critical that we better understand inhibition. The work presented here approaches these problems from a cellular and molecular level, and leads to a greater understanding of inhibition and the interplay between alcohol and inhibitory systems.

Crayfish are behaviorally sensitive to alcohol, becoming hyperexcitable and uncoordinated when exposed (Blundon & Bittner, 1992; Friedman et al., 1988; Swierzbinski et al., 2017). The similarity to human intoxication is convenient, and the ability to study behavior at a circuit and neuronal level allows unparalleled insight into a notoriously complex phenomenon. Alcohol was responsible for 1.5 million deaths in 2010, a number which has risen since 1990 (Rehm & Shield, 2013). In the US, almost 10% of deaths among working-age individuals are caused by alcohol, and excessive drinking cost the US $223.5 billion dollars in 2006 alone (Stahre et al., 2014). Consequently, alcohol is an important drug of study (Lobo & Harris, 2008). Despite this, the mechanisms underlying alcohol's many effects are not well understood: alcohol's molecular interactions are very complex, as it does not act through a single receptor (Wolf & Heberlein, 2003), but instead has activity at GABAergic (Kumar et al., 2009, Lobo & Harris, 2008), serotonergic (Lovinger, 1999), and glutamatergic (Peoples & Weight, 1995) neurotransmitter systems, among others (Wolf & Heberlein, 2003). Rodent models are not particularly well suited for the study of alcohol, due to the small

size of their neurons and relative complexity of their circuits. Contrastingly, the giant escape circuits of the crayfish is well understood, easily accessible, and sensitive to alcohol, providing an excellent model from which alcohol, and its interactions with inhibitory systems, can be studied (Swierzbinski et al., 2017).

The work presented in this dissertation advances our understanding of the lateral giant circuit and the three types of inhibition which can be studied using it. This work also aids in our understanding of the effects of alcohol on the inhibitory systems of crayfish.

2. Background

2.1. Lateral giant circuit

The primary method of evasion used by the crayfish is the tail-flip (Herberholz et al., 2004). Tail-flips may be evoked by three separate systems: two rapidly responding systems mediated by giant fibers, and one less well-understood system comprised of non-giant fibers, responsible for more variable responses (Wine & Krasne, 1972; Edwards et al., 1999). Rapid strikes against the cephalothorax, or threatening visual input, cause backwards tail-flips mediated by the medial giant (MG) neurons (Wine & Krasne, 1972; Edwards et al., 1999; Liden et al., 2010). Strikes against the abdomen cause an upwards tail-flip, mediated by the lateral giant (LG) neurons (Roberts, 1968; Wine & Krasne, 1972). Crayfish have decentralized nervous systems, in which much processing occurs in local ganglia along the nerve cords, and transmission between ganglia passes through interganglionic connectives **(Figure 2.1)**. The LG system consists of bilaterally coupled neurons in each segment, with septate (i.e., electrical) junctions adjoining each segment to their counterparts in neighboring segments (Johnson, 1924). The network receives input from electrically coupled (Herberholz et al., 2002), rapidly habituating sensory afferents in the tail, and drives the motor giant neurons in the anterior three segments of the abdomen through rectifying electrical synapses (Wine & Krasne, 1972; Wine, 1984; Edwards et al., 1999) near the third nerve root (Furshpan & Potter, 1959). The

arrangement of electrically coupled afferents, which tend to excite each other, and rectifying synapses, reducing the strength of inputs that do not arrive at the same time, allows the LG to respond selectively to stimuli with rapid onset (Wine & Krasne, 1972; Edwards et al., 1999; Herberholz et al., 2002).

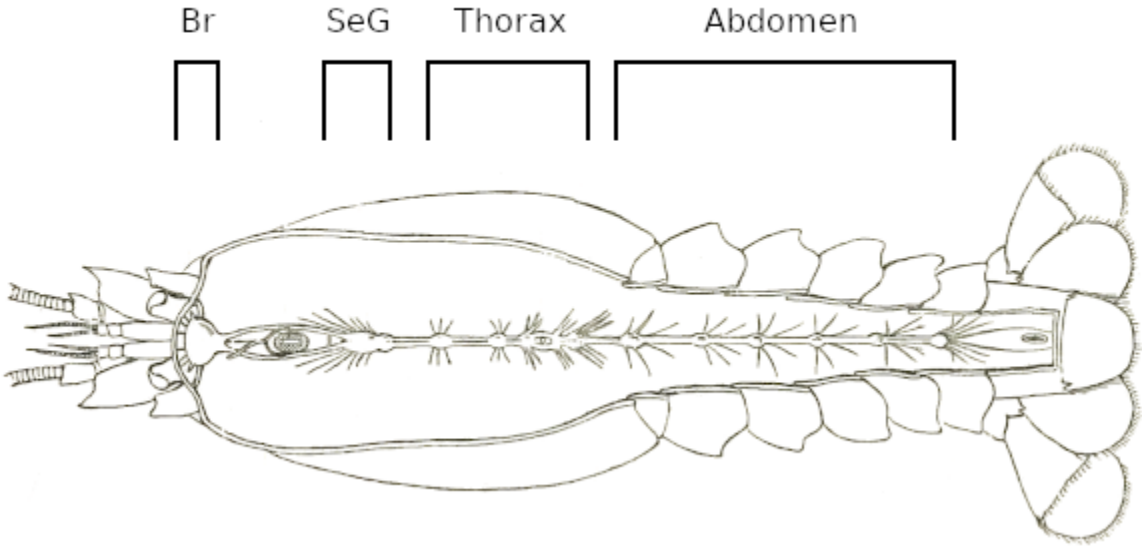

Figure 2.1. Schematic of the ventral nerve cord and drawing of its place in the crayfish. The ganglia in the crayfish, from rostral to caudal, are the brain (Br), the sub-esophageal ganglion (SeG), five thoracic ganglia, and six abdominal ganglia. Ganglia are numbered, rostral through caudal, as T1-T5 (in the thorax) and A1-A6 (in the abdomen). Nerves are also numbered from rostral to caudal, with three bilaterally paired nerves in each of the first five abdominal ganglia and seven nerves in A6. Image is adapted from Huxley, 1879.

The fast flexor muscles that mediate this tail-flip are innervated by the giant motor neurons (MoGs), as well as through a parallel pathway that is shared between both giant and non-giant tail-flips (Kramer & Krasne, 1984), which the LG drives through the segmental giants (Roberts et al., 1982). Due to the electrical coupling between each segmental LG and its contralateral, anterior, and posterior partners, an action potential in one LG segment will propagate to its contralateral partner, as well as its partner in

adjoining segments, and for most purposes, the entire LG system can be considered one neuron (Watanabe & Grundfest, 1961).

2.2. Inhibition in the lateral giant circuit

The LG circuit is subject to three distinct types of inhibition, and thus presents a unique model in which to study both the theoretical and mechanistic aspects of inhibitory phenomena. The LG's firing causes a rapid inhibition in the giant fiber itself, so that it does not fire repeatedly (autoinhibition); sensory input to the LG is followed by a delayed inhibition, which aids the LG in responding selectively to rapid stimuli (sensory-evoked inhibition); and the system is under a constant level of inhibition from the brain, which modulates the threshold of escape situationally (tonic inhibition). Due to its high chloride content, these inhibitory inputs cause the LG to depolarize, reducing its excitability by inactivating sodium channels and increasing conductance (Edwards, 1990).

This circuit, from sensory input to motor output, has been described in detail both anatomically and physiologically (Edwards et al., 1999) **(Figure 2.2)**. The firing of the LG causes inhibition in many systems associated with motor commands: proprioceptors are inhibited to prevent reflexive "correction" of tail posture (Eckert, 1961); sensory inputs to the LG are inhibited, to reduce movement-induced sensory feedback and protect chemical synapses from habituation (Kennedy et al., 1980; Kennedy et al., 1974; Kirk, 1985; Bryan & Krasne, 1977); and the motor giants and giant fibers are, themselves, inhibited (Roberts, 1968). Following an action potential in the LG, widespread, long-lasting autoinhibition of the LG occurs. The spiking of the MG interneurons also cause a

transient inhibition of the LG (Roberts, 1968). Spikes in either giant system cause primary afferent depolarizing interneurons (PADIs) to be stimulated, which are the mechanism behind the inhibition of LG afferent inputs. These PADIs also synapse onto the dendrites of the LG (Kirk, 1985), indicating that they may be involved in inhibition of the LG. However, the pathway involved is polysynaptic, and cannot account for the rapidity with which autoinhibition begins; additionally, the autoinhibition must involve non-dendritic receptors (Vu & Krasne, 1992; Vu et al., 1993). Despite the intense time and effort undergone to achieve this extensive mapping of the LG system **(Figure 2.2)**, the mechanisms underlying the LG's own autoinhibition have not been satisfactorily explained. This inhibition begins rapidly: by the falling phase of the LG action potential, depolarizing inputs are already active (Watanabe & Grundfest, 1961; Kao, 1960), which have been identified as inhibitory (Roberts, 1968). This inhibition must prevent the LG from firing during the execution of a tail-flip, so that the crayfish does not disrupt its own escape by initiating another (Roberts, 1968), as well as prevent the structure of the LG network from creating spikes which circulate endlessly, which the system's unique arrangement would otherwise allow (Kusano & Grundfest, 1965). While picrotoxin reduces the strength of the inhibition, it does not eliminate it (Roberts, 1968). There are inhibitory receptors along the spike initiation zone of the LG (Lee & Krasne, 1993), which may explain a portion of the autoinhibition (Vu et al., 1993).

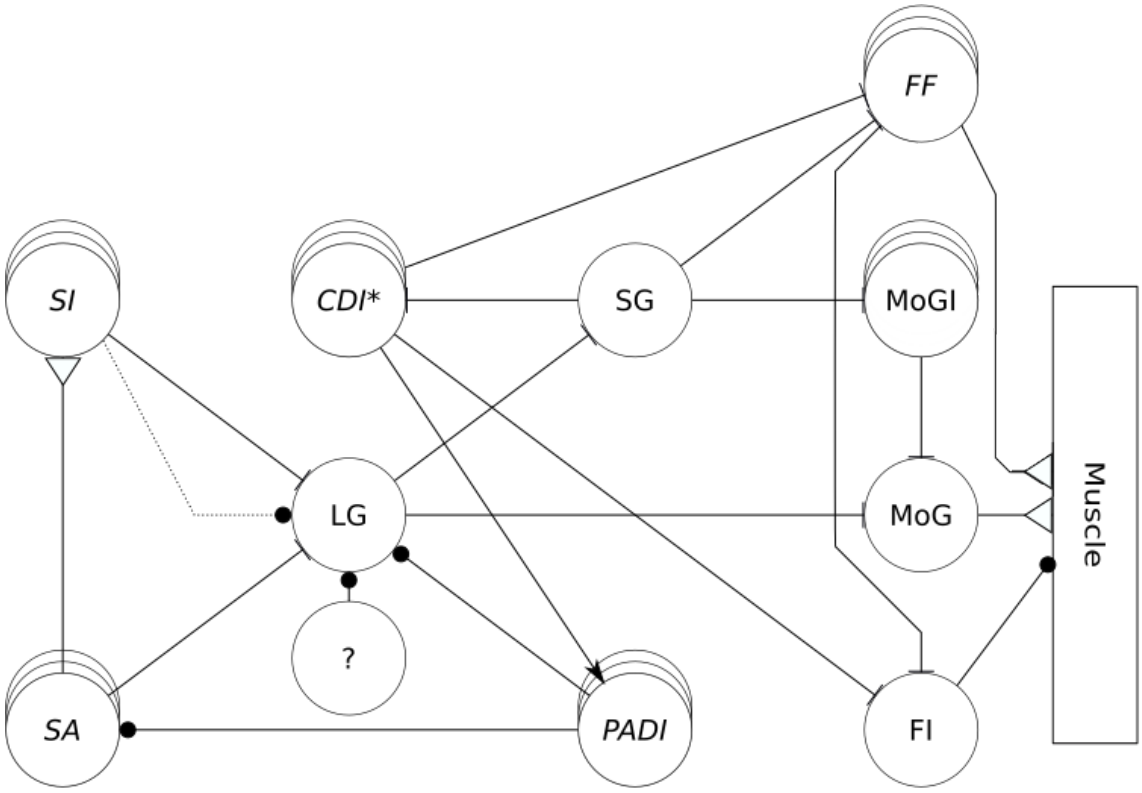

Figure 2.2. Partial diagram of the known LG circuit. Black circles are inhibitory synapses, flat terminations are electrical synapses, black arrows are unidentified excitatory synapses, and white triangles are excitatory chemical synapses. The black dotted line between the sensory interneurons and LG represent an undefined sensory-evoked inhibition. Individual circles represent individual neurons, while groups of circles represent populations. CDIs are specially marked to signify the fact that they are a particularly diverse group of neurons. Despite this understanding, the inhibition of the LG is not fully described. Acronyms: sensory afferent, SA; sensory interneuron, SI; lateral giant, LG; segmental giant, SG; fast flexor, FF; flexor inhibitor, FI; motor giant, MoG; motor giant inhibitor, MoGI; corollary discharge interneuron, CDI; primary afferent depolarizing interneuron, PADI.

The autoinhibition of the LG has several peculiar traits. It is rapid, beginning before the neuron has repolarized from its action potential **(Figure 2.3)**. The sensory afferents do not cause this inhibition directly (Calabrese, 1976), and this timing is too fast to allow the synaptic delay of more than one chemical synapse. This suggests that the rapid portion of the inhibition must either involve, at most, one chemical junction, or else be feed-forward in nature. Direct stimulation of the LG evokes a spike which is still

followed rapidly by inhibition (Roberts, 1968), however, suggesting that a feed-forward mechanism is unlikely. Additionally, the inhibition occurs relatively evenly throughout the axon of the neuron: the depolarizing inhibitory post-synaptic potential (dIPSP) is not substantially different in size whether measured near the spike initiation zone or between ganglia, while passively-flowing potentials like post-synaptic potentials (PSPs) are more strongly attenuated between those two points **(Figure 2.3),** suggesting that the dIPSP is at least partially due to inputs more rostral than the LG's dendrites. The inhibition occurs even in areas such as the brain connectives (Herberholz, personal communication), where there is no excitatory input and thus no clear reason to have autoinhibition. As the inhibition occurs throughout the axon, there is no clear place to begin searching for the inhibitory mechanism. However, the fact that the inhibition occurs relatively evenly throughout the neuron, even in areas such as the brain, implies that the locus is likely diffuse. These factors suggest that receptors at the spike initiation zone may not be a sufficient explanation.

Similarly to LG-derived autoinhibition, inhibition of the LG by sensory afferents has been characterized somewhat, but the mechanism that causes it remains undescribed. PSPs of the LG are made up of three distinct components: α, β, and γ (Krasne, 1969; **Figure 2.4**). The α component is due to direct electrical synapses from sensory afferents, while the β is more complex, but its early part, off of which the action potential rises, is due to electrical input from interneurons that receive cholinergic input from the sensory afferents (Krasne, 1969; Zucker, 1972; Wine & Krasne, 1972; Miller et al., 1992). The

later phase of the β component is more variable, as is the γ component, and both are due substantially to inhibition (Krasne, 1969; Vu et al., 1997). This sensory-evoked post-excitatory inhibition is partially responsible for the LG's selective response to phasic stimuli, as it ensures that the first afferents which fire in response to a slow stimulus prevent those which respond later from evoking an action potential (Vu et al., 1997). The interneurons involved have not been described, and while the inhibition is known to exist, the responsible neurotransmitter and receptors are not well characterized.

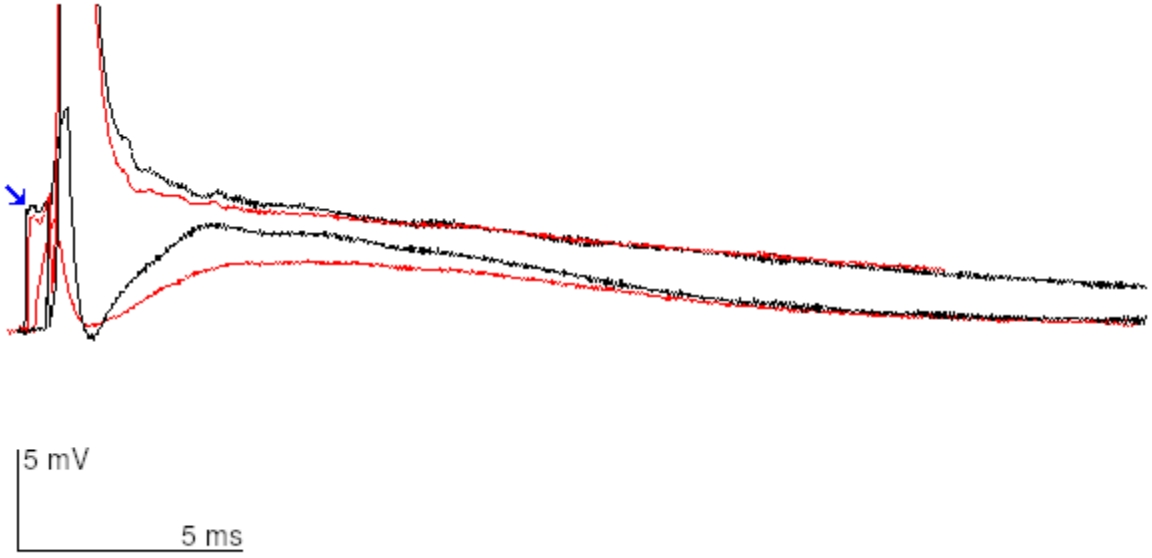

Figure 2.3. Direct-stimulation LG spike (truncated) and ensuing dIPSP, alongside a sensory afferent-evoked PSP. The black recordings are from near the A6 ganglion, where the afferent input occurs. The red recordings are from midway between A5 and A6. The blue arrow marks the stimulus artifact. Data is averaged over five recordings. Spiking traces are aligned to the upward limb of the spike, and PSP traces are aligned to the beginning of the voltage increase. The inhibition is visible as the long lasting depolarization following the spikes. The dIPSP is relatively unaffected by measured location, while the PSP is more strongly attenuated when it is measured further from the site of stimulation.

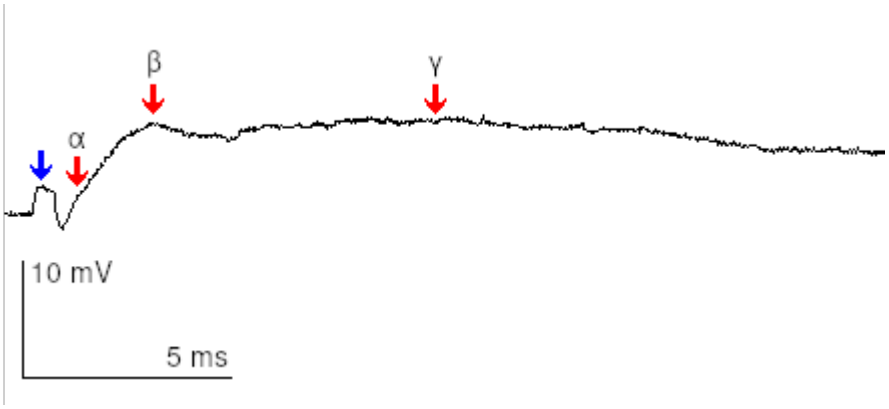

Figure 2.4. PSP of the LG after subthreshold electrical stimulation of sensory afferents, with all components labeled. The blue arrow marks the stimulus artifact. The α component is generated by direct electrical synapses from the sensory afferents, and is thus very consistent. The early β component consists of excitatory input from first-order interneurons. Both the late β and the γ component have substantial inhibitory input, and are more variable in size and shape.

Finally, the LG is under a constant level of inhibition, which descends from the brain, and modulates the threshold of escape (Krasne & Wine, 1975; Vu & Krasne, 1993; Vu et al., 1993; Swierzbinski et al., 2017). Like the other forms of inhibition in the LG circuit, this has received some theoretical and physiological attention, but is still poorly understood. The neurons responsible for it are not described, and other than its descending nature, dendritic locus, and sensitivity to picrotoxin, little else is known.

All three forms of inhibition are critical for the LG's proper functioning. The LG is therefore uniquely situated for studies of inhibition, as a single neuron which allows for intracellular recordings, and in which autoinhibition, sensory-evoked inhibition, and tonic inhibition can all be studied in detail. Despite this advantage, none of the inhibitions of the LG are fully understood. Other than its speed, duration, and sensitivity to picrotoxin, little is known about the autoinhibition. Similarly, while the time course of the sensory-evoked inhibition, as well as its response to picrotoxin, is known, the receptors involved

have not been identified. Tonic inhibition is similarly understudied, with little characterization other than the receptor location, sensitivity to picrotoxin, and importance of descending inputs from the brain. These gaps are notable in a literature that is otherwise very detailed, and which explains other facets of the LG circuit so thoroughly. The experiments presented in this dissertation substantially reduce these gaps and lay the groundwork from which inhibition can be further explored. This will aid in the interpretation of data and refinement of theories of inhibition, as prior invertebrate research has informed vertebrate research and significantly improved our understanding of the principles upon which nervous systems function (Pearson, 1998; Satelle & Buckingham, 2006).

2.3. Depolarizing inhibition

Studying inhibition in crayfish is complicated by the fact that most inhibition is depolarizing (Wine & Krasne, 1982). This relatively less known type of inhibition is present in mammals as well: in developing mammalian neurons, the chloride concentration differs from that found in adult neurons, due to differential expression of ion transporters (Owens & Kriegstein, 2002). Moreover, there are sites in mammalian adults where this occurs as well, such as the spinal cord (Melcangic & Bowery, 1996). In all of these cases, this depolarization is brought about because the electrochemical gradient between the cytosol and extracellular space favors chloride efflux. Consequently, the opening of chloride channels depolarizes the cell. The reversal potential for chloride is below threshold, so in a healthy preparation under normal physiological conditions,

chloride efflux alone cannot result in an action potential. Despite its depolarizing nature, chloride efflux results in powerful inhibition through several mechanisms: by opening chloride channels, the membrane conductance is increased, reducing the efficacy of excitatory events; voltage-gated potassium channels become more likely to open, further increasing conductance; and the probability that voltage-gated sodium channels will be open increases (Edwards, 1990). As sodium channel opening is followed by a period of inactivation, consistent depolarization results in a large number of sodium channels being unable to respond to any further depolarization, hence reducing the ability of the cell to reach the threshold required to generate an action potential. These mechanisms result in depolarizing inhibition having some qualities which other inhibition does not have. In particular, the inactivation of sodium channels eliminates the possibility of excitatory rebound (Edwards, 1990), a quality which is important in this circuit. However, this type of inhibition is more difficult to study than hyperpolarizing inhibition, as it is not immediately clear whether an observed depolarization is excitatory or inhibitory. Secondary tests are necessary, such as resistance and reversal potential measurements, use of a chloride channel blocker, or observing the cell's response to excitatory events (Roberts, 1968; Krasne, 1969; Krasne & Wine, 1975).

2.4. Glutamate in invertebrates

While crustaceans have historically been useful in the discovery and understanding of basic neural phenomena (Pearson, 1998; Satelle & Buckingham, 2006), there have been fewer widespread attempts to understand them when they differ from

mammals. These differences, however, often belie similarities (Pearson, 1998; Wolf & Heberlein, 2006). Consequently, invertebrate work has provided the foundation upon which much vertebrate research has been built (Satelle & Buckingham, 2006). For example, inhibition in vertebrates is generally thought of as being almost exclusively a GABAergic phenomenon, with additional receptors gated by glycine (Langosch et al., 1990) performing a supplementary role. This view is incomplete, as even in mammals, the main excitatory neurotransmitter, glutamate, can open chloride channels, albeit through a more complex, indirect route involving binding to its reuptake transporter (Fairman et al., 1995). In invertebrates, glutamate can more directly cause inhibition by binding to ligand-gated chloride channels (Wolstenholme, 2012), though it is also a ligand at sodium channels, as in vertebrates.

Glutamate-gated chloride channels (GluCls) are common in invertebrates, making controlled experimental design on inhibitory phenomena more difficult than it would be in an equivalent mammalian system. Fortunately, the GABA antagonist picrotoxin has activity at GluCls (Marder & Paupardin-Tritsch, 1978; Franke et al., 1986; Cleland, 1996), allowing pharmacological analysis. In addition, common pesticides are often directed at these receptors (Cully et al., 1996; Kane et al., 2000; Ikeda et al., 2003; Zhao and Salgado, 2010; Furutani et al., 2015; Wolstenholme & Rogers, 2006), a quality which makes the toxins relatively less effective in vertebrates. There are several subtypes of GluCls with varying properties. Though they are generally picrotoxin-sensitive, they differ in sensitivity (Raymond et al., 2000; Zhao et al., 2004). Additionally, some desensitize more completely than others (Zhao et al., 2004). There is often cross-

reactivity with GABA, and many compounds that affect GABA receptors also affect glutamate receptors. As inhibition in crayfish is generally depolarizing, and glutamate also acts as an excitatory neurotransmitter, it is not immediately obvious if a glutamate-induced membrane shift is due to sodium influx or chloride efflux. This fact and the presence of depolarizing inhibition combine to make the study of GluCls challenging. While glutamate as an inhibitory compound has been studied in the crayfish central nervous system (Heitler et al., 2001; Nagayama, 2005; Nagayama et al., 2004), and glutamate acts as an inhibitor on the post-synaptic side of the LG-MoG junction (Heitler et al., 2001), there has been no prior work suggesting that GluCls may be present on the LG and involved in its autoinhibition.

2.5. Glutamate as a signaling molecule

It had been suggested that the MG axons of the crayfish, and the giant axon of the squid, release glutamate when firing (Lieberman et al., 1994). More recent evidence suggests that this may not be the complete view: the axons of the MG neurons, which are responsible for the rapid backwards tail-flip escape, are known to contain N-acetylaspartylglutamic acid (NAAG), and release it when they fire (Kane et al., 2000; Urazaev et al., 2001). The enzyme glutamate carboxypeptidase II is present on the periaxonal glia, which causes the hydrolysis of NAAG to N-acetylaspartate and glutamate. Glutamate (and NAAG) activate several types of glial receptors (Urazaev et al., 2001; Gafurov et al., 2001; Gafurov et al., 2002; Urazaev et al., 2005) before eventually being taken up by the glia (Kane et al., 2000). Research thus far has primarily

focused on neuron-glia communication and the effects of glutamate and its derivatives on the glial cells, rather than how these compounds may affect giant axons themselves. Though the research on these phenomena has been performed on the crayfish MG and squid, the giant neurons share many similarities (Swierzbinski, 2016; Lieberman et al., 1994). It is therefore possible that the LG acts in a similar fashion, and communicates with its glia via glutamate or NAAG.

Both glutamate and GABA undergo reuptake by transporters that use electrochemical gradients as an energy source during transport. Glutamate transport is coupled to sodium and potassium (Kanner & Sharon, 1978), and GABA transport is coupled to sodium and chloride (Kanner, 1978). Altering ion (and substrate) concentrations can cause both of these transporters to operate in reverse, transporting their neurotransmitter to the extracellular space, if the electrochemical gradients shift (Szatkowski et al., 1990; Attwell et al., 1993). Periaxonal glia in the sheath surrounding the MG contain glutamate, and will readily take it up when it is present extracellularly (Kane et al., 2000). In rabbit astrocytes, glial exposure to a high potassium concentration results in a release of GABA, with no additional release found at concentrations higher than 10 mM above normal (Sellström & Hamberger, 1977). When the Na/K transporter was inactivated by ouabain, eliminating the primary method of potassium uptake, release was enhanced, and this effect persisted even without calcium. In crayfish, 110 mV depolarization of the MG for only two milliseconds released enough potassium to raise the concentration in the periaxonal space by 13 mM, but when actually measured, the concentration was increased by only 5 mM (Shrager et al., 1983), implying that it was

taken up rapidly. While the presence of ouabain did reduce the crayfish's rapid clearance of potassium, it did so only mildly, suggesting other mechanisms are involved. Taken together, these suggest that reversal of the glutamate transporter, causing potassium influx and glutamate efflux, may be one mechanism by which autoinhibition occurs.

2.6. Alcohol

Ethanol's effects on the GABAergic system contribute heavily to its modulation of behavior (Lobo & Harris, 2008). Ethanol appears to have strong effects on tonic inhibitory currents (Valenzuela & Jotty, 2015). Several types of extrasynaptic $GABA_A$ receptors appear sensitive to ethanol, including those containing δ subunits (Lobo & Harris, 2008; Smith & Gong, 2007; Santhakumar et al., 2007) and those containing ρ subunits (Wick et al., 1998; Yamakura & Harris, 2000; Blednov et al., 2017), which appear to be linked with alcoholism (Blednov et al., 2017) and can have differing responses to ethanol depending on which subunit type is present. For ease of reading, $GABA_A$-ρ and $GABA_A$-δ will be used throughout this dissertation as shorthand for "receptors containing a ρ/δ subunit." $GABA_A$-ρ receptors (previously known as $GABA_C$ receptors) are found in several places throughout the mammalian brain, but are most highly expressed in the retina, where they mediate slow and tonic currents (Olsen & Sieghart, 2009; Jones & Palmer, 2009). $GABA_A$-δ receptors mediate tonic inhibition, are found exclusively extrasynaptically (Farrant & Nusser, 2005), and are particularly sensitive to ethanol (Santhakumar et al., 2007). Interestingly, in crayfish, using a sucrose block or transecting the ventral nerve cord, thereby removing brain-derived descending

tonic inhibition from the LG (Vu et al., 1993), also lessens the excitation induced by ethanol in the LG neuron (Swierzbinski et al., 2017).

Globally, tobacco is the only drug that is deadlier than alcohol (Peacock et al., 2018). In 2015, excluding tobacco, alcohol killed four times more people than all other drugs combined. Study of alcohol is complicated by its interactions with multiple neurotransmitter systems (Wolf & Heberlein, 2003), making it important to find simple models in which to tease its cellular and molecular effects apart. Promisingly, crustaceans respond to many of the same drugs humans do. Common drugs of human abuse have very similar effects in crayfish: morphine, amphetamines, and cocaine can induce place preference (Imeh-Nathaniel et al., 2009; Panksepp & Huber, 2004). Of particular note is their behavioral response to alcohol. When placed in a solution of ethanol and water, they begin to take up ethanol through their gills and into their bloodstream, and respond with a similar behavioral pattern to that observed in humans as intoxication progresses: first, crayfish become excitable, and take an elevated stance; this is followed by disinhibition, with uncontrolled spontaneous tail-flipping throughout the tank, a behavior which only occurs naturally in the presence of a threat. Eventually the animals lose coordination, ending on their backs unable to right themselves (Swierzbinski et al., 2017). If they are allowed to take more ethanol up at this point, death follows.

The circuits underlying crayfish escape behavior are a convenient target; they are understood at the level of the individual cell, the circuit, and the behavior, and can be accessed at each of these points. This allows for the complex interactions between the levels to be studied, as well as the changes that drug application causes. The clear

behavioral reaction to alcohol administration in crayfish allows the observation of behaviors brought about by ethanol application in freely behaving animals, while also allowing the use of electrophysiology to probe into the underlying mechanisms for these behaviors. Crayfish therefore make ideal subjects for disentangling the multifaceted cellular effects of alcohol and its interaction with inhibition.

Despite its importance in human addiction, the effects of social exclusion are underappreciated (Heilig et al., 2016). As previously noted, crayfish undergo the same behavioral response to alcohol that humans do. Recent research has shown that this effect is socially modulated, with isolated animals becoming drunk more slowly than communally housed ones (Swierzbinski et al., 2017). Discovering the etiology of these differences may aid in our understanding of the effects of social experience on human alcohol responses as well.

Because of the tremendous societal cost of alcohol use, attaining a better understanding of its effects is a high priority. Swierzbinski et al. (2017) and Swierzbinski and Herberholz (2018) have begun to delineate the effects of ethanol on the LG and MG circuits. However, research on the interplay between ethanol and the GABAergic system in the LG circuit does not exist. My research explores these interactions, providing a better understanding of how ethanol interacts with $GABA_A$ receptors in the LG, as well as new knowledge about which receptor subtypes may be present in the circuit. This work, at the poorly-understood intersections of alcohol intoxication, inhibitory mechanisms, and social experience (Heilig et al., 2016; Swierzbinski et al., 2017), will create a foundation upon which further studies can be performed, and help elucidate some of the

crucial mechanisms underlying the broader phenomena that are present in organisms of all complexities.

3. General methods

3.1. Animals

Adult *Procambarus clarkii* of both sexes were used in all experiments. All specimens were ordered from either Carolina Biological or Niles Biological Supply Company. Animals were shipped overnight and placed in housing tanks (described below) on the day of their arrival. Crayfish were only used if they had both claws and at least 7 walking legs. Animals were not used if they had molted recently or their carapace was notably soft. Each animal was only used once.

3.2. Housing

Communal animals were housed in 76*30*30 cm (L*W*H) aquaria upon arrival. Animals were fed twice a week. Each tank received two Formula One medium pellets (Ocean Nutrition) for each animal present in the tank. Tanks were filled with tap water, which was continuously filtered. Tank floors were covered in a thin layer of gravel, and PVC tubes were placed in tanks to provide hiding spots. All tanks were housed in an animal housing room at 22° C on a twelve hour light/dark cycle.

Social differences are known to affect the response of crayfish to pharmacological agents, including ethanol. In order to explore this, some animals were socially isolated before experiments. Isolated animals were placed in small (15*8*10 cm) covered tanks

with a thin layer of gravel and an air stone. Animals were fed two pellets upon isolation. Animals were used between seven and ten days after their initial isolation.

3.3. Equipment

Intracellular electrodes were made of borosilicate glass capillary tubes (World Precision Instruments) and pulled using a P-97 electrode puller (Sutter Instruments). Electrodes were held with electrode holders, and silver wires were used as the conductive contact, with 2 M potassium acetate used for the electrolytic solution. Extracellular electrodes were fabricated from coated silver wire (A-M Systems) with 0.005 or 0.008 inch diameter. All instruments, including superfusion-related pump tubing, were held with micromanipulators (World Precision Instruments). Experiments took place in a copper Faraday cage, grounded to building earth. Intracellular electrodes were mounted on HS-1A headstages (Axon Instruments), and signals were amplified using a model 900A intracellular electrode amplifier. Axoclamp Commander was used to control the electrodes. Extracellular electrodes were connected to a model 1700 differential AC amplifier (A-M Systems). When used for stimulation, outputs were passed through an SIU5 stimulus isolation unit (Grass). Superfusion inflow was performed by a Fisher Scientific FH100 peristaltic pump.

All petri dishes were lined with sylgard, and Minutien pins were used to secure experimental tissue.

3.4. Superfusion

Superfusion was performed at a flow rate of 5 ml/minute. All solutions were held in separate aspirator bottles, which were connected via electronically actuated solenoid valves to the inflow pump. A separate pump was used for outflow. The experimental dishes used held approximately 40 ml of fluid. Because superfusion involves a continuous flow of fluid, any changes in superfusion fluid are not instant, instead occurring slowly as the new solution is mixed into the bath, replacing it over time. At 5 ml/minute, the concentration of superfusate in the dish reaches approximately 95% of its maximum after 24 minutes. As the bath itself is gradually replaced, any compounds applied will diffuse throughout the tissue, affecting all cells which are sensitive to their effects.

3.5. Procedures

Animals were anesthetized with ice for 15 minutes prior to any experimental manipulations. The abdomen was removed with scissors and the ventral carapace of the abdomen cut bilaterally down to the tail fan with a smaller pair of scissors. The ventromedial strip of carapace was then removed with forceps, exposing the ventral nerve cord. Deeper incisions were made along the lateral sides of the tail to remove connections between the nerve cord and innervated tissue. The scissors were then placed in the phasic tail flexor muscles, dorsal to the nerve cord, and used to further disconnect the third nerve root from its targets. Incisions were made along the very caudal end of the tail interior, to

cut the nerves of the sixth abdominal ganglion (A6). The nerve cord was then lifted with forceps and placed in the experimental dish with saline. The nerve cord was pinned down with Minutien pins, and in the case of experiments utilizing the Picospritzer, fine forceps were used between A5 and A6 to tear the sheath surrounding the nervous system.

The dish was placed in a holder in the experimental cage, to which its fluid was grounded. Extracellular electrodes were then placed, depending on experimental requirements. Intracellular electrodes were used to impale the neurons under study. All baseline measurements were performed with the flow active. Experimental methods specific to particular preparations are explained in the relevant chapters.

3.6. Saline

All physiological solutions were made using a modified van Harreveld's (1936) saline recipe (205 mM NaCl, 5.4 mM KCl, 13.5 mM $CaCl_2$, 2.6 mM $MgCl_2$, and 2.4 mM HEPES). pH was balanced to between 7.5 and 7.6 using sodium hydroxide and hydrochloric acid. All solutions used were made by dissolving substances of interest in saline. Information on all drugs used in experiments are detailed in the relevant chapters.

3.7. Data analysis

Data was obtained using ClampEx 10.4, and data extraction was performed using Clampfit 10.4 and 10.7. Statistics and figure generation were performed using R version 3.6.1 (R core team, 2019). The R packages used were broom 0.5.2 (Robinson & Hayes, 2019), plyr 1.8.4 (Wickham, 2011), e1071 1.7.2 (Dimitriadou et al., 2019), lme4 1.1.21

(Bates et al., 2015), lmerTest 3.1.0 (Kuznetsova et al., 2017), nlme 3.1.140 (Bates et al., 2019), ggplot2 3.2.1 (Wickham, 2016), and ggsignif 0.6.0 (Ahlmann-Eltze, 2019).

For graphical data presentation, p values were represented as * for $0.05 > p > 0.01$, ** for $0.01 > p > 0.001$, and *** for $p < 0.001$. In text, p values are given to three decimal places. If the value is less than 0.001, it is given in scientific notation with one significant figure. Due to the high density of statistical information generated by the experiments involving ethanol, p values and other statistical information in chapter 5 are presented in tables.

4. Autoinhibition

4.1. Summary

Crayfish respond to threats via tail-flip escapes. The lateral giant circuit used to elicit one of these escapes undergoes rapid inhibition along its axon following action potentials. Though this autoinhibition is known to be sensitive to the GABA antagonist picrotoxin, little else is known about its cause. It occurs throughout the LG, with no clear locus. Here I use several methods to explore the reactions of the lateral giant neurons to both GABA and glutamate, which sometimes has inhibitory function in crayfish, and whose receptors are inhibited by picrotoxin. I show that the neurons are sensitive to both GABA and glutamate, and that the effects of glutamate can be reduced by high concentrations of picrotoxin. I further show that the axon itself is sensitive to these compounds. I then discuss the implications of these findings.

4.2. Research questions

The rapid onset of the depolarizing inhibitory post-synaptic potential (dIPSP), and its diffuse nature, occurring in areas with no known inputs or outputs, suggest that a non-synaptic mechanism may be responsible for the earlier part of the inhibition, and that the axon may be sensitive to the action of inhibitory compounds generally, rather than at particular synaptic sites. The inhibition of the LG is chloride mediated and sensitive to

the $GABA_A$ receptor blocker picrotoxin. My initial attempts to localize GABA and GABA receptors in the sheath **(Figure 4.1, Figure 4.2)** using immunohistochemistry were not successful, leading me to question whether or not GABA is the relevant neurotransmitter.

Figure 4.1. Underside of the fifth abdominal ganglion (A5). Rostral is left. Green is GABA, red is $GABA_A$ receptors. GABA is generally localized to neuronal bodies, while the receptors are diffusely present throughout the neuropil, where connections are made. Nerve 3 is visible coming off the cord in the upper right of the image.

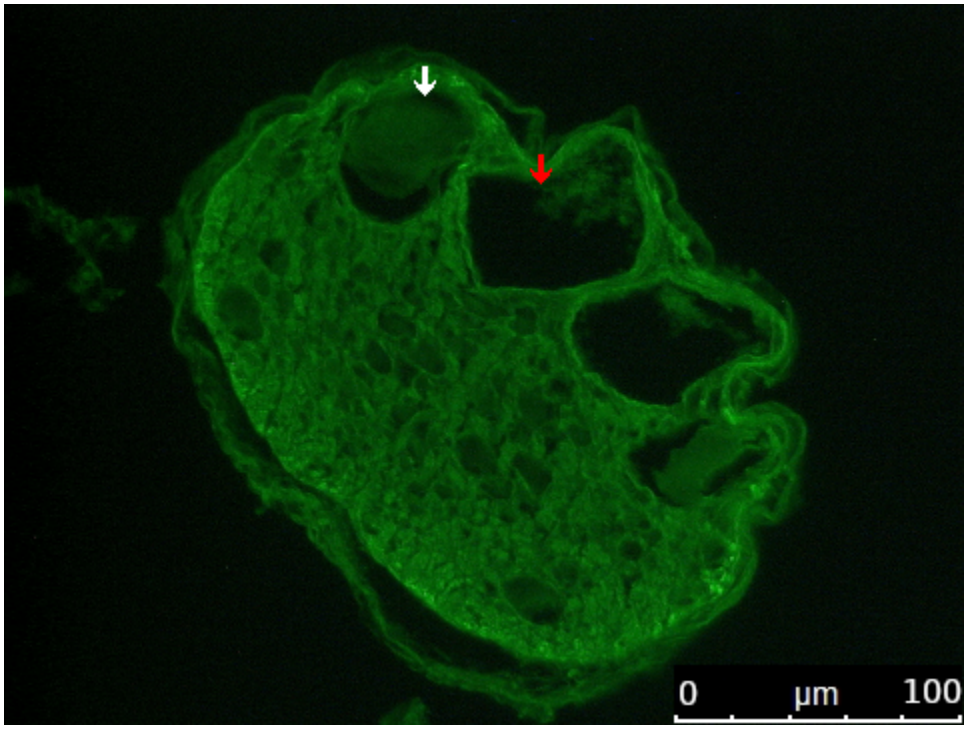

Figure 4.2. Interganglionic section of the abdominal nerve cord. The red arrow points to the MG, the white to the LG. Though the stain for GABA (green) was not specific, the glial sheaths are visible encircling the axons.

Invertebrates are known to possess chloride channels which are gated by glutamate; these channels are also sensitive to the antagonistic effects of picrotoxin, though often more resistant than GABA channels. Notably, glutamate mediates inhibition at several crayfish synapses, including the synapse between the LG and the MoG, and the glutamatergic compound NAAG, which is hydrolyzed into aspartate and glutamate in the extracellular space, is involved in communication between the MG and its glial sheath. Furthermore, the autoinhibition of the LG is not eliminated by picrotoxin. While it has been assumed that GABA is responsible for this autoinhibition, none of the evidence to date rules out the possibility of it being mediated by glutamate. I examine the possibilities that:

- The neurotransmitter release is non-synaptic in nature, and possibly caused by transporter reversal
- This inhibition is not localized, and occurs at least partially on the axon itself
- The inhibition is mediated by glutamate

Here I present work investigating these questions, and show that the LG axon is sensitive to GABA *and* glutamate in a manner which is reduced by the chloride channel blocker picrotoxin.

4.3. Methods

4.3.1. Immunohistochemistry

Images shown in the above section were made from tissue fixed and stained using GABA and $GABA_A$ receptor antibodies. Fixation and staining was accomplished using a modified version of Mulloney's fixation protocol (Mulloney & Hall, 1990). For the sectioned sample, the Sylgard containing the dissected out nerve cord was placed in an Eppendorf tube with 1 ml water and a small amount of protease from Streptomyces griseus dissolved in it for five minutes prior to fixation. This step is required to desheath the cord, and was necessary for successful staining. The sample was then moved to an Eppendorf tube with 1 ml of 4% formaldehyde and 0.2% glutaraldehyde in crayfish saline for 20 minutes at room temperature. 100 µl of 1.2% picric acid was then added, and the solution was left in the refrigerator at 4 degrees Celsius for six hours. Following this period, the cord was left in a 0.1 M glycine solution overnight. The procedure followed

for the whole-mount sample was identical, except that the primary fixative was 4% formaldehyde in crayfish saline and the secondary fixative was 2% formaldehyde in saline.

Tissue was incubated in several washes of 5% goat serum and 0.3% Triton X-100 in crayfish saline (wash buffer) for 3-5 hours. The tissue was then immersed in wash buffer with 1:750 rabbit anti-GABA and/or 1:100 mouse anti-$GABA_A$ receptor antibodies and left on an orbital shaker at 4 ºC overnight. Tissue was then incubated in several washes of wash buffer for 5-6 hours, and immersed in 1:100 Atto-488 conjugated goat anti-rabbit and 1:100 Atto-596 conjugated goat anti-mouse antibodies on an orbital shaker at 4 ºC overnight.

After staining, whole mount tissue was immersed for one hour in 50% glycerol, 50% deionized water, then moved to a 90% glycerol solution for an hour before being mounted in 100% glycerol. Slides were sealed using clear nail polish.

For sectioned tissue, the sample was dehydrated through an ethanol series of 70%, 90%, 95%, and 100% ethanol. The tissue was submersed in each concentration for five minutes. After this it was submersed in 100% xylene for five minutes, then the xylene bath was replaced with a fresh one for another five minutes. The tissue was moved into an oven at 60 ºC and left in a 1:1 xylene/paraffin solution for an hour. It was then moved to a solution of 100% paraffin for an hour, followed by a second 100% paraffin bath for an hour, then was moved into a mold filled with paraffin. The sample was allowed to rest in this mold until it sunk to the bottom, at which point it was moved out and held on a hot plate while being oriented. The hot plate was then turned off until the sample had

solidified. Paraffin-embedded tissue was sectioned on a microtome into 20 μm thick ribbons. The ribbons were adhered to subbed slides and left on a hot plate overnight, after which they were stored for later processing.

Slides with paraffin sections adhered were immersed in xylene for thirty minutes to deparaffinize them. They were then rinsed with ethanol and mounted in 100% glycerol.

4.3.2. No-calcium saline

In order to gauge the importance of calcium in the LG's autoinhibition, an isolated nerve cord was impaled with intracellular electrodes between the fifth (A5) and sixth (A6) abdominal ganglia, with an extracellular hook on the ipsilateral sensory afferents and another between A3 and A4. The afferents were stimulated at 85% of their threshold, and the cord was stimulated directly with 10 V, increased to 15 V if the spike began failing. Saline was made by replacing calcium chloride with an equimolar quantity of magnesium chloride and superfused over the preparation (Zucker, 1974). The β component of the PSP is due to interneurons which receive chemical (cholinergic) input, so it should be eliminated if there is insufficient extracellular calcium for neurotransmitter release. The PSP size was therefore used to discern whether the calcium concentration in the bath was insufficient for synaptic transmission. The dIPSP should fail at the same time as the PSP if it is produced by synaptic mechanisms, and would likely be unaffected if not.

4.3.3. Drugs

As an action potential in the LG initiates a complex array of neural activity, and the receptors may not be concentrated at any specific site, a high concentration of neurotransmitter might be needed to cause measurable effects. 5 mM was selected for the concentration of GABA, a higher concentration than has been previously used to study the relatively smaller LG PSP (Vu & Krasne, 1993).

For the preliminary experiment to test the possibility of glutamate, 0.5 mL of 400 mM monosodium glutamate was added via pipette to a dish containing an isolated abdominal nerve cord. The cord was stimulated directly between A5 and A6, and recording was taken between A3 and A4.

As both the exploratory glutamate and the GABA superfusion experiments appeared successful, 5 mM was also selected for glutamate, but following ambiguous results, the experiments were repeated with 10 mM glutamate. When utilizing a picospritzer, both GABA and glutamate solutions were 1 molar, corresponding to the highest concentration of glutamate used by Heitler et al. (2001) in their study of the MoG.

Glutamate gated chloride channels in crayfish muscle need up to 1 mM picrotoxin before becoming inhibited (Franke et al., 1986). I first selected 100 µM to test the effect of picrotoxin on the depolarizations that I observed during glutamate application. As this was successful, I also performed experiments with 50 µM and 25 µM picrotoxin.

4.3.4. Superfusion

An extracellular hook electrode was placed on the nerve cord between A5 and A6. This electrode was used to directly apply 10 V stimulation for a period of 0.5 ms in order to evoke action potentials in the LG. As the LG was stimulated directly, there was no concern of habituating its afferent input, so a 60 second inter-stimulus interval was used. While its afferents rapidly habituate (Krasne, 1969), the lateral giant itself reliably spikes when stimulated directly with cord electrodes, even when repeated over a long period of time (Algarin et al., 2019). Intracellular electrodes were inserted into the LG, ipsilateral to each other, between A3 and A4, each approximately one third from the nearest ganglion **(Figure 4.3)**. Following stimulation, the more rostral intracellular electrode was used to inject current at -100 nA, -50 nA, 50 nA, and 100 nA. Each injection was 20 ms in duration, and separated by 200 ms. Saline vehicle was superfused for 15 minutes, then drug (GABA or glutamate) was superfused for 30 minutes, followed by saline for 30 minutes to wash out any effects. During superfusion, the bath is slowly replaced with another containing the compound of interest, which results in a slow ramp-up and ramp-down in concentration.

To reduce electrical noise, data gathered were compared to the average membrane potential 20 ms prior to the stimulus artifact. While the dIPSP does not have clear discrete components like the LG's PSP, I decided to analyze several time points in case there was a difference between the effects of GABA and glutamate early, medium, and late in the response. The membrane potential was measured 3 ms, 5 ms, and 10 ms after

the stimulus artifact, averaged over a window of ± 50 microseconds (0.05 ms) **(Figure 4.4)**. The potential was also measured over the last 5 ms of each current injection step, to allow quantification of resistance changes. Resistance was calculated by dividing the membrane potential shift, in Volts, by the current injected, in Amperes.

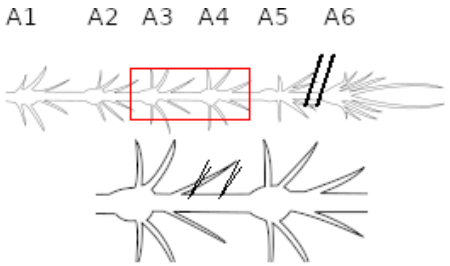

Figure 4.3. Experimental setup for superfusion experiments. On top is the abdominal nerve cord, oriented so that the right is caudal. Each bulge is a ganglion, with A1 furthest left and A6 furthest right. The thick black lines between A5 and A6 represent the stimulating hook electrode. Inset: a zoomed view of A3 and A4, with intracellular electrode tips shown in their recording positions. Nerve cord image is adapted from Huxley, 1879.

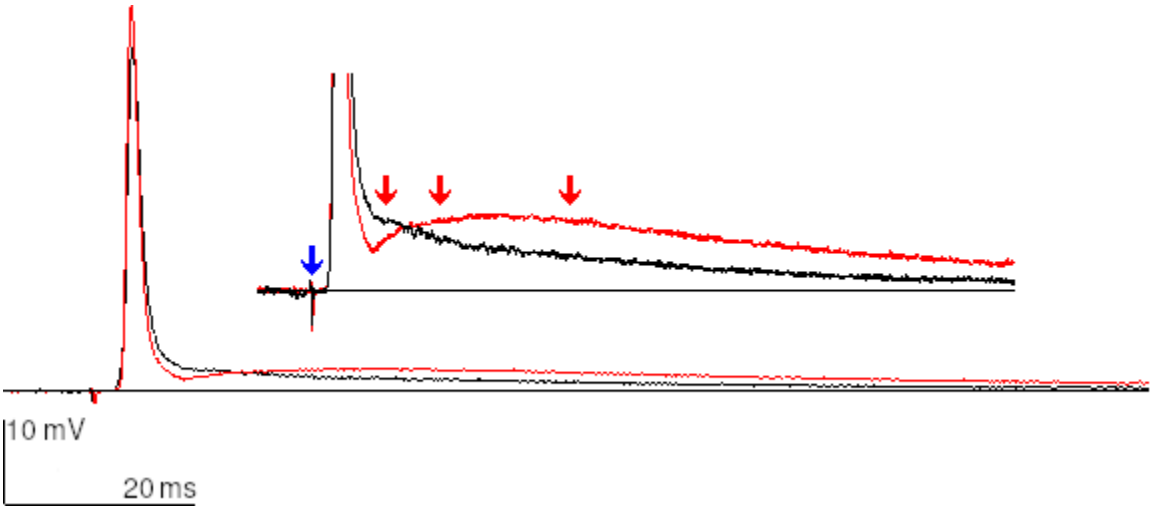

Figure 4.4. View of two dIPSPs, with zoomed inset. The shape of the dIPSP varies, and sometimes includes a slight depolarization following the spike. The depolarization in the example shown is particularly large, and most dIPSPs have shapes that lie between those of the two examples shown. The blue arrow indicates the stimulus artifact, and red arrows indicate 3 ms, 5 ms, and 10 ms post-stimulus, which were selected for analysis. The solid black lines indicate the baseline membrane potential. The LG action potential is truncated in the inset.

As it became clear that a desensitization-like effect was occurring after prolonged neurotransmitter exposure, and the effects of both GABA and glutamate occurred rapidly (see results sections), drug phase analysis was performed on data gathered 5 minutes after initial drug application, rather than 30 minutes.

4.3.5. Picospritzer

Experiments involving drug ejection utilized a General Valve Picospritzer II. The Picospritzer was fed by a nitrogen gas cylinder. All ejections were performed with a pressure of 20 PSI. I successfully elicited a GABA response with ejection pulses as short as 1 ms during early experiments, so this was selected as the ejection time for this protocol. Initially, I used a 1 ms ejection time for glutamate as well, but this proved too short for reliable results, so all glutamate data presented here was produced with 5 ms ejection times. In all experiments, a 120 second inter-stimulus interval was used, to allow a more complete recovery from drug ejection. This value was selected based on crayfish work showing that up to two minutes is required for EPSP recovery after glutamate application to the motor giant synapse (Heitler et al., 2001). Stimulation occurred 10 seconds after the picospritzer was used to eject the chemical under study. It was difficult to properly align the picospritzer tip and recording electrode, but both GABA and glutamate caused a depolarization of the LG membrane potential when properly ejected **(Figure 4.5, Figure 4.6)**, presumably due to the opening of chloride channels, so depolarization was used as a proxy for appropriate placement. Only experiments in which

ejection caused at least a 0.5 mV depolarization, when measured after 5 seconds, were used.

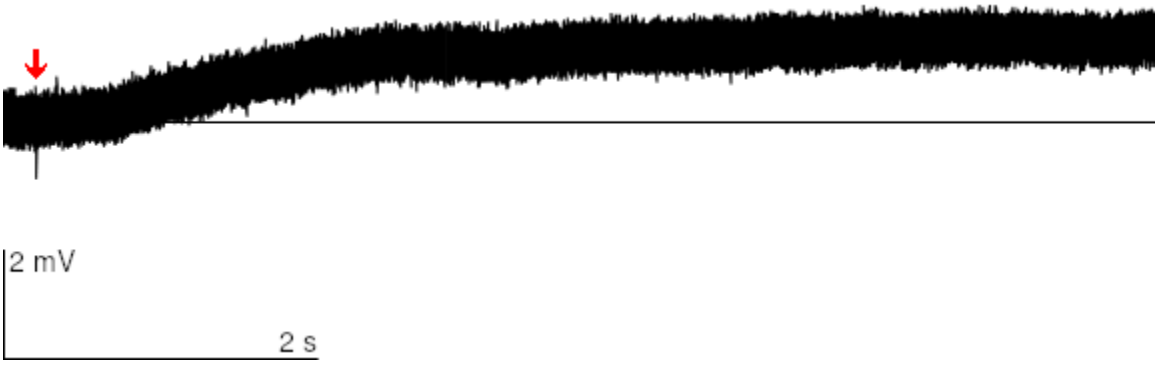

Figure 4.5. Membrane potential of the LG in response to a 1 ms ejection of 1 M GABA. The black line indicates the baseline membrane potential. The red arrow is the point at which GABA was applied. GABA causes a slow depolarization. The slope of onset, magnitude and time of peak depolarization (not visible), and time course of return to baseline are all highly variable among preparations, likely due to differences in picospritzer placement. This example is characteristic of the slower responses.

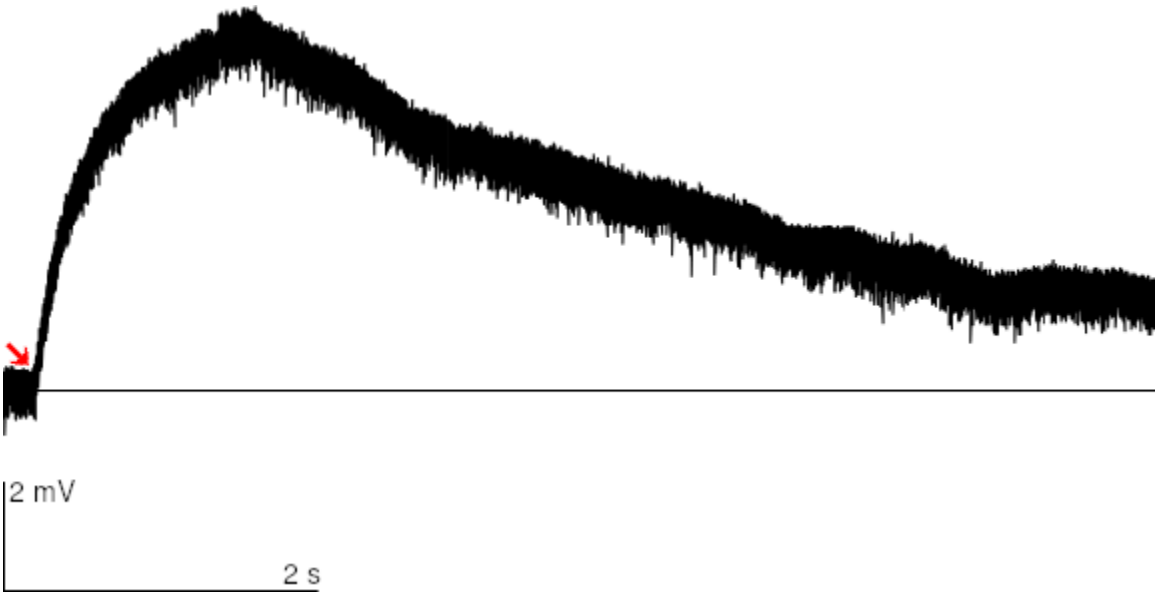

Figure 4.6. Depolarization due to a 5 ms ejection of 1 M glutamate. The black line indicates the baseline membrane potential. The red arrow is the point at which glutamate was applied. As with GABA, glutamate ejection caused a depolarization, which varied in its magnitude and time course between preparations. This example is characteristic of rapid (and strong) depolarization and repolarization.

Because the locus of inhibition may be diffuse (and the effect of local application thus weakened), I decided to test the presence of inhibition with subthreshold afferent stimulation in addition to testing with action potentials generated via direct cord stimulation. This has several advantages: if the effect of localized application is weak, it is more likely to be detected using a PSP; as a PSP is substantially less complex than an action potential, the effects of the neurotransmitter may be clearer; and PSPs do not regenerate themselves along axons, which should enhance the relative effect of the picospritzer by reducing voltage-gated currents through membrane patches near the recording site. Testing on action potentials was eventually ceased, as the effect seen in early trials was weak, and the PSP experiments were sufficient to examine the possibility of an axonal sensitivity to inhibitory compounds. PSP amplitudes were measured relative to the membrane potential averaged across 1 second before stimulation. Depolarization at 5 seconds post-ejection was measured over a one second time window, relative to pre-spritz voltage. Despite the long inter-stimulus interval, the ejection-induced depolarization underwent an attenuation *(GABA: N = 8; first trial (1.15 mV, SD = 0.49) to third trial (0.57 mV, SD = 0.34) Wilcoxon: p = 0.002; glutamate: N = 7; first trial (4.17 mV, SD = 2.99) to third trial (2.84 mV, SD = 3.15) Wilcoxon: p = 0.005)*, indicating desensitization. For this reason, I decided to use only the first two drug trials for analysis.

Measurements were taken 3 ms, 5 ms, and 10 ms post-stimulus, averaged over a 50 microsecond window **(Figure 4.7)**. These times correspond to the early and late β

component of the LG's PSP **(Figure 2.4)**, as well as the period of post-excitatory inhibition (Krasne, 1969; Vu et al., 1997). Unfortunately, in many cases the PSP attenuation due to passive propagation resulted in a rostral PSP that was too small to be analyzed reliably at 3 ms, so only the 5 ms and 10 ms time points were used.

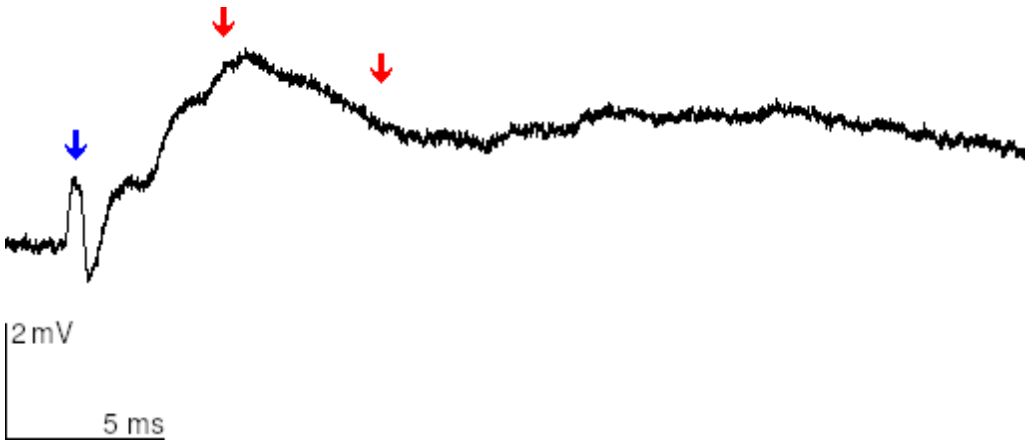

Figure 4.7. LG PSP. Arrows indicate 5 ms and 10 ms. The blue arrow indicates the stimulus artifact.

In all experiments, an extracellular stimulating electrode was placed on the lateral nerve roots of A6, which contain the sensory afferents to the LG, and a portion of the nerve cord between A5 and A6 was mechanically desheathed. The stimulation voltage used was 85% of the threshold for evoking an action potential. The torn sheath was pinned down with fine Minutien pins. One electrode was placed in the desheathed area, and the picospritzer tip was placed as close as possible. Another electrode was placed in the LG in a non-desheathed area near A6, to serve as a comparison **(Figure 4.8)**. The PSP size recorded in the rostral, drug-applied area was divided by the PSP size seen in the caudal control area. This ratio was used as the quantified measure of drug-induced axonal inhibition.

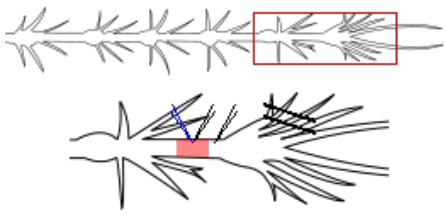

Figure 4.8. Experimental setup for experiments utilizing a picospritzer. On top is the abdominal nerve cord, oriented so that the right is caudal. Inset: a zoomed view between A5 and A6. The extracellular hook electrode used for stimulation of sensory afferents is represented by the thick black lines on the sensory nerves. The intracellular recording electrodes are represented by the thin black pinpoints, and the tapered blue pinpoint represents the tip of the picospritzer. The red overlay on the connective signifies the area which has been desheathed. Nerve cord image is adapted from Huxley, 1879.

Saline was superfused across the cord for the duration of the experiment, to prevent the build-up of ejected neurotransmitter or the diffusion of neurotransmitter onto nearby ganglia. The experiment consisted of three trials with no drug ejection, three trials with drug ejection, and three "washout" trials without drug ejection. Statistics were performed on values obtained by averaging the values within each experimental phase (pretreatment, drug application, washout).

In addition, several preparations had picrotoxin washed over them while glutamate was ejected in order to demonstrate that chloride channels were involved. These preparations were exposed to 100 µM, 50 µM, or 25 µM picrotoxin for 20 minutes. Afterwards, saline washout was attempted for 30 minutes. The depolarization was measured 2 seconds after glutamate ejection.

To analyze these experiments, a linear mixed model was fitted with picrotoxin concentration, time, and their interaction as fixed effects, a random intercept and slope for

each subject, and an autocorrelation structure of order 1. A separate model with identical structure was fitted for the washout phase.

4.4. Results

4.4.1. No-calcium saline

I hypothesized that perhaps high external potassium concentration following a spike causes the GABA or glutamate transporters to reverse, releasing neurotransmitters into the extracellular space and causing the dIPSP during autoinhibition. In order to test this, saline with reduced levels of calcium was used, as this eliminates synaptic neurotransmitter release in response to action potentials (Fatt & Katz, 1952). As the β component of the PSP requires chemical input, the afferents were stimulated and the disappearance of the β component was used to indicate that the calcium concentration was insufficient for synaptic transmission. Several preparations with no-calcium saline followed by picrotoxin were attempted, but the PSP loss could never be reversed, making it impossible to rule out the possibility that its disappearance was simply due to threshold changes. Eventually, a preparation was exposed to an hour of no-calcium saline, and I found that this treatment was effective at eliminating the dIPSP **(Figure 4.9)**. The dIPSP was restored upon superfusion with normal saline. While this suggests vesicular involvement, rather than non-synaptic events, it does not exclude the possibility of an axonal locus to the inhibition. If it is synaptic, however, its source must be local, as its

size remains unaffected if the cord is cut or ligated rostral to the next ganglion (Herberholz, personal communication).

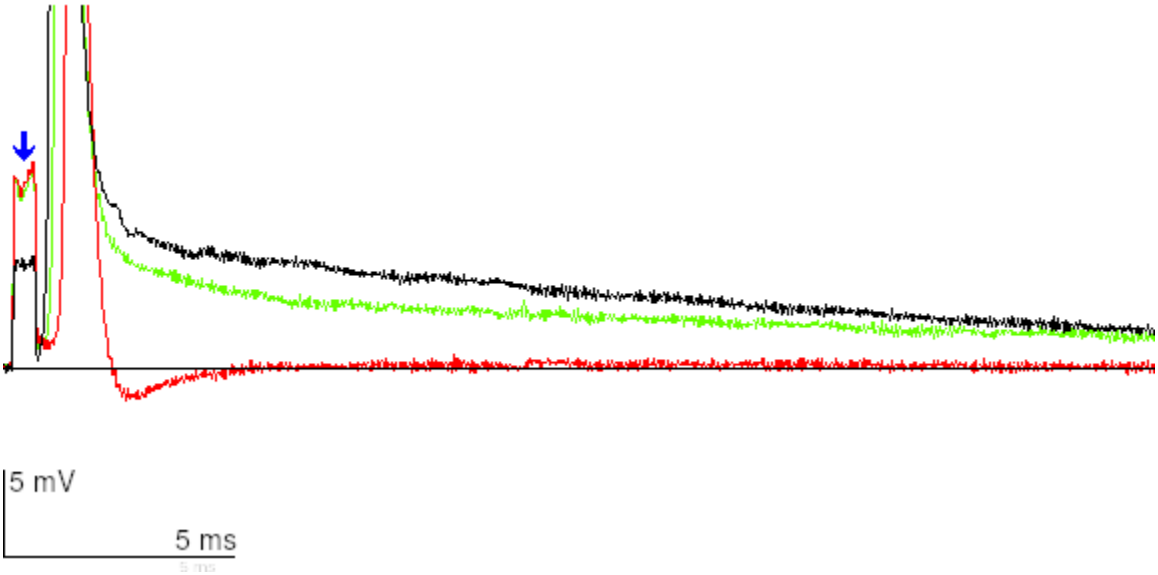

Figure 4.9. dIPSP following no-calcium saline superfusion. The black trace is before no-calcium saline was superfused, the red trace after 54 minutes of superfusion, and the green trace after 20 minutes of normal saline. The blue arrow marks the stimulus artifact. Stimulus artifacts are not identical as the stimulation voltage had to be increased following spike failure. The dIPSP following the (truncated) action potential is eliminated fully, allowing the LG to undershoot its baseline. This is reversed if calcium is returned to the bath.

4.4.2. GABA

4.4.2.1. Superfusion

GABA exposure *(N = 6)* caused a rapid decline in the dIPSP amplitude, suggesting that the effects of GABA occlude the dIPSP, but this effect rapidly reversed, typically while GABA was still superfused **(Figure 4.10).** Compared to the dIPSP amplitude before drug application, 5 minutes of exposure to 5 mM GABA caused a substantial reduction in size at **3 ms** *(Friedman: p = 0.002; pretreatment (4.23 mV, SD = 1.73) to drug (3.49 mV, SD = 1.63) Wilcoxon: p = 0.031)*, **5 ms** *(Friedman: p = 0.002;*

pretreatment (4.23 mV, SD = 1.04) to drug (3.33 mV, SD = 0.96) Wilcoxon: p = 0.031), and **10 ms** *(Friedman: p = 0.011; pretreatment (4.25 mV, SD = 1.47) to drug (3.24 mV, SD = 1.03) Wilcoxon: p = 0.031).* At the end of washout, dIPSP sizes had increased at all time points *(3 ms: drug to washout (5.50 mV, SD = 1.44) Wilcoxon: p = 0.031; 5 ms: drug to washout (4.90 mV, SD = 0.77) Wilcoxon: p = 0.031; 10 ms: drug to washout (4.26 mV, SD = 0.85) Wilcoxon: p = 0.031)*, overshooting the pretreatment size at **3 ms** *(Wilcoxon: p = 0.031)* and **5 ms** *(Wilcoxon: p = 0.031)*, though it is important to note that the reversal began during the drug exposure phase **(Figure 4.10)**. There was no clear difference in resistance *(Friedman: 0.115; pretreatment (70800 Ω, SD = 8400); drug (64800 Ω, SD = 10200); washout (76600 Ω, SD = 15900))*, nor between baseline membrane potential before and after 5 minutes of treatment, though there was a decrease in membrane potential during washout *(Friedman: p = 0.011; pretreatment (-92.99 mV, SD = 5.56) to drug (-92.54 mV, SD = 5.36) Wilcoxon: p = 0.688; drug to washout (-97.35 mV, SD = 5.68) Wilcoxon: p = 0.031)*, and the means in all five measurements followed identical trends (change during early drug exposure, followed by a reversal and often overshoot of pretreatment value).

While these experiments show that GABA application is effective at reducing the dIPSP, suggesting competition for GABA receptors, they do not test if the inhibition is occurring at any particular locus. In an attempt to clarify both the location of the inhibition and the effect of acute exposure, I performed new experiments, utilizing a picospritzer for fine spatial and temporal control of neurotransmitter application.

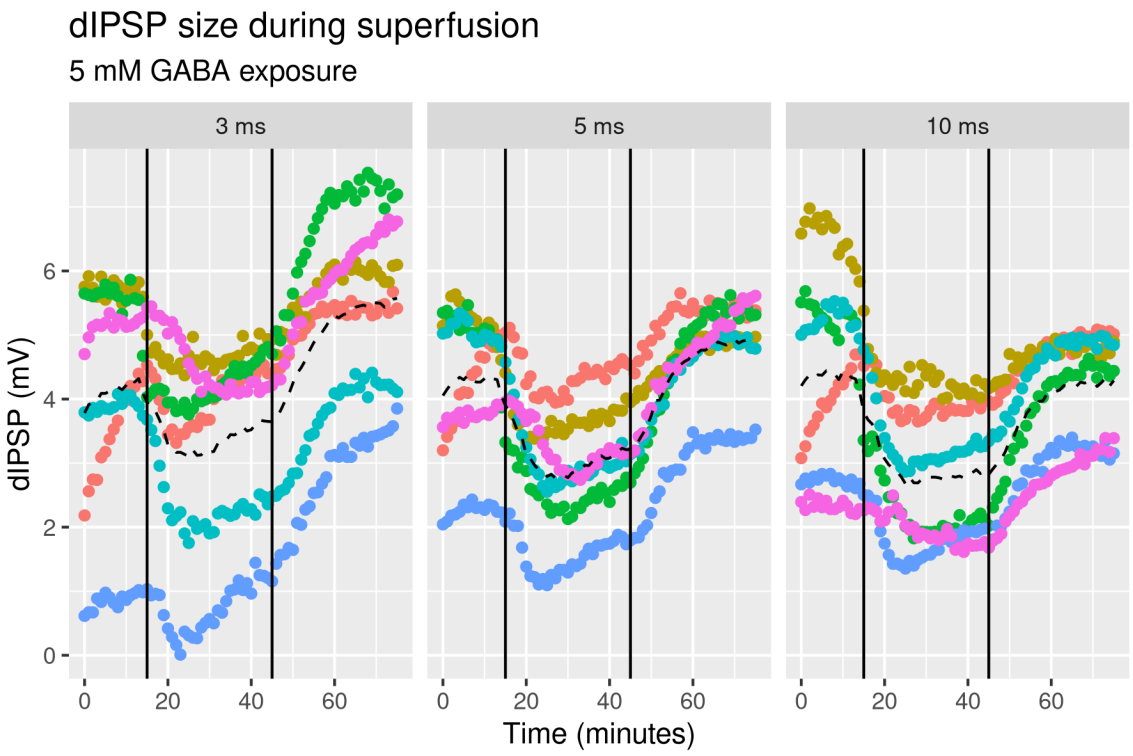

Figure 4.10. dIPSP size at 3 ms, 5 ms, and 10 ms during the GABA superfusion experiment. Each preparation is graphed in a separate color, with the mean represented by the dotted line. The solid black vertical lines demarcate the beginning and end of GABA superfusion. During superfusion, all preparations experience a rapid decline in dIPSP size at all three time points, but this began to reverse between ten and fifteen minutes of GABA exposure, suggesting desensitization.

4.4.2.2. Picospritzer

Saline was continually superfused and GABA applied via a picospritzer. Application of GABA *(N = 8)* caused a clear depolarization in the rostral electrode **(Figure 4.5)**, and had a clear effect on the afferent-evoked LG PSP recorded in the desheathed area **(Figure 4.11)** at both **5 ms** *(Friedman: p = 0.005; pretreatment (2.70 mV, SD = 1.25) to treatment (2.09 mV, SD = 0.74) Wilcoxon: p = 0.016; treatment to posttreatment (2.79 mV, SD = 0.97) Wilcoxon: p = 0.008)* and **10 ms** *(Friedman: p = 0.002; pretreatment (2.87 mV, SD = 1.71) to treatment (2.08 mV, SD = 0.76) Wilcoxon:*

p = 0.008; treatment to posttreatment (3.02 mV, SD = 1.43) Wilcoxon: p = 0.008), as well as having an effect on the ratio between the two recording electrodes **(Figure 4.12)** at **5 ms** *(Friedman: p = 0.008; pretreatment (0.60, SD = 0.13) to treatment (0.54, SD = 0.16) Wilcoxon: p = 0.023; treatment to posttreatment (0.61, SD = 0.16) Wilcoxon: p = 0.008)* and **10 ms** *(Friedman: p = 0.010; pretreatment (0.68, SD = 0.11) to treatment (0.61, SD = 0.13) Wilcoxon: p = 0.016; treatment to posttreatment (0.71, SD = 0.15) Wilcoxon: p = 0.008)*. This effect only occurred on trials where GABA was applied; the PSP size and ratio increased in post-treatment trials, returning to pretreatment levels.

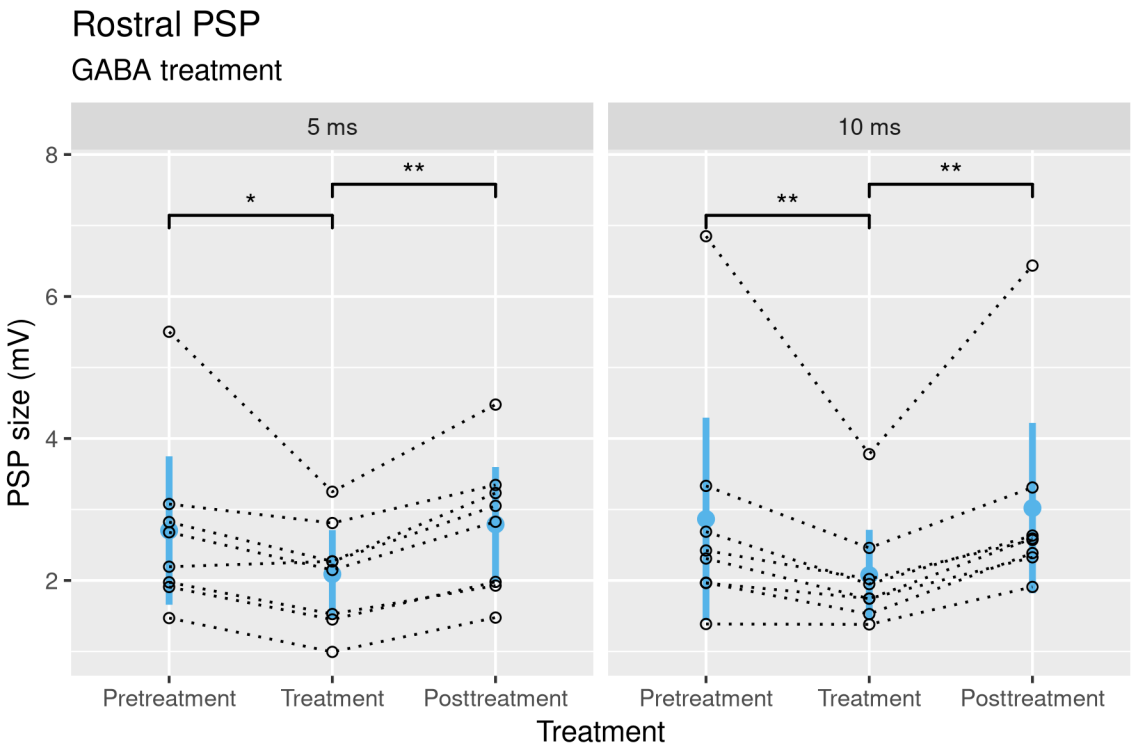

Figure 4.11. PSP size in response to GABA ejection. Filled circles are means, lines are ± one standard deviation. Hollow circles, linked by dotted lines, represent individual preparations. The presence of GABA reduces the size of the PSP, but this effect is rapidly reversed, and the PSP recovers to its pretreatment size.

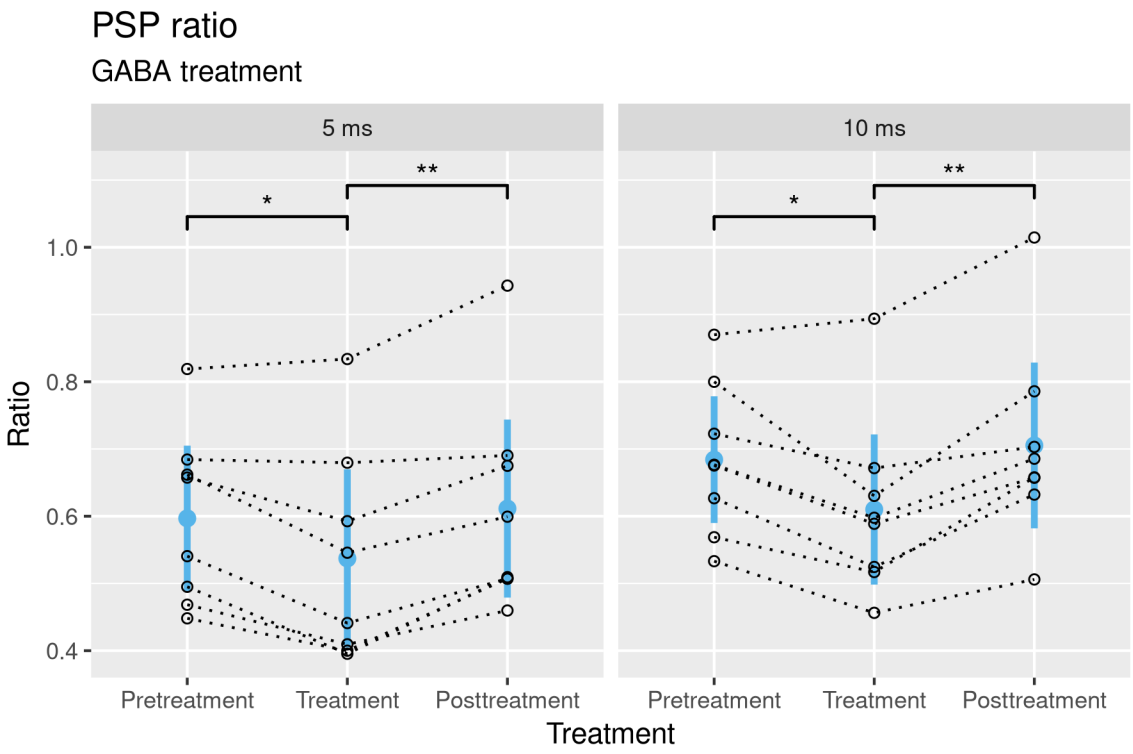

Figure 4.12. PSP ratio in response to GABA ejection. Filled circles are means, lines are ± one standard deviation. Hollow circles, linked by dotted lines, represent individual preparations. The presence of GABA reduces the strength of the PSP in the interganglionic space relative to that of the proximal PSP. The ratio returns rapidly to normal in the absence of GABA.

4.4.3. Glutamate

4.4.3.1. Rationale for glutamate testing

When exploring the possibility of glutamate being involved, as opposed to solely GABA, exploratory experiments *(N = 2)* were conducted. 0.5 mL of 400 mM monosodium glutamate was added to a dish containing an isolated abdominal nerve cord. This resulted in a drastically reduced dIPSP **(Figure 4.13)**. The dIPSP did not return during washout, though the spike widened. Based on this preliminary result, a series of more controlled experiments were performed.

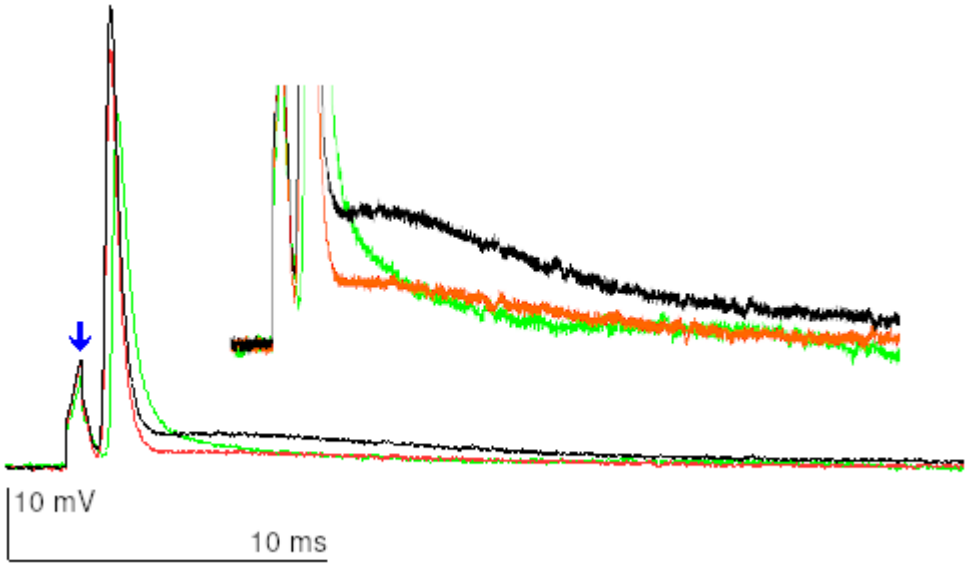

Figure 4.13. Effect of glutamate application on the shape of the LG spike and dIPSP. The blue arrow marks the stimulus artifact. The black trace is pretreatment, the red is after six minutes of glutamate application, and the green is twenty minutes after washout started. Glutamate exposure substantially reduced the dIPSP amplitude, and modestly reduced the height of the action potential peak. These effects persisted during washout. Inset: zoom of the spike and ensuing dIPSP.

4.4.3.2. Superfusion - 5 mM

Unlike GABA, superfusion of 5 mM glutamate (N = 6) did not induce many clear effects, though it appears some preparations responded more than others **(Figure 4.14)**. While there was an increase in dIPSP amplitude by the end of the experiment at **3 ms** *(Friedman: p = 0.009; pretreatment (4.22 mV, SD = 1.09) to washout (5.22 mV, SD = 1.41) Wilcoxon: p = 0.031)* and **5 ms** *(Friedman: p = 0.011; pretreatment (4.53 mV, SD = 1.42) to washout (5.27 mV, SD = 1.50) Wilcoxon: p = 0.031)*, though there was not for **10 ms** *(Friedman: p = 0.311)*, and in all cases the difference followed a monotonically increasing trendline. At no measurement point did drug application result in a robust weakening of the dIPSP *(3 ms: pretreatment (4.22 mV, SD = 1.09) to drug (4.04 mV, SD*

= 1.23) Wilcoxon: p = 0.563; 5 ms: pretreatment (4.53 mV, SD = 1.42) to drug (4.62 mV, SD = 1.26) Wilcoxon: p = 0.688). Similarly, while resistance increased over the course of the experiment, *(Friedman: p = 0.002; pretreatment (69800 Ω, SD = 11000) to drug (72500 Ω, SD = 11400) Wilcoxon: p = 0.031; drug to washout (87700 Ω, SD = 19900) Wilcoxon: p = 0.031)*, it increased monotonically. There was no change in baseline membrane potential over the course of the experiment *(Friedman: p = 0.846)*. The lack of finding of a robust decrease in dIPSP is somewhat surprising in light of the clear trend displayed by many preparations at 3 ms and 5 ms **(Figure 4.14)**. This might be explained by the fact that some preparations appeared to be relatively resistant to glutamate, while most displayed some weakening during exposure. As glutamate's effect at chloride channel can be less robust than GABA's (Heitler et al., 2001), the same experiment was performed with a doubled concentration of glutamate.

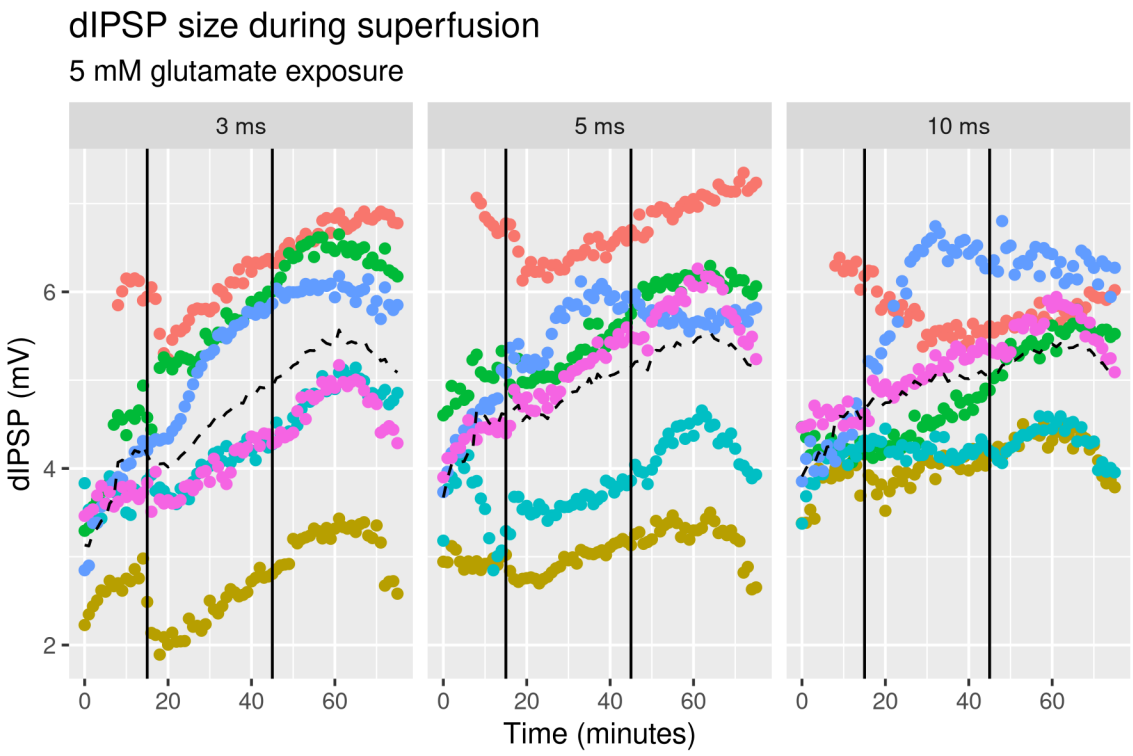

Figure 4.14. dIPSP size at 3 ms, 5 ms, and 10 ms during the 5 mM glutamate superfusion experiment. Each preparation is graphed in a separate color, with the mean represented by the dotted line. The solid black lines demarcate the beginning and end of glutamate superfusion. Some preparations do appear to have responded to glutamate exposure, but the effect was less dramatic than it was with GABA, and reversal always began earlier than it did with GABA.

4.4.3.3. Superfusion - 10 mM

Preparations *(N = 6)* were exposed to a higher concentration of glutamate in an attempt to amplify any possible effects. The measures used to quantify dIPSP change at 5 mM GABA and glutamate application proved inappropriate due to severe disinhibition late in the experiment (however, dIPSP strengths during each trace are shown in **Figure 4.15**). Three preparations produced multiple spiking, a relatively rare phenomenon. This always occurred in the washout phase. In one preparation, one stimulation evoked 271

action potentials over 445 milliseconds (**Figure 4.16**). In this preparation, unusual double spikes were observed. Despite the lack of clear effect of glutamate superfusion on the LG dIPSP, its washout appears to cause an unusual amount of disinhibition.

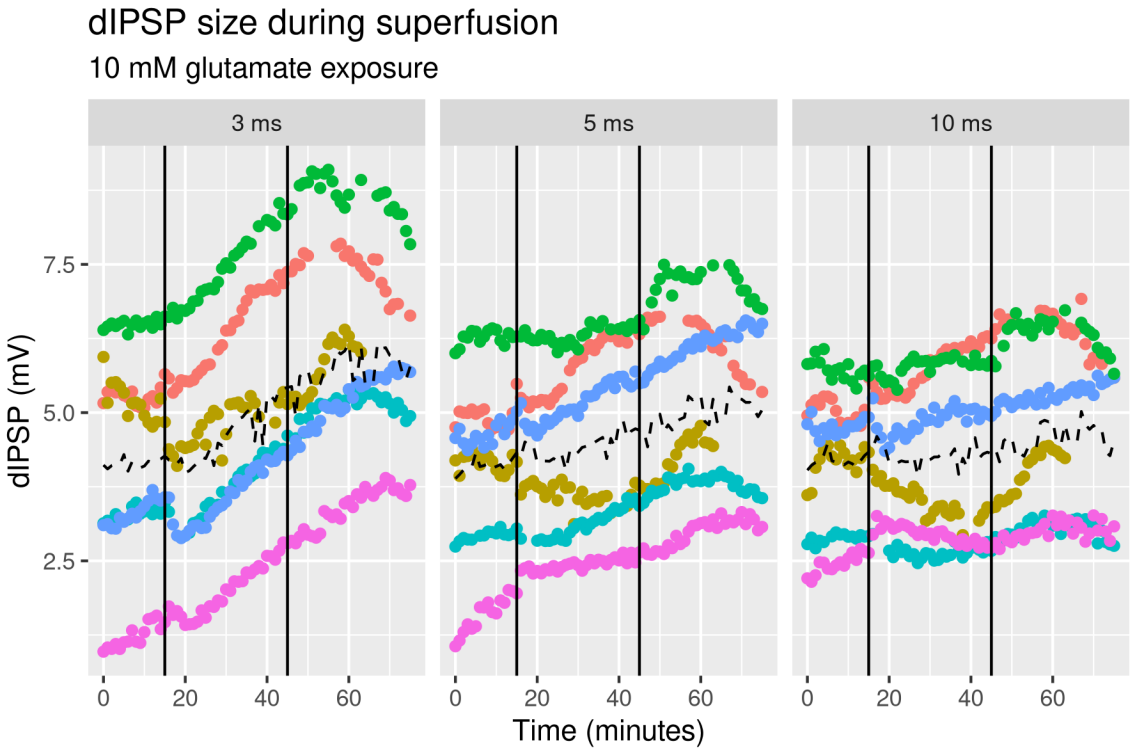

Figure 4.15. dIPSP size at 3 ms, 5 ms, and 10 ms during the 10 mM glutamate superfusion experiment. Each preparation is graphed in a separate color, with the mean represented by the dotted line. The solid black lines demarcate the beginning and end of glutamate superfusion. Action potentials were removed. As before, it appears that there is a sharp decrease following glutamate exposure, but only in some preparations.

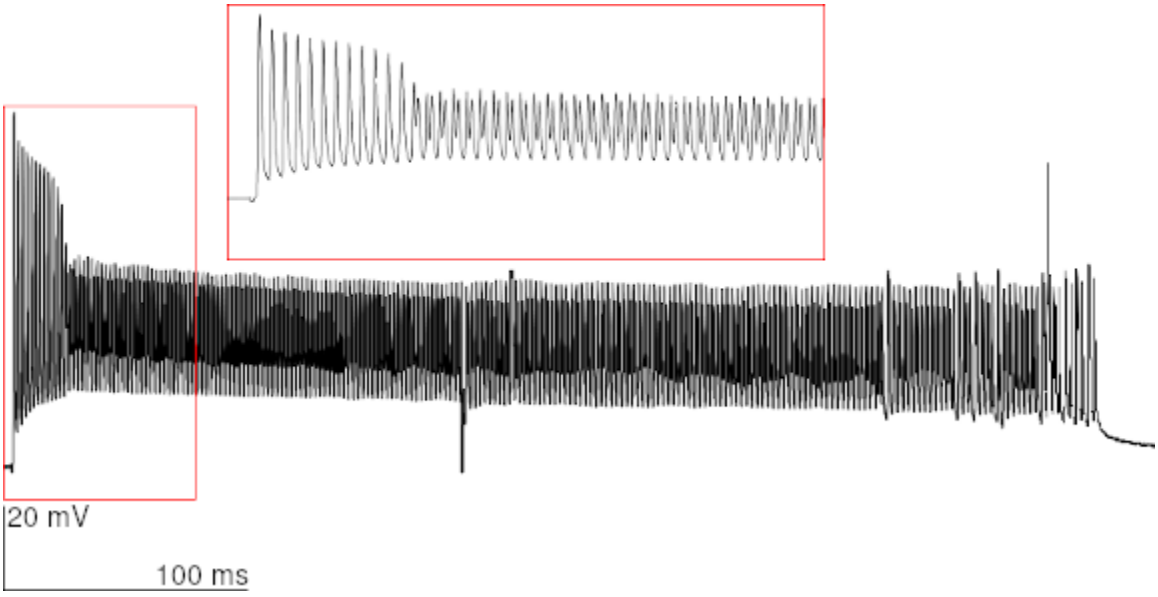

Figure 4.16. Rapid spiking following glutamate washout. Figure shows the 500 ms containing the longest spike train seen. Inset: zoomed view of the initial spikes.

Taken together, these results do not cleanly support the hypothesis that glutamate acts as an inhibitory neurotransmitter on the LG, although the washout disinhibition shows that it does have some effect. It is clear that the presence of GABA induces inhibition, and while the preliminary experiment suggested that acute exposure to high glutamate concentrations suppressed the dIPSP, the results of chronic glutamate exposure using bath superfusion are inconclusive. A Picospritzer was used to clarify glutamate's effect.

4.4.3.4. Picospritzer

Ejected glutamate application *(N = 7)* had a very similar effect to that of GABA. Ejection of glutamate caused a depolarization **(Figure 4.6)**, a substantial decrease in PSP size at **10 ms** *(Friedman: p = 0.018; pretreatment (1.84 mV, SD = 0.74) to treatment (1.57 mV, SD = 0.86) Wilcoxon: p = 0.031; treatment to posttreatment (1.86 mV, SD =*

0.77) Wilcoxon: p = 0.016) **(Figure 4.17)**, and a decrease in the ratio between rostral and caudal electrodes at both **5 ms** *(Friedman: p = 0.028; pretreatment (0.61, SD = 0.14) to treatment (0.54, SD = 0.15) Wilcoxon: p = 0.031; treatment to posttreatment (0.63, SD = 0.13) Wilcoxon: p = 0.031)* and **10 ms** *(Friedman: p = 0.018; pretreatment (0.70, SD = 0.11) to treatment (0.60, SD = 0.15) Wilcoxon: p = 0.031; treatment to posttreatment (0.72, SD = 0.09) Wilcoxon: p = 0.016)* **(Figure 4.18)**, though the p value for the decrease in PSP size at **5 ms** was elevated beyond 0.05 *(Friedman: p = 0.066)*. As with GABA, these effects disappeared immediately during postreatment.

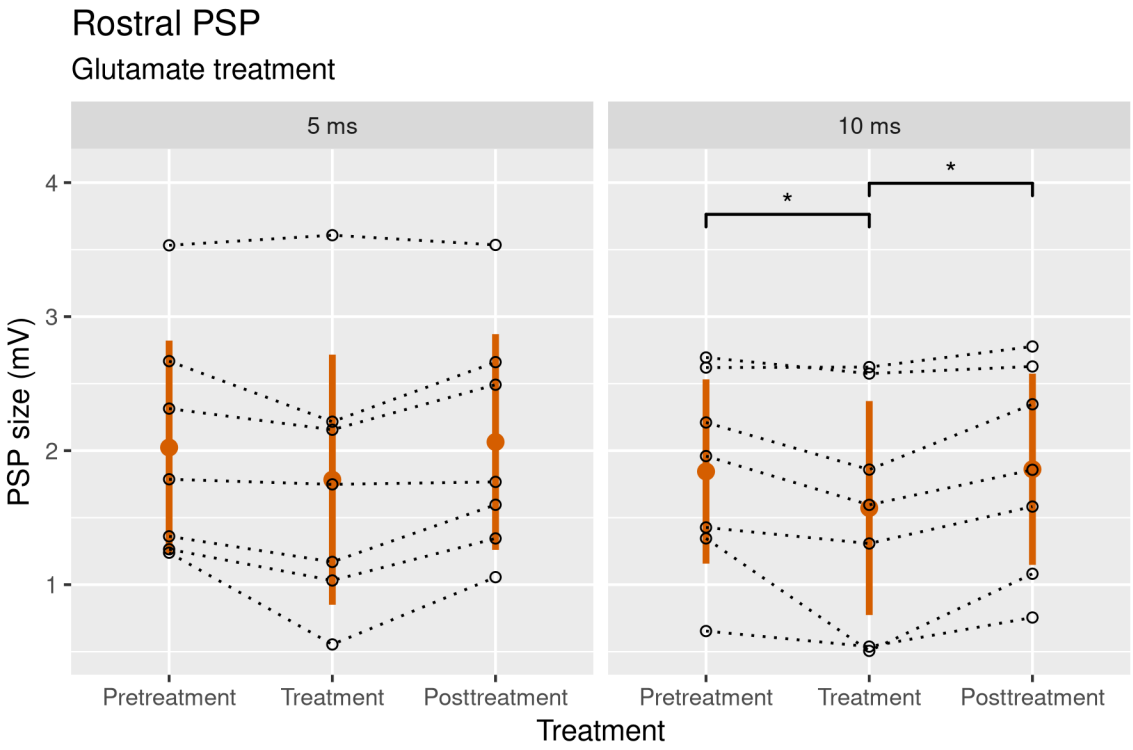

Figure 4.17. PSP size in response to glutamate ejection. Filled circles are means, lines are ± one standard deviation. Hollow circles, linked by dotted lines, represent individual preparations. The presence of glutamate reduces the size of the PSP at 10 ms, but the PSP recovers if not exposed. The effect follows the same general pattern at 5 ms, but less consistency resulted in a p value of 0.066.

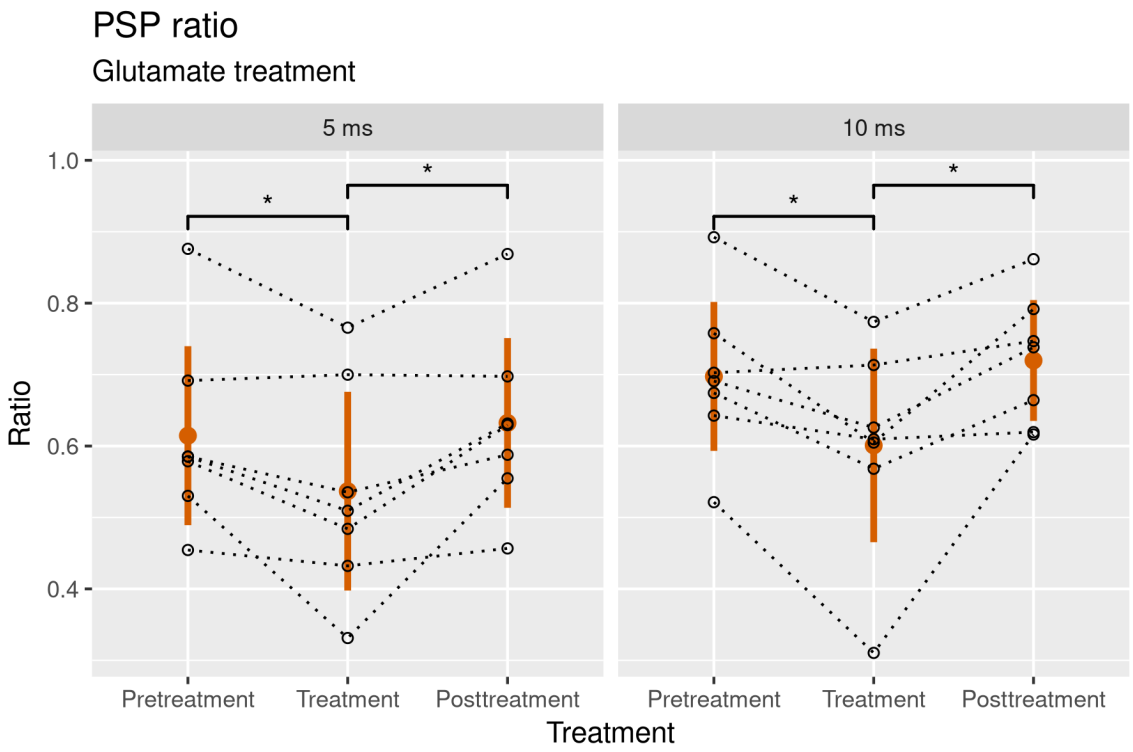

Figure 4.18. PSP ratio in response to glutamate ejection. Filled circles are means, lines are ± one standard deviation. Hollow circles, linked by dotted lines, represent individual preparations. The presence of glutamate reduces the ratio of the interganglionic to proximal PSPs at both 5 ms and 10 ms. As before, this effect is limited to trials where glutamate is applied.

4.4.3.5. Picrotoxin

Several preparations *(100 µM, N = 1; 50 µM, N = 3; 25 µM, N = 2)* were superfused with picrotoxin. Picrotoxin should bind GluCls, preventing glutamate from opening the channels and thereby reducing the response seen to ejection. When superfused with 100 µM picrotoxin, the depolarization induced by glutamate was inhibited rapidly, with a dramatic decrease after four minutes of exposure **(Figure 4.19)**. Exposure to 25 µM picrotoxin also inhibited this effect, but more slightly **(Figure 4.20)**. A linear mixed model fit to the baseline and picrotoxin exposure phases showed no effect based on time *($p = 0.195$)*, but did show a combined interaction effect between time and

concentration *(p = 0.019)*, consistent with the possibility that picrotoxin superfusion reduces depolarization brought about by glutamate ejection. The same model fit to the washout phase found no interaction effect *(p = 0.547)* or main effect of time *(p = 0.318)*. Picrotoxin is difficult to wash out, and has long lasting effects on the LG (Roberts, 1968), so the lack of recovery is not surprising. The model fit after picrotoxin exposure had finished (i.e., to the washout phase) found weak evidence that picrotoxin concentration made a difference in depolarization strength *(p = 0.063)*, while there was no evidence for this during pretreatment and picrotoxin exposure *(p = 0.490)*, further supporting the idea that picrotoxin blocks glutamate-mediated depolarization of LG.

The dish in which the experiments took place held a fairly large amount of fluid (40 ml), so the change in picrotoxin concentration brought about by superfusion took some time. The weakening of the depolarization for the lower picrotoxin concentrations continued during washout phase **(Figure 4.21)**, as the highest concentration of picrotoxin occurred at the end of superfusion and the beginning of washout.

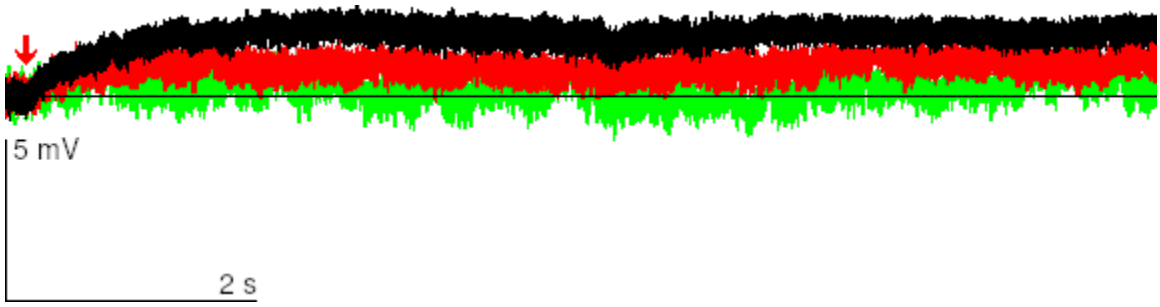

Figure 4.19. Glutamate based depolarization with 100 µM picrotoxin treatment. The black trace is immediately before picrotoxin is superfused, the red trace is after four minutes of picrotoxin, and the green trace is after 20 minutes of superfusion. The red arrow marks the point at which glutamate was ejected, and the black line represents the baseline membrane potential. Picrotoxin rapidly blocks the depolarization, and by 20 minutes there is no clear effect of glutamate.

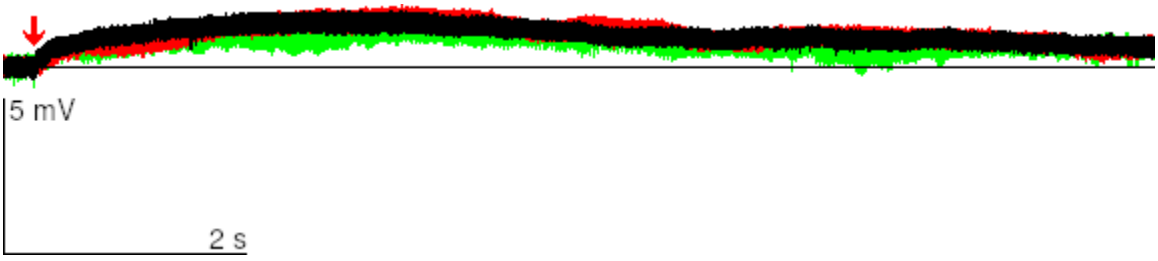

Figure 4.20. Glutamate based depolarization with 25 µM picrotoxin treatment. The black trace is immediately before picrotoxin is superfused, the red trace is after four minutes of picrotoxin, and the green trace is after 20 minutes of superfusion. The red arrow marks the point at which glutamate was ejected, and the black line represents the baseline membrane potential. At a lower concentration, picrotoxin still has some effect, but it is much slower and less complete.

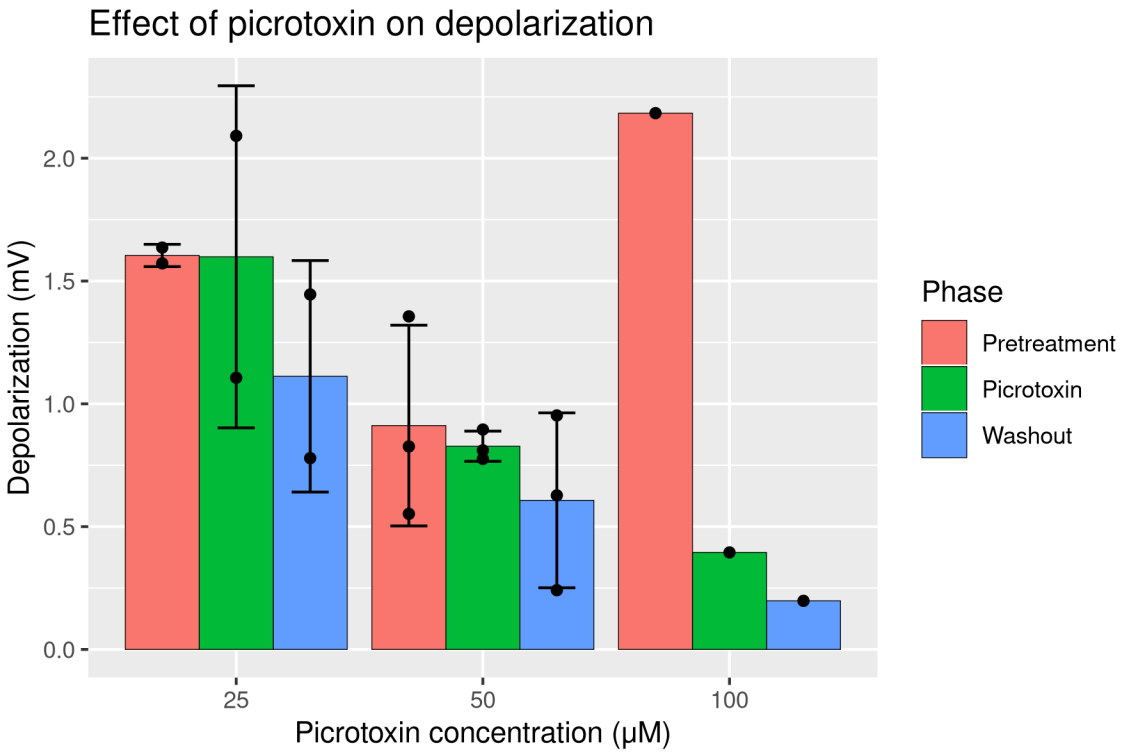

Figure 4.21. Mean glutamate-evoked depolarization for different picrotoxin concentrations before, during, and after picrotoxin superfusion. The last two trials of each condition (20 minutes for picrotoxin, 30 minutes for washout) were averaged. Height is the mean across all preparations in each condition, and bars are ± one standard deviation. Individual preparations are plotted as points. Picrotoxin was vastly more effective at the 100 µM concentration. The attenuation for 25 µM and 50 µM occurred in late picrotoxin exposure and early washout, when the concentration was highest.

4.5. Discussion of autoinhibition

I attempted to discern the mechanism of the LG's autoinhibition. I investigated the possibility that the mechanism of release is non-synaptic, that the axolemma itself is involved, and that glutamate is involved in an inhibitory capacity. I tested both glutamate and GABA in superfusion- and picospritzer-based application paradigms. As superfusion allowed the solution to flow completely throughout the system, its effects were less conclusive and the results less easy to interpret than those of the picospritzer experiment.

Since the autoinhibition does not decrease substantially in size further from the LG's dendrites, and occurs too quickly to be explained by a polysynaptic circuit, a non-synaptic release of neurotransmitters, either by the axon (Lieberman et al., 1994; Kane et al., 2000; Urazaev et al., 2001) or by its glia (Lieberman et al., 1994; Villegas, 1984), could be responsible. I therefore investigated whether or not the mechanism of release could involve a reversal of the transporter, leading to neurotransmitter release and causing the dIPSP, by eliminating calcium from the bath. The result of this experiment strongly suggests that transporter reversal is not the cause of the inhibition, or at least not the major contributor. If it were, then the removal of calcium should have had little effect. Calcium could still be important for a non-synaptic mechanism if the glial release of inhibitory transmitter involved metabotropic receptors and a second messenger cascade, but the speed with which the dIPSP occurs makes that unlikely. A more probable explanation is that the release of inhibitory neurotransmitters is coupled to vesicular release. However, a single synapse as a locus seems unlikely, as the dIPSP occurs so

strongly in the connective between the ganglia. There are several possible sources of a vesicular neurotransmitter release: the giant axons themselves, their supporting glia, or an inhibitory interneuron. The giant axons themselves do contain vesicles, and while along the axon they appear mostly to be results of endocytosis (Viancour et al., 1987), the LG's synapses onto the MoGs also appear to have pools of vesicles (Hama, 1961; Stirling, 1972). However, given the diffuse nature of the inhibition, and the fact that the large vesicle pools are generally near the LG's synapses, this possibility is somewhat remote.

The most likely explanation is that an interneuron, either excited directly by the LG or the segmental giant through electrical synapses, makes synaptic contact at various points along the axon. Near the LG-MoG synapse, there is a small neuron with GABAergic vesicles that makes contact with both the MoG and LG, which are heavily intertwined through branching dendrites (Stirling, 1972; Leitch et al., 1990). Furthermore, while most afferent contact with the LG occurs in the dendrites, the LG axon has contact with cells containing vesicles with shape common to those containing GABA, which synapse onto the LG through openings in its glial sheath (Krasne & Stirling, 1972). Occasional, dispersed axonal connections to an inhibitory interneuron would result in a diffuse dIPSP, as is seen in my preparations. Inhibition which is present at many locations along the axon, but which is not due to a more general LG membrane or glial phenomenon, would also explain why picospritzer experiments similar to mine near the MoG synapse did not find any evidence that the LG is responsive to glutamate (Heitler et al., 2001).

When applied via bath, 5 mM GABA caused a number of effects. The size of the dIPSP, when measured at 3 ms, 5 ms, or 10 ms after stimulation, decreased after 5 minutes of treatment, suggesting a possible occlusion of receptors. This effect washed out, and the dIPSP size continued to increase over pretreatment levels at 3 ms and 5 ms. Despite this, there was no significant effect of treatment on either the LG membrane resistance or the baseline membrane potential.

In addition to GABA, glutamate can be an inhibitory neurotransmitter in crayfish, and mediates inhibitions in some portions of the LG circuit (Heitler et al., 2001). It was therefore important to repeat the experiments with glutamate, as it could also mediate the autoinhibition. While the application of 5 mM glutamate did not cause robust effects (though there was a brief reduction in the mean upon glutamate exposure), preparations sometimes became highly disinhibited upon washout when a stronger concentration of glutamate was used. The multiple spiking is probably due to an action potential circling around a portion of the LG's ladder-like structure (Kusano & Grundfest, 1965), and its occurrence in these experiments on inhibition suggests that one important purpose of the recurrent inhibition is to prevent the LG's structure from locking the animal in a flexed position. It is worth noting that stimulation in the superfusion experiment was direct; multiple spiking could not have been due to presynaptic responses in the system. If the double spikes seen after glutamate exposure are counted as singlets, then the spiking frequency is near the 250 Hz found when a circular current develops along two segments of the LG system (Kusano & Grundfest, 1965). Higher frequencies are possible; several spikes can occur at near 500 Hz in fully intact animals (Wine & Krasne, 1972), so even

counting doublets separately, this rate is not unheard of. This disinhibition is a plausible consequence of washing off a substance which induces inhibition. The fact that glutamate does not appear to have an effect, but its washout does, is surprising. It may be that the concentrations selected were too high. If this is the case, and the receptors are susceptible to desensitization, then it is possible that the high concentrations of glutamate ended up masking their own effects, leaving their receptors less responsive, and the system in a state of disinhibition. This effect may also be due to the nature of chronic exposure and the slow build up during superfusion. Any discernible signal will be preceded by a marginally weaker activation of the receptors as the concentration slowly increases. If the build up is sufficiently slow, then the desensitization brought about by this activation may be enough to disrupt the effect which would otherwise be seen. If the receptors were completely desensitized, however, it is difficult to see how washout would increase excitation. This suggests that perhaps multiple receptor subtypes are present. While some glutamate receptors do not desensitize easily, other desensitize rapidly and powerfully, an effect which may last for minutes (Cleland, 1996). It is possible that a portion of the receptors were agonized while others were desensitized, and that during washout, the inhibition was reduced more rapidly than the desensitization. Crayfish have GluCls which are not desensitized by GABA (Franke et al., 1986), so it is not surprising that this effect did not occur following 5 mM GABA administration.

While suggestive of an inhibitory effect of glutamate, the previous experiments involved slow application of inhibitors over many minutes. Additionally, the neurotransmitters were superfused evenly across the entire cord, making it impossible to

determine whether or not any effects were due to inputs on the dendrites or at some other neuronal location. To clarify the involvement of the neurotransmitters, as well as the locations at which they act, I ejected GABA and glutamate with a picospritzer. This protocol restricted their effects to a localized area on the axon and for a shorter time period. The results of these experiments were much clearer and more interesting. The local application of GABA to the desheathed axon of the LG induces inhibition in that area, whether measured absolutely or in relation to a control electrode nearer the dendrites. This effect ceases when the GABA is washed away, though there is sometimes a lingering reduction in sensitivity to GABA lasting for at least two minutes. The inhibition is visible as a depolarization following GABA ejection, resulting in a weakened PSP caused by sodium channel inactivation and increased potassium and chloride conductance (Edwards, 1990). Ejection of glutamate onto the desheathed LG causes the same effects. Importantly, application of picrotoxin appears to block the depolarization due to glutamate.

These effects show that there are inhibitory receptors along the axon of the lateral giant, not merely the dendrites and spike initiation zone, that these receptors respond to glutamate as well as GABA, and that those channels are permeable to chloride, as picrotoxin blocks them. Picrotoxin's effects were most pronounced at 100 μM and lower when the picrotoxin concentration was reduced. This is not surprising, as even in the earliest studies of GluCls, it was clear that, while concentrations near 1 mM could cause a nearly complete block of chloride conductance, picrotoxin became less effective even at the relatively high 100 μM concentration that I used (Franke et al., 1986). This could also

explain why the attenuation that occurred with 25 μM and 50 μM picrotoxin attenuation occurred during the end of exposure and beginning of washout, when the picrotoxin concentration was at its highest level.

In summary, I investigated the possibilities of non-synaptic release of glutamate, a locus of inhibition spread across the axon, and the involvement of glutamate as an inhibitor. It is clear that the LG reacts to both GABA and glutamate application via depolarization, and that this depolarization reduces the effect of excitatory inputs. This depolarization can be blocked by picrotoxin, consistent with the hypothesis that GluCls are behind this apparent inhibition. This all occurs along the axon itself, showing that these effects are not confined to the areas of the spike initiation zone or the ganglionic dendrites. Experiments in saline without calcium, together with other observations, suggest that the inhibition is likely due to synaptic release.

The ultimate source of the dIPSP still remains unknown. The results are not compatible with a mechanism solely involving transporter reversal. Imaging has thus far not been able to clearly identify the hypothesized neurons that are involved in the dIPSP, which is not surprising if the synapses are sparsely distributed. It is possible that sectioning along a sagittal or coronal axis would aid in this identification by allowing easier tracing of neurites. Due to the timing of the dIPSP, all synapses between the LG and the hypothesized inhibitory interneurons must be electrical. It should therefore also be possible to inject a dye into the LG and trace it to candidate neurons. Dye tracing of the LG is sometimes complicated by its rectifying synapses (Antonsen & Edwards, 2003), so the tracing will likely need to be combined with repeated stimulation of the LG

if the dye is charged. The ideal experiment to show the mechanism of the dIPSP would be to record from and stimulate the inhibitory neuron or neurons responsible, obtaining physiological evidence of their action, and perform a dye fill through the same electrode, anatomically characterizing the cells involved.

Though the mechanisms of inhibition suggested here are not as common as synaptic inhibition via GABA, they are paralleled in other organisms, including mammals. Axonal GABA receptors are present in mammals, and mammalian cells sometimes have chloride concentration gradients along their axons, leading to depolarization when exposed to GABA (reviewed by Trigo et al., 2008). As the axons of mammalian neurons are relatively small, making intracellular recordings from them more difficult, the LG neuron presents an appealing alternative model in which to study the details and mechanics of axonal receptors. Similarly, while GluCls are unique to invertebrates, they are similar to the glycine receptors present in mammals (Wolstenholme, 2012). Study of these glutamate receptors is therefore not merely of intellectual interest, but has practical benefits as well. The comparison between vertebrate and invertebrate systems provides a method by which light is shed on the proper functioning of both clades. Studying invertebrate inhibitory mechanisms will uncover basic functions that can advance research of mammalian systems in the long term.

5. Sensory-evoked inhibition

5.1. Background

The second focus of this dissertation is on the LG's sensory-evoked inhibition, which occurs shortly after an excitatory stimulus to the LG neuron, as well as its tonic inhibition. The circuitry of the excitatory inputs to the LG has been largely mapped out, and its immediate outputs to the motor systems are well-described. The sensory-evoked inhibitory input, however, comes from unidentified neurons which synapse on to (presumably GABAergic) receptors of unidentified subtype. Similarly, the receptors responsible for tonic inhibition have not been described. In this chapter, I attempt to fill in some of these gaps in the literature. Additionally, I will explore the interactions that alcohol has with these inhibitions of the LG.

The LG receives input from mechanosensory afferents and interneurons. Both connect to the LG via electrical synapses, and the afferents synapse onto the interneurons via cholinergic synapses (Herberholz et al., 2002; Zucker, 1972; Wine & Krasne, 1972; Miller et al., 1992). The PSP of the LG is made of three broad components, α, β, and γ **(**See **Figure 2.4)**. The α component is due to the electrical synapses made directly by the afferents. The early β component is due to excitatory input from the first-order interneurons. The later β component and the γ component are of mixed origin. There is substantial delayed inhibitory input in the late β component (Vu et al., 1997). This input aids in temporal filtering: stimuli which are slow will recruit sensory afferents over a

longer time span than quick stimuli, and the afferents which fire earlier will begin inhibiting the LG shortly after they are recruited. This sensory-evoked postexcitatory inhibition thus ensures that only rapid stimuli cause the LG to fire. However, this inhibition is poorly characterized, and it is only known that a GABAergic, picrotoxin-sensitive inhibition generates the latter part of the β component of the PSP, and that the inhibitory inputs are on the LG's dendrites (Vu et al., 1997). Here I will present work that furthers our understanding of this inhibition, utilizing alcohol and other modulators of GABA receptors.

Despite alcohol's status as one of the most destructive and economically damaging drugs worldwide, our understanding of its effects at the cellular level are limited. Crayfish are an ideal organism in which to study the effects of alcohol on individual cells, small circuits, and receptor/subtype distributions. The study of the effects of alcohol on the escape circuits of crayfish is therefore of broader interest than it would first appear. In order to truly understand the effects of alcohol, which affects many neurotransmitter systems in complex ways, the different neurotransmitters' contribution must be teased apart. The GABAergic system is an excellent starting point, as GABA receptors are strongly modulated by ethanol (EtOH) and represent a major target for its actions (Lobo & Harris, 2008; Santhakumar et al., 2007). Work on the interplay between alcohol and inhibition in the MG circuit of crayfish have given some insight (Swierzbinski & Herberholz, 2018), but a more thorough investigation in the more accessible LG neuron has not been performed.

Crayfish also provide insight into the interaction between social status, or social isolation, and EtOH consumption. It has been found that crayfish which have spent their time in communal tanks have differing responses to EtOH exposure, both behaviorally and physiologically, than animals which have been isolated for a period of one week (Swierzbinski et al. 2017). Crayfish have a longer latency to disinhibition after social isolation, measured as the first alcohol-induced tail-flip. This effect is paralleled on the level of single neurons: lower concentrations of EtOH were required to increase LG excitability in animals which were communally housed than in isolated ones, perhaps due to differences in descending tonic inhibition (Swierzbinski et al., 2017). The etiology of this difference is not known, but may have to do with receptor redistribution elicited by different social experiences.

The work presented here, on the GABAergic side of the LG circuit, will clarify the pharmacology of the sensory-evoked inhibition of the LG. I will examine the effects of several modulators on this post-excitatory inhibition. I will also examine agonists which may have activity on tonic inhibitory receptors. Together, the experiments performed on the autoinhibition and the experiments presented in this chapter improve our knowledge about three separate types of inhibition, all of which affect the LG neuron. Moreover, they help clarify the effects that social status has on $GABA_A$ receptor distributions. Finally, this work will guide a more detailed analysis of the effects of EtOH on other neurotransmitter systems.

I will use picrotoxin, which non-competitively blocks currents at chloride channels, and muscimol, which is an agonist at $GABA_A$ receptors, to explore the sensory-

evoked inhibition of the LG, and I will measure how social experience modulates their effects. Muscimol has been used previously to study crayfish escape circuits. Swierzbinski and Herberholz (2018) found that exposure to muscimol did not appreciably change the PSP of the MG neuron. However, when muscimol was followed with saline in an attempt to wash out its effects, the MG's PSP was dramatically reduced. Conversely, exposure to EtOH increased the PSP. Most interestingly, preexposure to muscimol prevented this EtOH-induced increase in MG excitability. These effects were explained by positing $GABA_A$-ρ receptor activity. Muscimol is a partial agonist to these receptors, so it could be competing with endogenous GABA, resulting in little effect when applied to the crayfish preparation. Since muscimol's effects on this receptor subtype are weaker than those of GABA, washout would likely cause inhibition. Additionally, these receptors are different from most other GABA receptors in that EtOH can act on them as an inhibitor, increasing net excitation, an effect that muscimol might reduce by competition. Altogether, this hypothesis explains the data seen in the MG neuron, suggesting the possible presence of receptors similar to mammalian $GABA_A$-ρ receptor in the crayfish. No experiments directly targeting these receptors have been performed in the LG, so I decided to use a $GABA_A$-ρ receptor antagonist in an attempt to identify their possible existence in the crayfish nervous system. I selected TPMPA as an antagonist for these receptors, due to its availability and relatively high selectivity when used at lower concentrations (Ragozzino et al., 1996).

As with the other forms of inhibition, the receptors underlying tonic inhibition have not been identified. Tonic inhibition has to be dendritic (Vu & Krasne, 1992; Vu &

Krasne, 1993; Vu et al., 1993), so that it can be overridden by sufficient excitation when situations warrant escape (Lee & Krasne, 1993), but beyond this basic characterization, little is known about the mechanisms. One receptor candidate is the aforementioned $GABA_A$-ρ receptor. $GABA_A$-ρ receptors are found in the vertebrate CNS, with a high expression at some synapses in the retina, and are slowly desensitizing, which probably allows them to modulate activity over longer periods of time (reviewed by Zhang et al., 2001). This quality would be useful when modulating either tonic or sensory-evoked inhibition, as it would prevent continuous stimuli from desensitizing the receptors and thereby disinhibiting the circuit. Another receptor candidate is the $GABA_A$-δ receptor. These receptors often mediate tonic inhibition in mammals. They are extrasynaptic, and respond strongly to low concentrations of GABA, making them an ideal mediator of this type of inhibition. As with $GABA_A$-ρ receptors, I decided to test the presence of $GABA_A$-δ receptors in the LG circuit. To probe the possible role of these receptors, I selected the agonist THIP (also known as Gaboxadol), which has strong activity at receptors with δ subunits (Stórustovu & Ebert, 2006).

Additionally, it appears that $GABA_A$-δ receptors are particularly sensitive to EtOH (Santhakumar et al., 2007), suggesting a possible mechanism for the social modulation of EtOH's effects previously reported in crayfish (Swierzbinski et al., 2017). As discussed earlier, the firing threshold of the LG is modulated via tonic inhibition (Vu & Krasne, 1992; Vu & Krasne, 1993; Vu et al., 1993), and this inhibition appears to be modulated by social status (Swierzbinski et al., 2017). Descending tonic inhibition is absent in the preparations used in my research, leaving the receptors which mediate it

free to bind any ligands. My experiments will investigate the possibility that GABA receptors which are similar to the mammalian receptors containing ρ or δ subunits are present in crayfish, and may be distributed differently in animals with different social experiences. This work will thus aid in our understanding of the less studied subtleties of inhibition in the LG, as well as help build a framework in which to study the intersection of social experience, inhibition, and alcohol in a variety of animal systems.

5.2. Research questions

The combination of two socialization statuses (communal and isolate) and five drug conditions (saline, picrotoxin, muscimol, TPMPA, and THIP) used in this chapter creates a large number of groups and interactions for analysis. It is important to formulate specific questions so that there is a common framework in which the large quantity of data are interpreted. My experiments attempt to answer the following questions:

- How does each drug affect the LG neuron in an isolated nerve cord?
- What are the interactions between each drug and EtOH?
- Are the effects of each drug, or their interaction with EtOH, modulated by the social experience of the animal?

5.3. Methods

5.3.1. Drugs

200 mM solutions of EtOH, 25 μM solutions of picrotoxin, 25 μM solutions of muscimol, 10 μM solutions of methyl(1,2,3,6-tetrahydropyridin-4-yl)phosphinic acid (TPMPA), and 10 μM solutions of 4,5,6,7-tetrahydroisoxazolo(5,4-c)pyridin-3-ol (THIP) were used for alcohol pharmacology. The concentration of alcohol was increased from that used by Swierzbinski et al. (2017) in juvenile crayfish after initial testing showed that adult nerve cords are less responsive to EtOH than those of juveniles. This difference is reflected in behavior, as juvenile crayfish are more sensitive to the effects of EtOH than adults (Herberholz lab, unpublished results). The concentration selected here corresponds roughly to the EtOH levels seen in the hemolymph of adult crayfish following an hour of EtOH exposure (Herberholz lab, unpublished results).

The picrotoxin concentration selected was between that used by Roberts (1968) and Vu et al. (1997). This concentration, as well as the selected concentration for muscimol, was used by Swierzbinski and Herberholz to study alcohol effects in the MG circuit (2018), so using the same concentration will facilitate comparisons between the two crayfish escape systems. The concentration of TPMPA was selected to modulate $GABA_A$ receptors containing the ρ subunit without appreciable effects on other subtypes (Ragozzino et al., 1996), and the concentration of THIP was selected to activate δ subunit-containing $GABA_A$ receptors without activation of other subtypes (Stórustovu & Ebert, 2006).

5.3.2. Procedure

An extracellular hook electrode was placed on the lateral nerve roots of A6 to stimulate sensory afferents, and a 90 second inter-stimulus intervals was used, to avoid habituation **(Figure 5.1)**. An intracellular electrode was placed in the LG, as close as possible to A6. Extracellular stimulation voltage was adjusted until the LG's firing threshold was found to within 0.2 V. The voltage was then reduced to 75% of the threshold voltage, rounded to the nearest 0.2 V. If the stimulation could not induce spikes, even at its maximum of 15 V, the point at which the intracellularly recorded EPSPs no longer increased with increasing stimulation voltage was selected for stimulation instead.

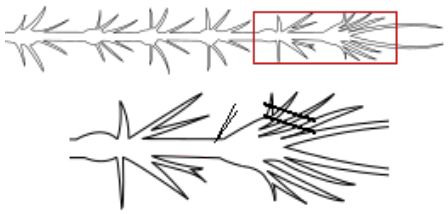

Figure 5.1. Experimental setup for superfusion experiments involving EtOH. Inset is a zoomed view of the ventral nerve cord between A5 and A6. The thick black lines represent the extracellular stimulating electrode on the sensory nerves. The thin pinpoint represents the intracellular electrode. Nerve cord image is adapted from Huxley, 1879.

The periods chosen for analysis were 3 ms, 5 ms, and 10 ms. These correspond to the early β component, off of which the action potentials rises **(Figure 5.2)**, the approximate peak of the β component, and a late phase of the β component, when post-excitatory inhibition is quite strong (Krasne, 1969; Vu et al., 1997). Due to the natural variation in the timing and strength of the later parts of the β component, the peak does

not always occur at 5 ms, and there is some variability in the shape of the later PSP. The early β component is due to a monosynaptic pathway, and is relatively similar across preparations.

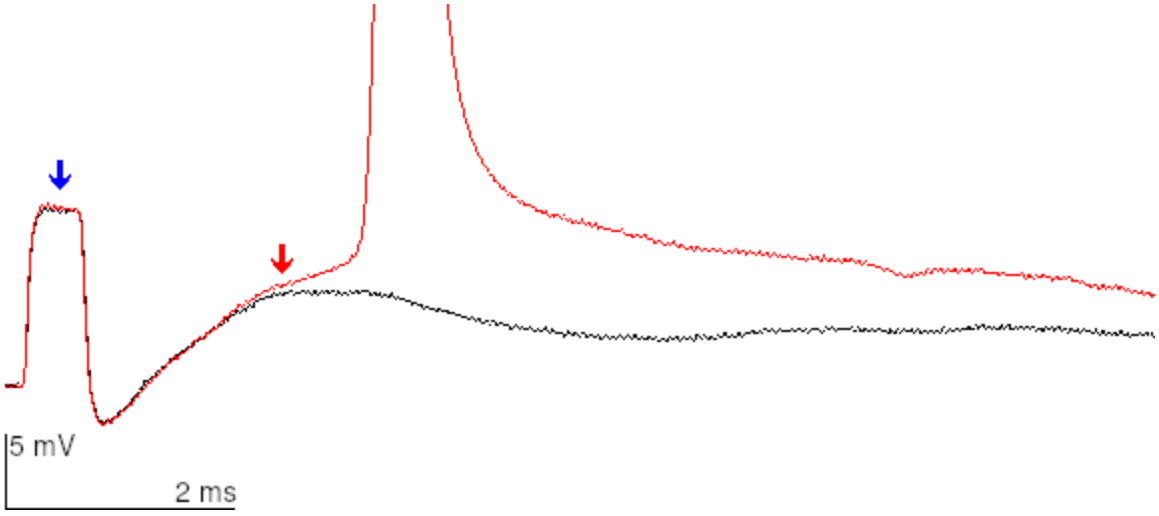

Figure 5.2. Truncated LG action potential (red), compared to subthreshold PSP (black). The black recording was taken during saline superfusion, and the red recording was taken after nine minutes of EtOH superfusion, using the same stimulus voltage. The red arrow marks 2.5 ms, and the blue arrow marks the stimulus artifact. This image is typical of an action potential in the LG, which generally occurs 2-3 ms after a superthreshold stimulus.

5.3.3. Data analysis

Occasionally, strong (~10 mV) 60 Hz (or harmonics of 60 Hz) electrical noise was present in recordings, usually only for several traces. Any experimental traces contaminated by this noise were removed from analysis. Experiments consisted of four phases, including the pretreatment baseline. The pretreatment phase consisted of fifteen minutes of saline superfusion, and was used to ensure the preparation was stable. Preparations were considered stable if they had at least eight pretreatment measurements where the average PSP size (measured intracellularly, near A6) was at least 0.8 mV at 3

ms, 5 ms, and 10 ms post-stimulus, the coefficient of variation for each of these time points was less than 0.2, and they generated no action potentials. Pretreatment was followed by thirty minutes of superfusion of the pharmacological treatment or saline control ("drug phase"), then thirty minutes of EtOH superfusion ("EtOH phase"). Finally, saline was superfused for thirty minutes in an attempt to bring the preparation back to its pretreatment state ("washout phase"). For each phase, the value used for analysis was the average PSP size of the final three trials of that phase. As noted in previous chapters, superfusion involves a replacement of the bath solution over time, leading to a slow increase in drug concentration. As only the final recordings of each phase were used, however, the solute concentration in the bath is near the concentration of the prepared solution in the data presented here.

If a spike occurred before the time point chosen for measurement, the recorded value was changed to 120% of the maximum value seen in that preparation at that time point, a procedure previously used by Teshiba et al (2001). The extremely high likelihood of action potential generation in preparations treated with picrotoxin presented a problem for this type of analysis. Nearly every preparation generated action potentials in the alcohol, and spiking continued in washout phases. The quantification method used on other preparations (replacing spike-contaminated values with 120% of the maximum PSP seen previously in the preparation) may have resulted in an arbitrary value based on how much a cell depolarized without spiking in the traces preceding the spikes. Consequently, an analysis on picrotoxin experiments (and saline controls) was also performed on the cumulative number of spikes that had occurred by the end of each phase. If more than

one spike occurred during a trial, which was usually the case, each spike was counted as a separate event. Statistics were performed using nonparametric tests after removing preparations which were missing data from any phase.

I used a linear mixed model, with phase, drug, and socialization (and their interactions) as fixed factors and subject as a random intercept, to analyze PSP data. A restricted maximum likelihood estimation was used. Effect size confidence intervals were generated using a profile likelihood ratio. Within-group descriptive graphs use sample means and standard deviations. Main effects were analyzed by a similar model without socialization as a factor. As crayfish readily form dominance hierarchies to determine access to future resources (Bovbjerg, 1953; Graham & Herberholz, 2009; Herberholz et al., 2001; Herberholz et al., 2016; Herberholz et al., 2007), preparations from communal tanks likely came from animals of varying social status. Because this possible confound of social dominance is not present in isolates, the isolate saline group was chosen as the reference condition for statistical analyses.

Because there is no widely agreed upon definition of degrees of freedom in a mixed model, calculations for p values are not well defined. Satterthwaite's degrees of freedom approximation was used when estimating p values, and used in a two-tailed t-test. Unadjusted p values are given here for several reasons:

1) While the questions that this chapter attempts to answer can all be viewed under the broad umbrella of inhibition, the individual treatments each ask different questions, as each of the selected drugs has a distinct pharmacological profile.

2) While the possibility of a false-positive is of concern, so is the possibility of a false-negative. The research presented here includes a large exploratory component. For these questions, false-positive effects (e.g., THIP spuriously appearing to cause inhibition) will likely be rapidly corrected on any attempted follow-up, while false-negatives will dissuade further research, which may be exceptionally damaging given the relatively small size of the field.
3) It is more difficult to detect interactions than main effects with models of the type used here (Leon & Heo, 2009), and adjusting the p values to be more conservative would make this even more difficult. The best solution would be to increase sample sizes, but this is not a trivial task in electrophysiological research.

P values are interpreted as continuous measures of evidence for a hypothesis. P = 0.1 was used as a hard cutoff for interpretation of evidence for a hypothesis. For the purposes of this dissertation, values between 0.1 and 0.05 are considered very weak evidence, and values between 0.05 and 0.01 as some evidence. Interpretations are made in light of related evidence (e.g., other measures of the effect of a drug). Values are rounded to three decimal points; number smaller than 0.001 are given in scientific notation.

Skewness and kurtosis of model residuals was analyzed to assess deviations from normality. Residuals showed slight skewness at five milliseconds, and negligible skewness at other time points (3 ms: -0.18; 5 ms: 0.42; 10 ms: 0.05). Contrastingly, residuals showed a very high degree of kurtosis at early time points, as well as a

relatively high degree of kurtosis at ten milliseconds (3 ms: 2.71; 5 ms: 2.47; 10 ms: 1.66). However, when analyzing repeated measures or interaction effects at higher sample sizes, linear mixed models are fairly robust to both moderate skewness and extremely high kurtosis (Arnau et al., 2013).

Descriptive statistics for each group will be given first, describing the general trend of the data, followed by statistical analysis of the possible effects of interest. P values for main effects were calculated as compared to the previous phase, giving an estimate of the effect of the drug of interest, the interaction of that drug with EtOH, and the efficacy of washout. Additionally, p values were calculated for the difference between EtOH phase and pretreatment baseline, as an ambiguous drug effect and a weak interaction effect may combine to cause a clear difference from the effect seen from EtOH in controls. As the effects of combining alcohol with other drugs is a human health concern, the existence of a combined effect compared to that of EtOH exposure alone might be of interest. In order to more intuitively show the meaning of data, graphical display and model analysis of drug main effects will present effect estimates and confidence intervals which are adjusted to reflect their distance from zero, rather than from the reference condition. P value brackets will be solid when comparing within the saline group, and dashed when comparing between groups. In general, graphs of raw data display the sample mean and standard deviation, while graphs of models will display point estimates and 95% confidence intervals. In the spike analysis, bars representing standard deviations were truncated to remove negative values.

One of the benefits of a linear mixed model is the ability to include data from individuals which are missing some measurements. This results in a large number of separate sample sizes, as each phase may have a different number of samples, even within treatment/social groups. The range of samples (i.e., animals) in the following experiments was between 8 and 14, though the majority were 10 or 11. For ease of reading, rather than interspersing sample sizes throughout the text, a table containing sample sizes is included in the appendix. Sample sizes are presented in the spike analyses, as the removal of preparations which are missing data from any phase was necessary to use the statistical methods chosen. Additionally, due to space and clarity concerns, when raw data is plotted, only means and standard deviations are shown. Graphs including individual data points are presented in the appendix.

5.4. Results

5.4.1. Saline - control

Saline was superfused over isolate and communal preparations, followed by EtOH and a saline washout **(Figure 5.3).** While controls did occasionally undergo spiking, it was rare enough that no clear difference between phases was found in either **isolate** *(N = 10; Friedman: p = 0.392)* or **communal** preparations *(N = 11; Friedman: p = 0.050; pretreatment (0, SD = 0 spikes) to saline phase (0.6, SD = 1.8 spikes) Wilcoxon: p = 0.18; saline to EtOH phase (3.0, SD = 6.3 spikes) Wilcoxon: p = 0.109; EtOH to washout phase (1.0, SD = 2.4 spikes) Wilcoxon: p = 0.109).*

At **3 ms**, an increase in mean PSP following both saline and EtOH treatment was observed, and a decrease in washout, for both isolates and communals **(Table 5.1)**. The instability of PSPs during saline exposure has been seen before (Swierzbinski et al., 2017), though this is the first evidence of the isolated abdominal nerve cord undergoing facilitation. The same pattern seen at 3 ms was observed at both **5 ms** and **10 ms**, for both isolates and communals.

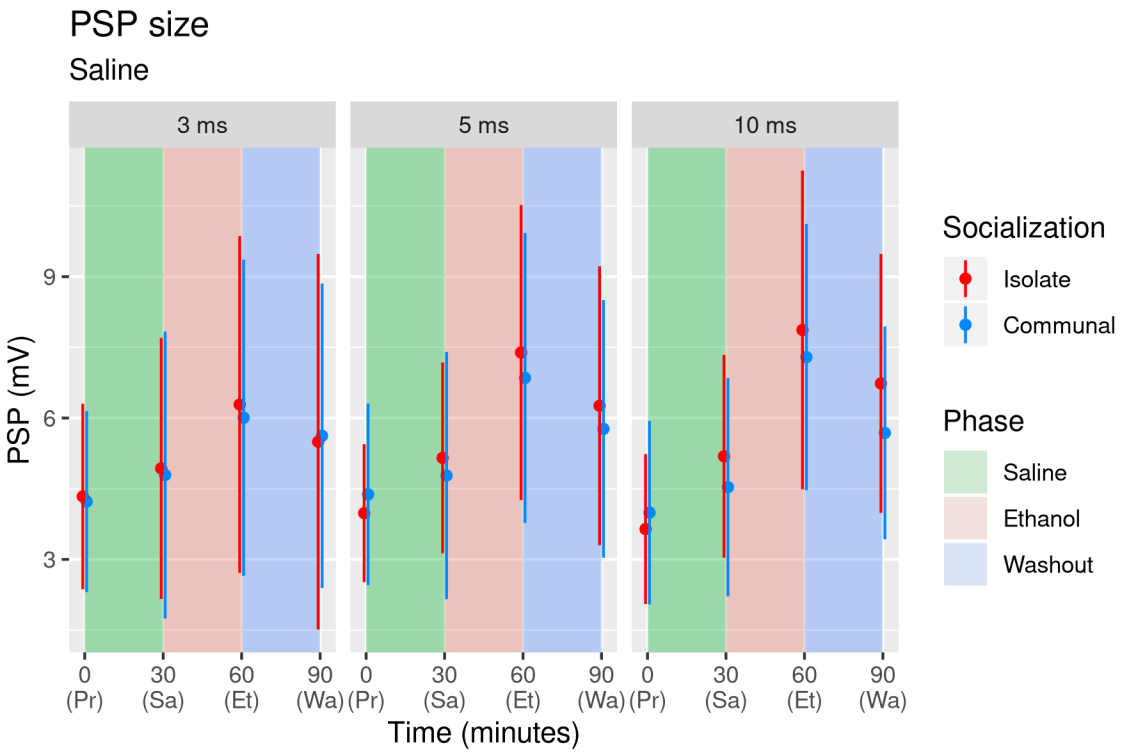

Figure 5.3. PSP size at the end of each phase for saline preparations. Both groups experience the same general trend of increasing LG PSP sizes during ethanol exposure, and a decrease during washout at all three time points. At 5 ms and 10 ms, there was a slight increase in PSP size during saline exposure. Colored circles are means, and lines are means ± one standard deviation. The x-axis is color-coded based on the solution being superfused at each time. Time points correspond to the end of pretreatment (Pr), saline (Sa), EtOH (Et), and washout (Wa).

Table 5.1. Descriptive data for saline condition. All units are millivolts.

Condition			3 ms		5 ms		10 ms	
Drug	Socialization	Phase	Mean	SD	Mean	SD	Mean	SD
Saline	Isolate	Pretreatment	4.34	1.97	3.98	1.46	3.64	1.59
Saline	Isolate	Drug	4.93	2.77	5.15	2.02	5.19	2.15
Saline	Isolate	Ethanol	6.29	3.57	7.39	3.13	7.87	3.38
Saline	Isolate	Washout	5.50	3.98	6.26	2.96	6.73	2.75
Saline	Communal	Pretreatment	4.23	1.92	4.38	1.93	3.99	1.95
Saline	Communal	Drug	4.79	3.04	4.78	2.62	4.53	2.32
Saline	Communal	Ethanol	6.01	3.35	6.85	3.08	7.29	2.83
Saline	Communal	Washout	5.62	3.23	5.77	2.73	5.68	2.26

Main effects were studied by aggregating data for both socialization **(Figure 5.4, Table 5.2).** At **3 ms**, there was weak evidence for a potentiating effect of saline, and strong evidence for a potentiating effect of EtOH, which was not substantially reduced by washout. At **5 ms**, both saline and EtOH appeared to facilitate the PSP size, and there was an attenuation during the washout phase. At **10 ms** these effects were heightened further. Saline and EtOH combined to clearly increase PSP, relative to pretreatment levels, at all time points *(3 ms: p = 1e-8; 5 ms: p = 1e-13; 10 ms: p = 1e-19).*

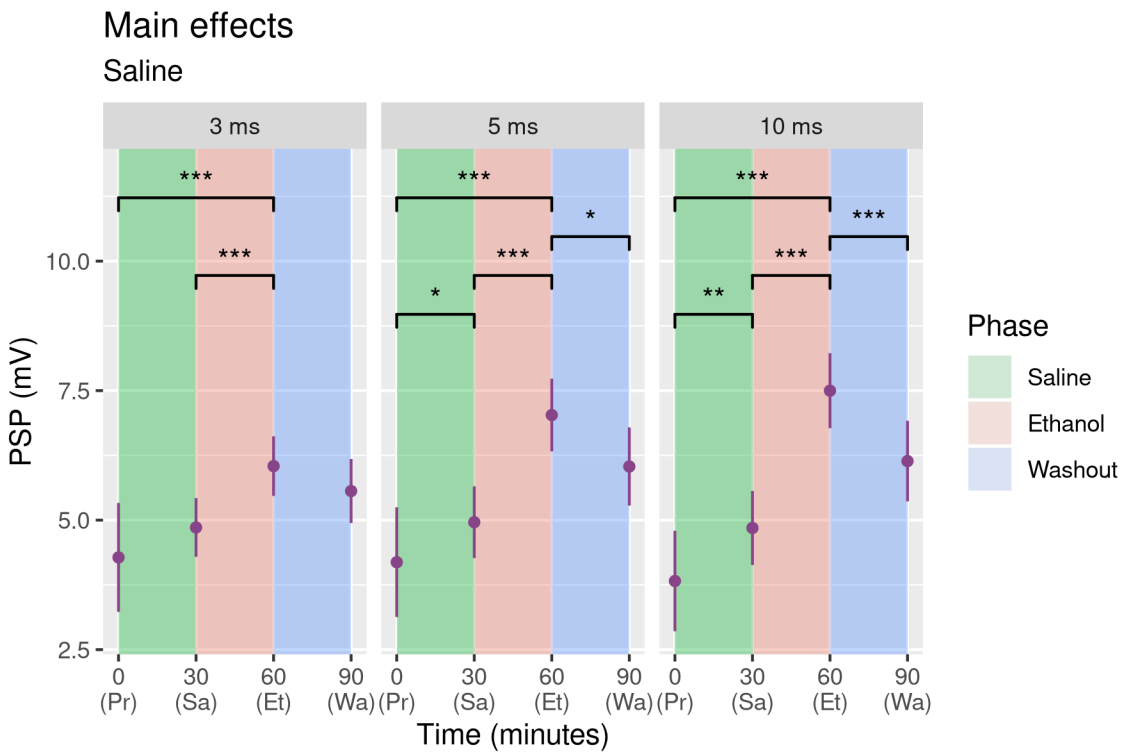

Figure 5.4. The effects of EtOH, aggregated over both social groups. The response to EtOH appears to be stronger in the late PSP, relative to the early PSP. Colored circles are point estimates, and lines are 95% confidence intervals. The x-axis is color-coded based on the solution being superfused at each time. Time points correspond to the end of pretreatment (Pr), saline (Sa), EtOH (Et), and washout (Wa).

Table 5.2. Main effects for saline condition. Estimate and 95% confidence interval are in millivolts. P values are calculated between a given phase and the preceding one.

Condition			Statistic		
Drug	Phase	Time	Estimate	95% CI	P-value
Saline	Pretreatment	3 ms	4.28	[3.23, 5.33]	
Saline	Drug	3 ms	4.86	[4.29, 5.43]	0.051
Saline	Ethanol	3 ms	6.04	[5.47, 6.62]	**1e-04**
Saline	Washout	3 ms	5.56	[4.94, 6.18]	0.138
Saline	Pretreatment	5 ms	4.19	[3.13, 5.25]	
Saline	Drug	5 ms	4.96	[4.27, 5.65]	**0.033**
Saline	Ethanol	5 ms	7.03	[6.33, 7.73]	**4e-08**
Saline	Washout	5 ms	6.04	[5.28, 6.79]	**0.012**
Saline	Pretreatment	10 ms	3.82	[2.85, 4.79]	
Saline	Drug	10 ms	4.85	[4.13, 5.56]	**0.006**
Saline	Ethanol	10 ms	7.50	[6.78, 8.22]	**1e-11**
Saline	Washout	10 ms	6.14	[5.36, 6.92]	**0.001**

The interaction between socialization and phase was studied for the saline group **(Figure 5.5, Table 5.3).** I found no evidence for a difference in responses to **saline** based on social status at any time point, nor for a difference in response to **EtOH**. I did, however, find some evidence that **washout** differed between social groups at 5 ms and 10 ms, with communals experiencing a stronger attenuation.

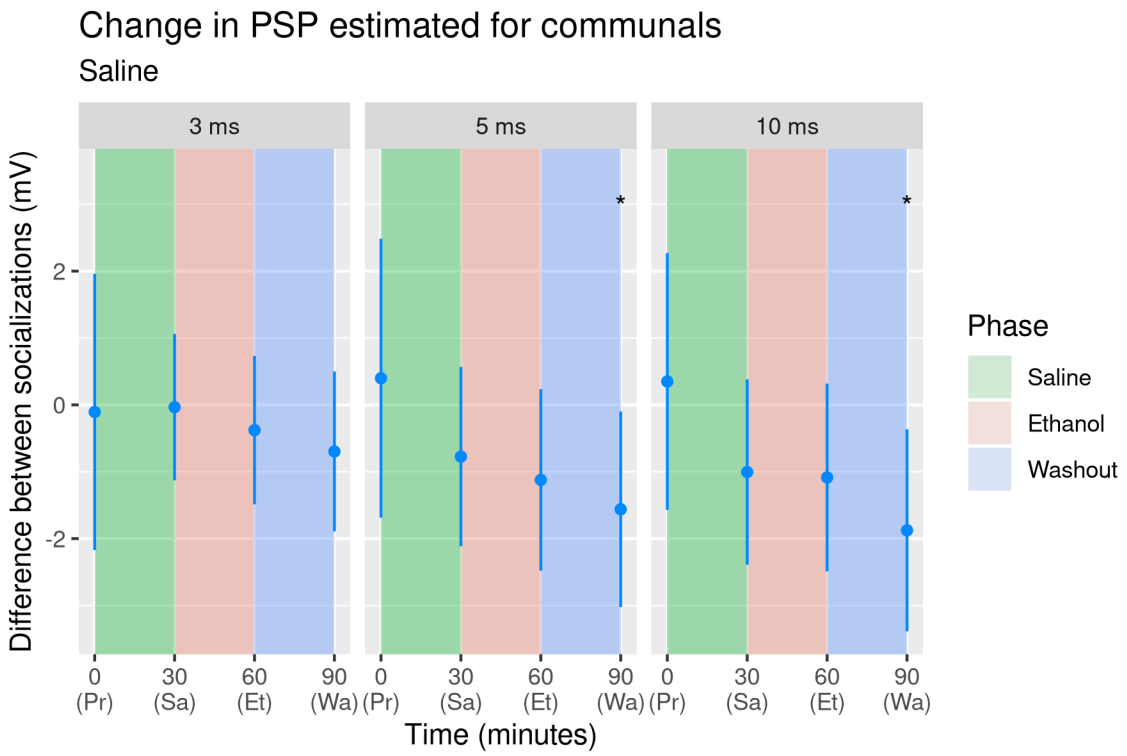

Figure 5.5. PSP difference observed between communals and isolates. The circles represent point estimates of the effect that communalization has during saline exposure, controlling for the main effects of saline exposure and phase. Lines are 95% confidence intervals. The x-axis is color-coded based on the solution being superfused at each time. Time points correspond to the end of pretreatment (Pr), Saline (Sa), EtOH (Et), and washout (Wa). The washout attenuation of EtOH's effect was stronger in communals.

Table 5.3. Social effects for saline condition. Estimate and 95% confidence interval are in millivolts, and represent the difference in PSP magnitude caused by communalization when controlling for all other factors.

Condition			Statistic		
Drug	Phase	Time	Estimate	95% CI	P-value
Saline	Drug	3 ms	-0.03	[-1.13, 1.06]	0.954
Saline	Ethanol	3 ms	-0.38	[-1.49, 0.73]	0.525
Saline	Washout	3 ms	-0.70	[-1.89, 0.50]	0.277
Saline	Drug	5 ms	-0.77	[-2.11, 0.57]	0.281
Saline	Ethanol	5 ms	-1.12	[-2.48, 0.24]	0.123
Saline	Washout	5 ms	-1.56	[-3.02, -0.10]	**0.047**
Saline	Drug	10 ms	-1.00	[-2.39, 0.38]	0.176
Saline	Ethanol	10 ms	-1.09	[-2.49, 0.32]	0.149
Saline	Washout	10 ms	-1.88	[-3.39, -0.37]	**0.021**

Overall, EtOH exposure increased LG PSP size at all time points in the isolated nerve cord. EtOH's effect did not appear to interact with social status, though there was a difference in washout between communal and isolates at 5 ms and 10 ms. This lack of interaction between social experiences and EtOH could be due to the absence of tonic inhibition in these experiments with isolated nerve cords (see discussion). Saline exposure alone also caused a mild facilitation of the PSP.

5.4.2. Picrotoxin - $GABA_A$ antagonist/EtOH interaction

To investigate the presence of local inhibition on the LG neuron (and its possible modulation by social status), I used the general $GABA_A$ antagonist picrotoxin, at a concentration of 25 μM**.** Picrotoxin is a potent chloride channel blocker, so if there is inhibition present in the LG PSP, it should be visible as an increase in PSP size or an increase in spike generation after picrotoxin exposure.

Picrotoxin exposed preparations responded to picrotoxin and EtOH exposure with spiking for both **isolate** *(N = 10; Friedman: p = 0.0003; pretreatment (0, SD = 0) to drug phase (4.4, SD = 6.7) Wilcoxon: p = 0.043; drug to EtOH phase (56.2, SD = 41.3) Wilcoxon: p = 0.012; EtOH to washout phase (30.9, SD = 34.1) Wilcoxon: p = 0.050)* and **communal** animals *(N = 10; Friedman: p = 0.00001; pretreatment (0, SD = 0) to drug phase (3.4, SD = 6.3) Wilcoxon: p = 0.043; drug to EtOH phase (83.6, SD = 49.7) Wilcoxon: p = 0.008; EtOH to washout phase (22.4, SD = 21.7) Wilcoxon: p = 0.008)* **(Figure 5.6)**. In both socializations, picrotoxin evoked some spiking, and EtOH caused a

clear and dramatic increase in the number of spikes. In both cases, this effect appears reversible, though in isolates the evidence for effective washout is weaker.

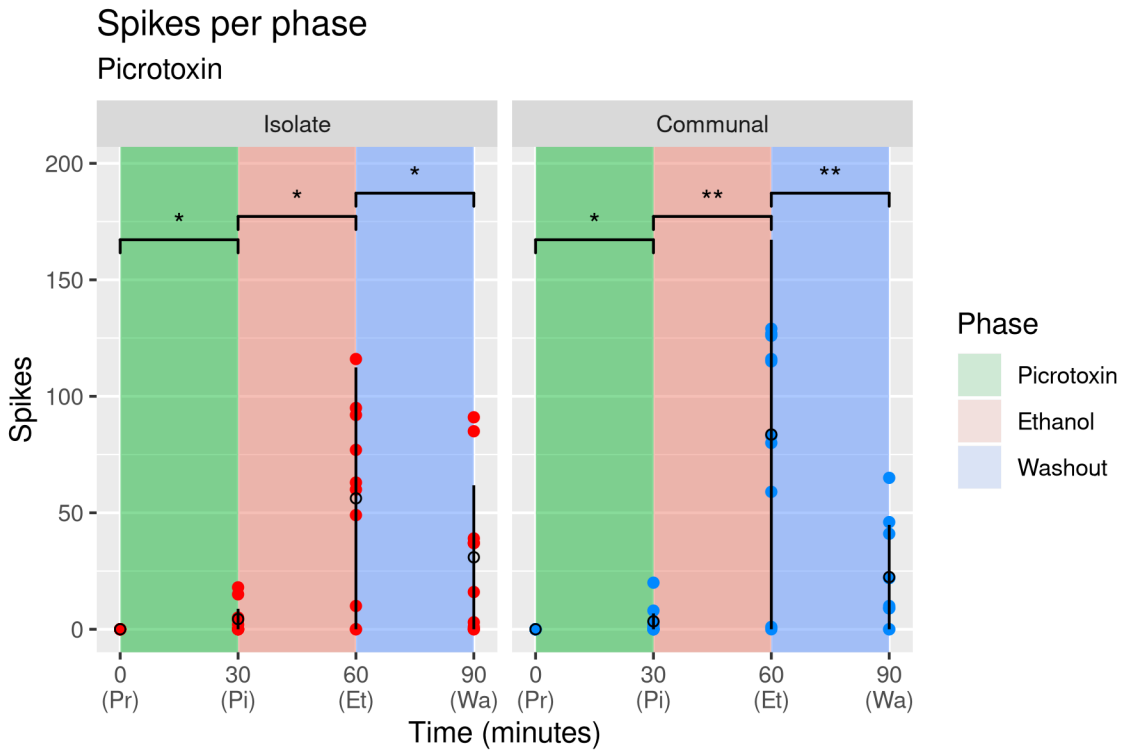

Figure 5.6. Spikes in each phase for picrotoxin exposed preparations. Filled points are individual preparations, and hollow circles and black lines are means ± one standard deviation, trimmed at zero. The x-axis is color-coded based on the solution being superfused at each time. Time points correspond to the end of pretreatment (Pr), picrotoxin (Pi), EtOH (Et), and washout (Wa). Picrotoxin caused an increase in the number of spikes. EtOH exposure following picrotoxin caused a dramatic increase in spike numbers. This was partially reversed during washout.

It is possible that most spikes occurred at the very beginning of each phase, in which case the effect could be primarily due to the previous treatment (e.g., EtOH's spikes may occur primarily in the first few trials, when there is a low EtOH concentration but still a substantial picrotoxin concentration). In order to rule this out, the analysis was repeated using only the spikes that occurred on the final trial of each phase **(Figure 5.7)**. This procedure did not appreciably change the analysis in **isolates** *(Friedman: $p = 0.003$;*

pretreatment (0, SD = 0 spikes) to drug phase (0.9, SD = 1.2 spikes) Wilcoxon: p = 0.060; drug to EtOH phase (3, SD = 2.4 spikes) Wilcoxon: p = 0.027; EtOH to washout phase (0.7, SD = 1.5 spikes) Wilcoxon: p = 0.027) nor **communals** *(Friedman: p = 0.0002; pretreatment (0, SD = 0 spikes) to drug phase (1.2, SD = 1.7 spikes) Wilcoxon: p = 0.042; drug to EtOH phase (4.2, SD = 2.7 spikes) Wilcoxon: p = 0.027; EtOH to washout phase (0.3, SD = 0.5 spikes) Wilcoxon: p = 0.011)*, though when using this measure, the evidence for picrotoxin's effect on spiking in isolates was weaker.

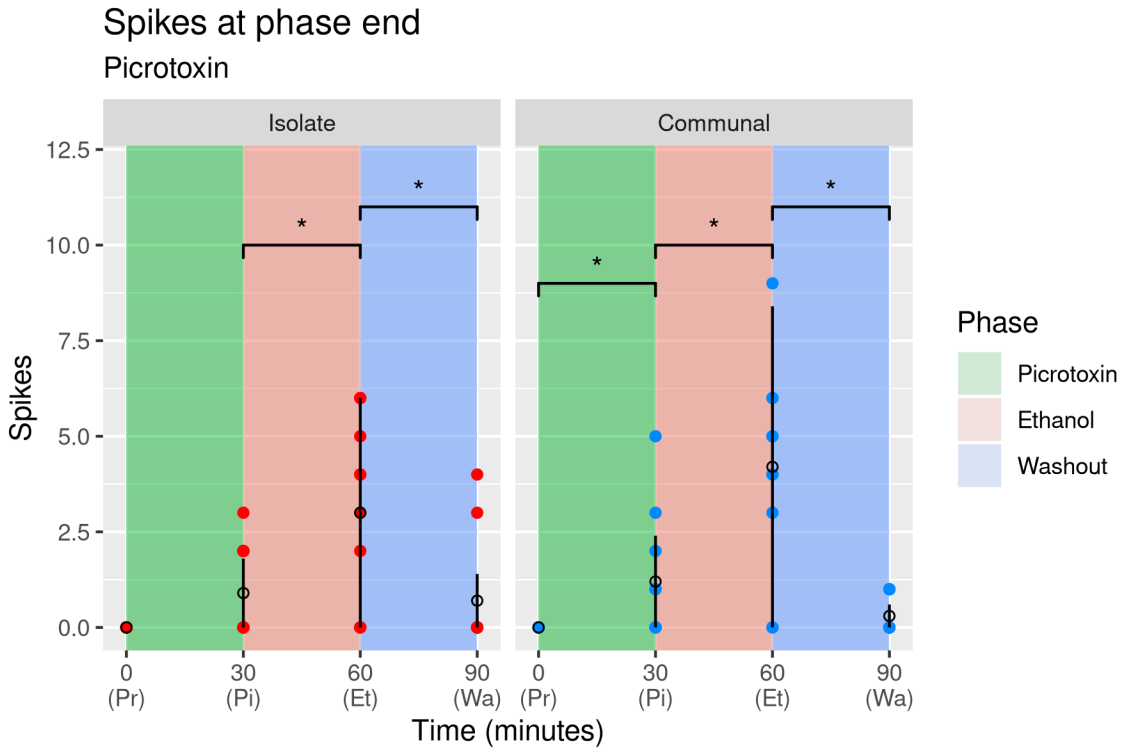

Figure 5.7. Spikes in the final trial of each phase for picrotoxin exposed preparations. Filled points are individual preparations, and hollow circles and black lines are means ± one standard deviation, trimmed at zero. The x-axis is color-coded based on the solution being superfused at each time. Time points correspond to the end of pretreatment (Pr), picrotoxin (Pi), EtOH (Et), and washout (Wa). Picrotoxin caused an increase in the number of spikes in communals, though the effect was less clear in isolates. EtOH caused an increase in spike number in both cases, which washed out. Despite the high variance of EtOH's effects in communals, washout was largely complete in all preparations, while in isolates several preparations showed a resistance to washout.

In summary, while some preparations spiked following saline exposure, this was rare, especially in isolates. Picrotoxin caused a similar increase in spike number in animals of both socializations, and this effect was greatly magnified by EtOH exposure. While this reversed following thirty minutes of saline superfusion in both cases, several isolate preparations maintained a relatively high spiking rate even late in washout.

PSP data was also analyzed following picrotoxin exposure. When measured at **3 ms (Figure 5.8, Table 5.4)**, picrotoxin caused no clear effect on isolates' PSP sizes. Picrotoxin caused a mean increase in excitation in communals, but alcohol did not further this effect, nor did it wash out.

At **5 ms**, there was a large variance in isolates that made responses unclear in any phase, though the trend was an increase in PSP during picrotoxin and EtOH and a facilitation during washout. Communals experienced a similar trend, but had far less variance. As in saline, the trend seen at 5 ms was also present at **10 ms**, but sharper in both isolates and communals.

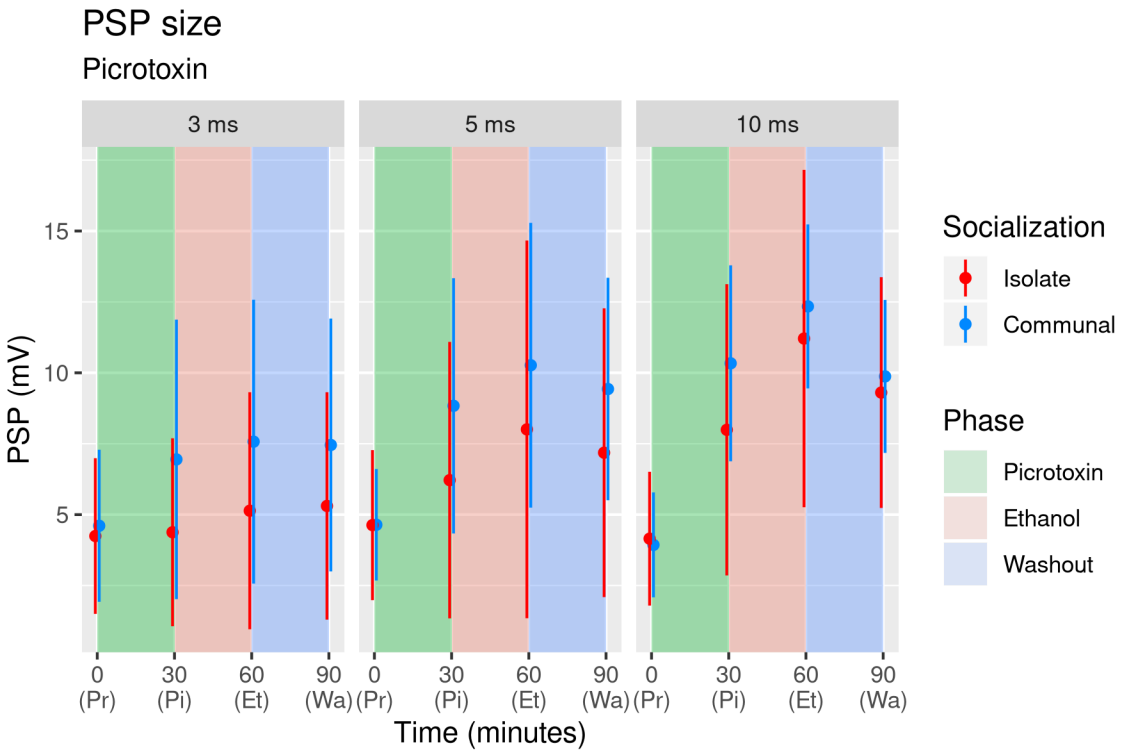

Figure 5.8. LG PSP values at the end of each phase for picrotoxin exposed preparations. Colored circles are means, and lines are means ± one standard deviation. The x-axis is color-coded based on the solution being superfused at each time. Time points correspond to the end of pretreatment (Pr), picrotoxin (Pi), EtOH (Et), and washout (Wa). Picrotoxin caused excitation in communals, an effect which remained present throughout EtOH exposure and washout. In isolates, there was no strong effect at early time points, though there were similar trends when compared to communals. Picrotoxin had a stronger effect on the late PSP.

Table 5.4. Descriptive data for picrotoxin condition. All units are millivolts.

Condition			3 ms		5 ms		10 ms	
Drug	Socialization	Phase	Mean	SD	Mean	SD	Mean	SD
Picrotoxin	Isolate	Pretreatment	4.24	2.74	4.63	2.64	4.15	2.36
Picrotoxin	Isolate	Drug	4.38	3.31	6.22	4.87	7.99	5.13
Picrotoxin	Isolate	Ethanol	5.14	4.18	8.01	6.66	11.21	5.95
Picrotoxin	Isolate	Washout	5.31	4.01	7.18	5.09	9.30	4.07
Picrotoxin	Communal	Pretreatment	4.61	2.68	4.64	1.96	3.93	1.85
Picrotoxin	Communal	Drug	6.95	4.93	8.84	4.50	10.34	3.45
Picrotoxin	Communal	Ethanol	7.57	5.00	10.27	5.02	12.34	2.89
Picrotoxin	Communal	Washout	7.46	4.46	9.43	3.92	9.87	2.70

The general effects (i.e., communals and isolates combined) of picrotoxin on LG PSPs were analyzed **(Figure 5.9, Table 5.5).** Picrotoxin exposure did not have a clear effect during any phase at **3 ms**. Picrotoxin exposure did increase PSP sizes at **5 ms**, but not during EtOH exposure or washout. At **10 ms**, the same pattern was discovered. Picrotoxin exposure and EtOH together was strong at 5 and 10, but not at 3 ms *(3 ms: p = 0.716; 5 ms: p = 0.003; 10 ms: p = 1e-11).*

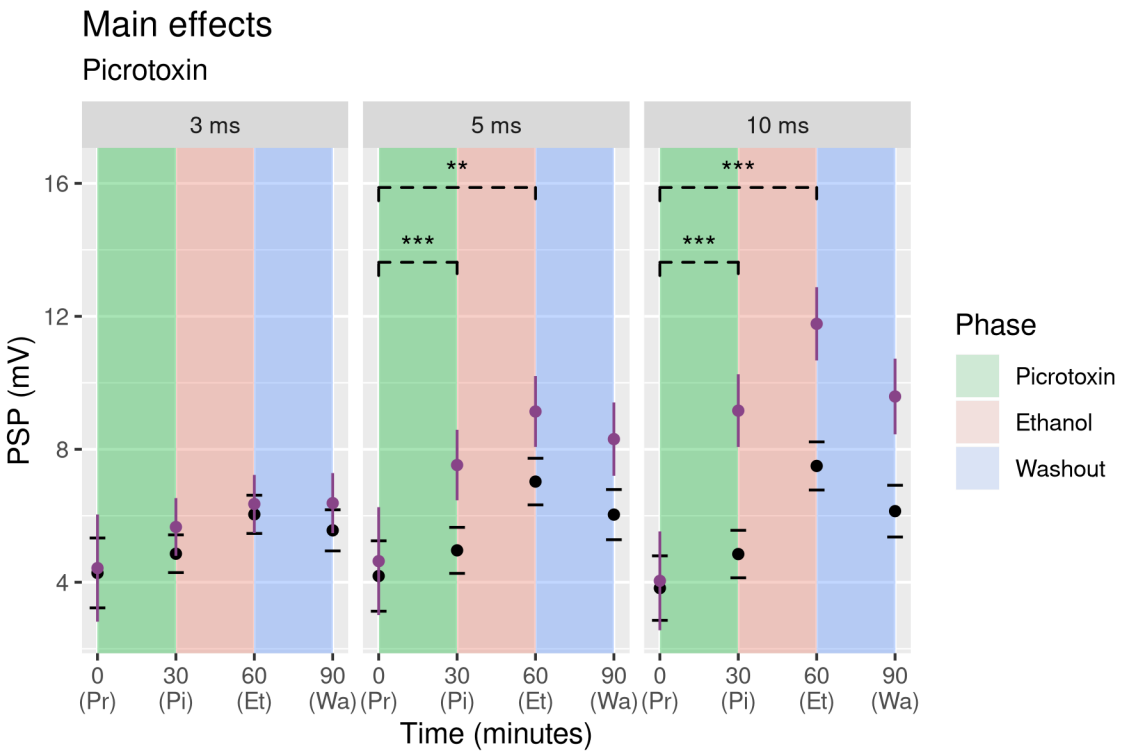

Figure 5.9. Main effects of picrotoxin across phases for each measurement time. Colored circles are point estimates, and lines are 95% confidence intervals. Black circles are saline control estimates, shown here for comparison, with black bars for the control confidence interval. The x-axis is color-coded based on the solution being superfused at each time. Time points correspond to the end of pretreatment (Pr), picrotoxin (Pi), EtOH (Et), and washout (Wa). Brackets for p values are broken to signify that comparisons are between the differences between phases when exposed to picrotoxin and the difference between phases when exposed to saline. Picrotoxin exposure causes a large increase over saline exposure at 5 ms and 10 ms, but does not strongly change the responses to EtOH or washout.

Table 5.5. Main effects for picrotoxin condition. Estimate and 95% confidence interval are in millivolts. P values are calculated between a given phase and the preceding one (e.g., Ethanol vs Saline).

Condition			Statistic		
Drug	Phase	Time	Estimate	95% CI	P-value
Picrotoxin	Pretreatment	3 ms	4.43	[2.81, 6.04]	
Picrotoxin	Drug	3 ms	5.66	[4.79, 6.53]	0.147
Picrotoxin	Ethanol	3 ms	6.35	[5.48, 7.23]	0.281
Picrotoxin	Washout	3 ms	6.38	[5.48, 7.28]	0.283
Picrotoxin	Pretreatment	5 ms	4.64	[3.01, 6.26]	
Picrotoxin	Drug	5 ms	7.53	[6.47, 8.59]	**2E-04**
Picrotoxin	Ethanol	5 ms	9.14	[8.07, 10.20]	0.410
Picrotoxin	Washout	5 ms	8.31	[7.20, 9.41]	0.777
Picrotoxin	Pretreatment	10 ms	4.04	[2.56, 5.53]	
Picrotoxin	Drug	10 ms	9.16	[8.07, 10.26]	**6E-12**
Picrotoxin	Ethanol	10 ms	11.78	[10.67, 12.88]	0.947
Picrotoxin	Washout	10 ms	9.59	[8.45, 10.73]	0.165

Picrotoxin was stronger in communals **(Figure 5.10, Table 5.6).** At all time points, picrotoxin exposure had a stronger effect in communals than isolates during **picrotoxin**, **EtOH**, and **washout** phases.

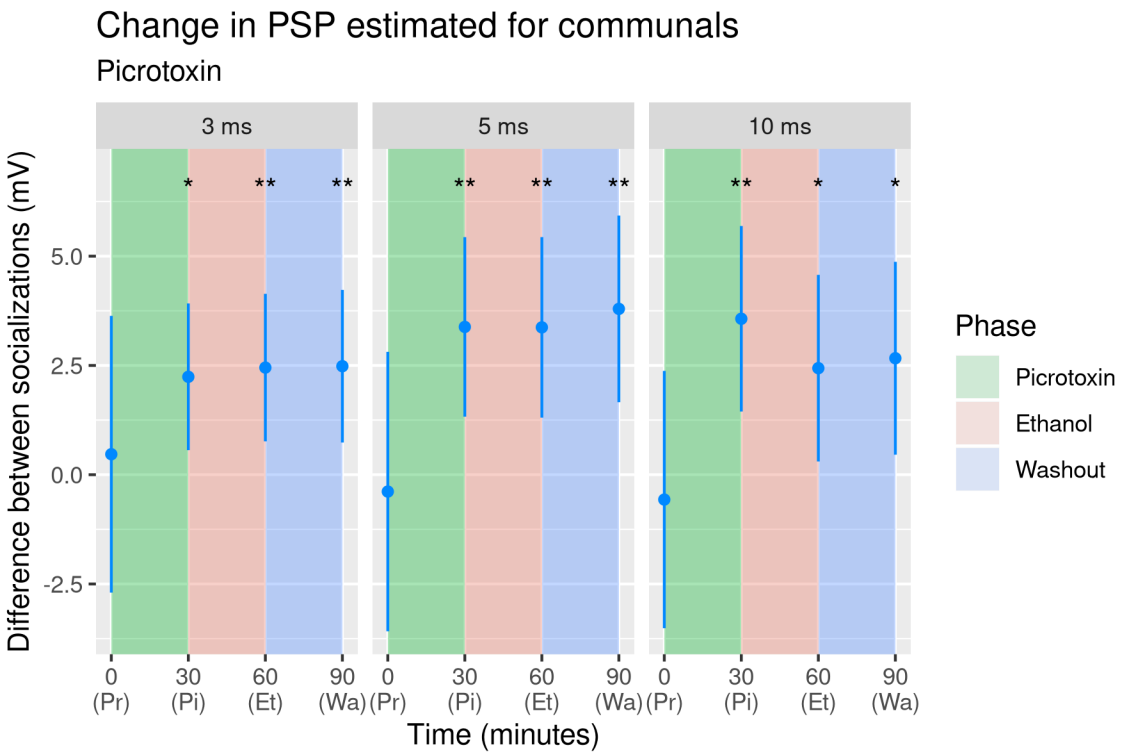

Figure 5.10. PSP difference observed between communals and isolates, controlling for the effects of picrotoxin and EtOH. The circles represent point estimates of the effect that communalization has. Lines are 95% confidence intervals. The x-axis is color-coded based on the solution being superfused at each time. Time points correspond to the end of pretreatment (Pr), picrotoxin (Pi), EtOH (Et), and washout (Wa). Picrotoxin had a stronger effect on communals at all time points. This difference remained stable during EtOH and washout.

Table 5.6. Social effects for picrotoxin condition. Estimate and 95% confidence interval are in millivolts, and represent the difference in PSP magnitude caused by communalization when controlling for all other factors.

Condition			Statistic		
Drug	Phase	Time	Estimate	95% CI	P-value
Picrotoxin	Drug	3 ms	2.24	[0.56, 3.92]	**0.013**
Picrotoxin	Ethanol	3 ms	2.45	[0.76, 4.14]	**0.007**
Picrotoxin	Washout	3 ms	2.48	[0.74, 4.23]	**0.008**
Picrotoxin	Drug	5 ms	3.38	[1.33, 5.43]	**0.002**
Picrotoxin	Ethanol	5 ms	3.37	[1.31, 5.44]	**0.002**
Picrotoxin	Washout	5 ms	3.79	[1.66, 5.93]	**0.001**
Picrotoxin	Drug	10 ms	3.57	[1.45, 5.69]	**0.002**
Picrotoxin	Ethanol	10 ms	2.44	[0.30, 4.57]	**0.034**
Picrotoxin	Washout	10 ms	2.66	[0.46, 4.87]	**0.025**

In summary, picrotoxin consistently excited animals at 5 ms and 10 ms, but did not appear to change the effects of EtOH. The excitatory effect of picrotoxin was restricted to communals, who responded much more strongly to picrotoxin exposure than isolates. Interestingly, this disinhibition occurred even at 3 ms, which differs from previous research suggesting that picrotoxin's effect on PSP begins around 4 ms post-stimulus (Vu et al., 1997)**.** However, the interpretation of picrotoxin's effect at a time when input is presumably excitatory is complicated by the possibility of picrotoxin interfering with cholinergic transmission (Miller et al., 1992). Picrotoxin's effect on blocking cholinergic transmission requires a higher concentration than the effect on GABA, so if this is the cause, picrotoxin's effects should change when concentration in the dish increases (i.e., at later times within the drug exposure period). This did not occur, however: communal LG PSPs began to increase in size early during picrotoxin exposure, presumably before the concentration could affect acetylcholine, while isolate PSPs did not **(Figure 5.11)**.

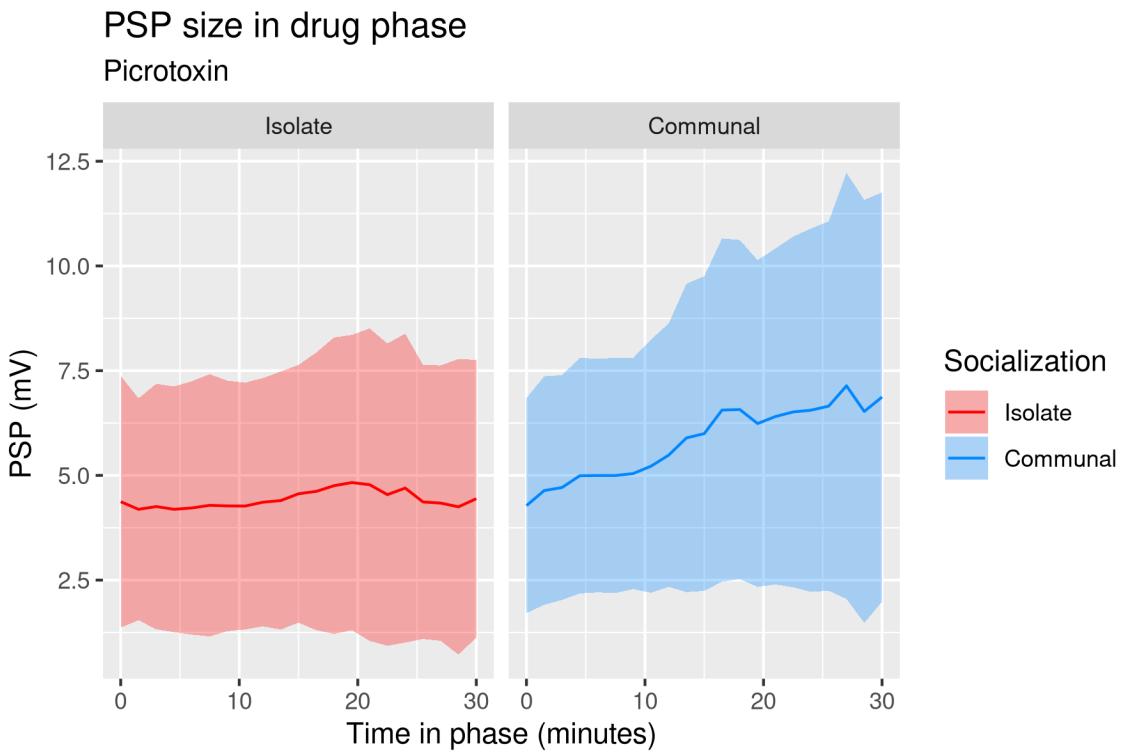

Figure 5.11. Effect of picrotoxin on PSP size during exposure. The shaded area is ± one standard deviation. Communals showed a relatively steady increase in PSP size even when drug concentration was still low, while isolates PSPs maintained a flat trajectory.

5.4.3. Muscimol - $GABA_A$ agonist/EtOH interaction

The effects of antagonists are only visible when their targets are active. In order to study the possibility of quiescent inhibitory machinery (which may be modulated in socially-dependent ways), I used the general $GABA_A$ agonist muscimol **(Figure 5.12, Table 5.7)**, at a concentration of 25 µM, to study the LG PSPs after stimulating the sensory afferents. The **3 ms** PSPs of isolates were generally attenuated by muscimol, facilitated by EtOH following muscimol, and unaffected by washout, though there was

high variance. Communal animals exposed to muscimol became facilitated upon EtOH washout, rather than attenuated as happened with saline and picrotoxin.

At **5 ms**, the PSP of isolates underwent a similar trend, though again with high variance. Preparations from communal animals did not clearly respond consistently to muscimol, but were facilitated by EtOH exposure and, again, during washout.

At **10 ms**, the PSP of isolates were attenuated by muscimol and washout, and facilitated by EtOH, but with very high variance. The communal PSPs were facilitated by EtOH and washout, but slightly attenuated by muscimol.

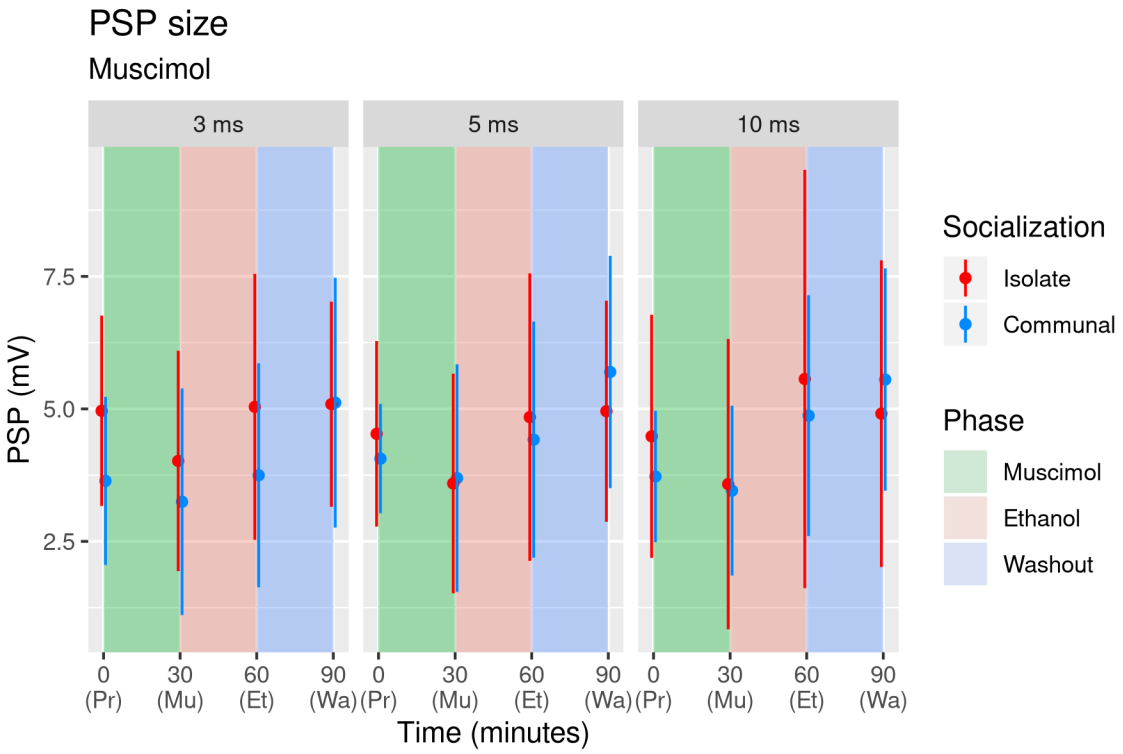

Figure 5.12. PSP at the end of each phase for muscimol exposed preparations. Colored circles are means, and lines are means ± one standard deviation. The x-axis is color-coded based on the solution being superfused at each time. Time points correspond to the end of pretreatment (Pr), muscimol (Mu), EtOH (Et), and washout (Wa). PSPs of communal animals were weakly affected by muscimol and EtOH, but underwent a facilitation in washout. In isolates, muscimol exposure attenuated the PSP, and EtOH exposure slightly facilitated it, but no effect emerged during washout.

Table 5.7. Descriptive data for muscimol condition. All units are millivolts.

Condition			3 ms		5 ms		10 ms	
Drug	Socialization	Phase	Mean	SD	Mean	SD	Mean	SD
Muscimol	Isolate	Pretreatment	4.96	1.80	4.53	1.75	4.48	2.29
Muscimol	Isolate	Drug	4.02	2.08	3.59	2.07	3.58	2.74
Muscimol	Isolate	Ethanol	5.04	2.51	4.84	2.71	5.56	3.95
Muscimol	Isolate	Washout	5.09	1.94	4.96	2.09	4.91	2.89
Muscimol	Communal	Pretreatment	3.64	1.59	4.06	1.03	3.73	1.24
Muscimol	Communal	Drug	3.25	2.14	3.69	2.15	3.46	1.60
Muscimol	Communal	Ethanol	3.75	2.11	4.42	2.23	4.87	2.27
Muscimol	Communal	Washout	5.12	2.36	5.70	2.19	5.55	2.10

When combining data from both social groups, muscimol generally attenuated the PSP, and, surprisingly, caused preparations to undergo a facilitation during washout, though its effects on EtOH exposure were ambiguous **(Figure 5.13, Table 5.8).** At **3 ms**, there was PSP attenuation and an apparent facilitation in washout, but no interaction with EtOH. This was similar at **5 ms**, though there was also some evidence for an EtOH interaction. **10 ms** displayed the same pattern, except evidence for blockage of EtOH's facilitatory effects was weaker. The attenuation of PSPs by muscimol, and its attenuation of EtOH's effects, were potent at all time points *(3 ms: $p = 4e\text{-}4$; 5 ms: $p = 1e\text{-}5$; 10 ms: $p = 2e\text{-}5$).*

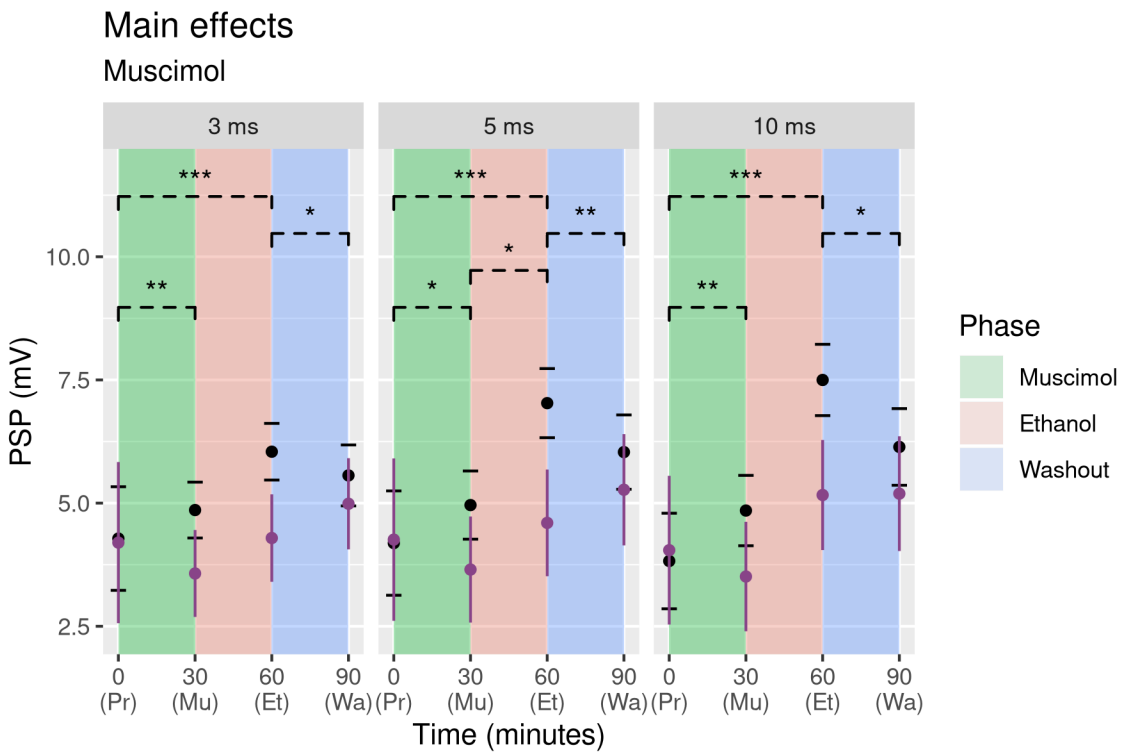

Figure 5.13. Main effects of muscimol across phases for each measurement time. Colored circles are point estimates, and lines are 95% confidence intervals. Black circles are saline control estimates, shown here for comparison, with black bars for the control confidence interval. The x-axis is color-coded based on the solution being superfused at each time. Time points correspond to the end of pretreatment (Pr), muscimol (Mu), EtOH (Et), and washout (Wa). Brackets for p values are broken to signify that comparisons are between the differences between phases when exposed to muscimol and the difference between phases when exposed to saline. Muscimol attenuated the PSP relative to saline. It also interacted with EtOH at later time points, resulting in a drastic reduction of PSP relative to EtOH exposure in controls.

Table 5.8. Main effects for muscimol condition. Estimate and 95% confidence interval are in millivolts. P values are calculated between a given phase and the preceding one.

Condition			Statistic		
Drug	Phase	Time	Estimate	95% CI	P-value
Muscimol	Pretreatment	3 ms	4.20	[2.56, 5.83]	
Muscimol	Drug	3 ms	3.57	[2.69, 4.45]	**0.009**
Muscimol	Ethanol	3 ms	4.29	[3.40, 5.18]	0.315
Muscimol	Washout	3 ms	4.99	[4.06, 5.91]	**0.015**
Muscimol	Pretreatment	5 ms	4.26	[2.61, 5.91]	
Muscimol	Drug	5 ms	3.65	[2.57, 4.73]	**0.015**
Muscimol	Ethanol	5 ms	4.60	[3.52, 5.68]	**0.048**
Muscimol	Washout	5 ms	5.27	[4.14, 6.40]	**0.005**
Muscimol	Pretreatment	10 ms	4.04	[2.53, 5.55]	
Muscimol	Drug	10 ms	3.51	[2.40, 4.62]	**0.008**
Muscimol	Ethanol	10 ms	5.16	[4.05, 6.28]	0.088
Muscimol	Washout	10 ms	5.19	[4.03, 6.36]	**0.023**

Social group did not appreciably interact with muscimol except during washout **(Figure 5.14, Table 5.9). Muscimol's** direct effects did not differ between social groups, nor did **EtOH's** effect following it. However, the data suggest that muscimol's **washout** caused facilitation in communals, but not isolates, at 3 ms, with stronger evidence that it did at 5 ms and 10 ms.

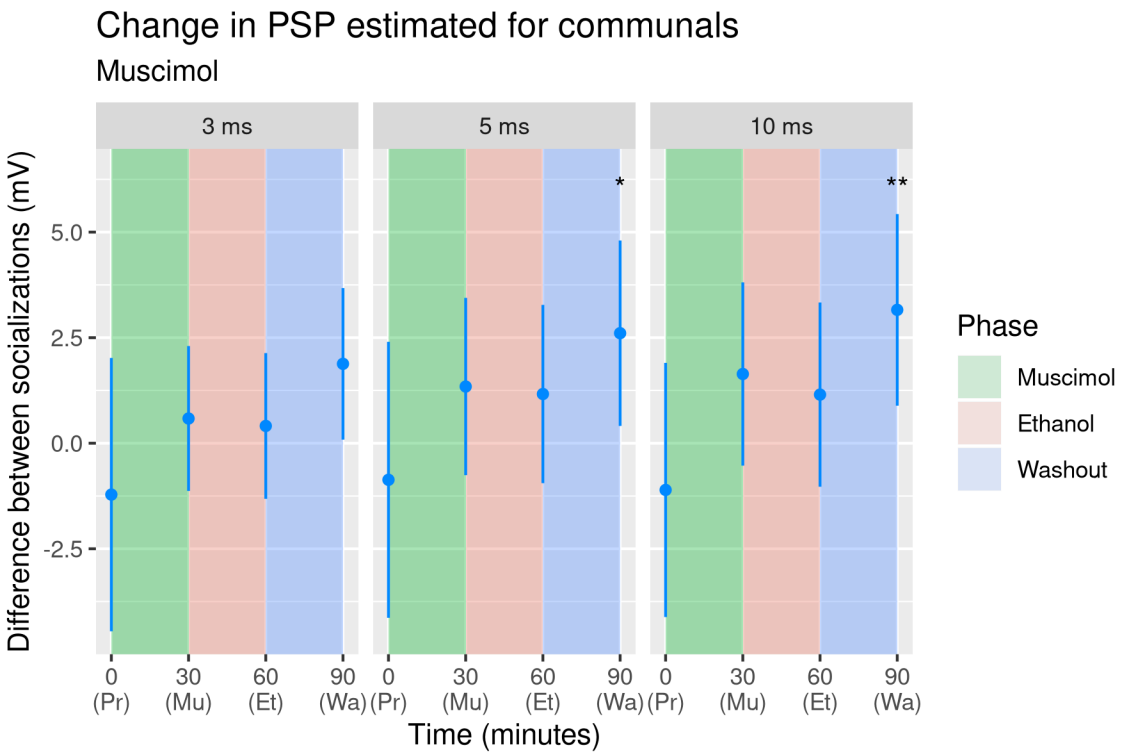

Figure 5.14. PSP difference observed between communals and isolates, controlling for the effects of muscimol and EtOH. The circles represent point estimates of the effect that communalization has. Lines are 95% confidence intervals. The x-axis is color-coded based on the solution being superfused at each time. Time points correspond to the end of pretreatment (Pr), muscimol (Mu), EtOH (Et), and washout (Wa). Muscimol's effect was not strongly modulated by social group, nor was EtOH's following it, but there was a difference in washout, such that communals experienced a facilitation of PSP.

Table 5.9. Social effects for muscimol condition. Estimate and 95% confidence interval are in millivolts, and represent the difference in PSP magnitude caused by communalization when controlling for all other factors.

Condition			Statistic		
Drug	Phase	Time	Estimate	95% CI	P-value
Muscimol	Drug	3 ms	0.59	[-1.13, 2.30]	0.524
Muscimol	Ethanol	3 ms	0.41	[-1.32, 2.13]	0.658
Muscimol	Washout	3 ms	1.88	[0.08, 3.68]	0.051
Muscimol	Drug	5 ms	1.34	[-0.76, 3.44]	0.233
Muscimol	Ethanol	5 ms	1.17	[-0.95, 3.28]	0.303
Muscimol	Washout	5 ms	2.61	[0.41, 4.80]	**0.027**
Muscimol	Drug	10 ms	1.64	[-0.53, 3.81]	0.159
Muscimol	Ethanol	10 ms	1.15	[-1.03, 3.33]	0.325
Muscimol	Washout	10 ms	3.16	[0.89, 5.43]	**0.010**

Overall, muscimol caused an attenuation relative to saline exposure, and this appeared to disrupt the effect of EtOH facilitation seen in controls. Interestingly, muscimol's washout tended to facilitate the PSPs, mediated primarily by a strong effect in communals.

5.4.4. TPMPA - $GABA_A$-ρ mediated inhibition

Swierzbinski et al. (2017) suggested that the difference between LG responsivity to alcohol in isolate and communal LG neurons may have been due to differences in GABA receptor distributions, and that this difference may persist in isolated nerve cords. Swierzbinski and Herberholz (2018) found that the MG's PSP was facilitated by muscimol, but that this attenuated the effects of EtOH, and suggested that this may be due to the presence of $GABA_A$-ρ receptors. $GABA_A$-ρ receptors do not quickly desensitize, allowing them to modulate inhibition during slower events, which may be useful during either tonic or post-excitatory inhibition. While the LG is known to be inhibited through several mechanisms, the specific receptor subtypes responsible for any forms of its inhibition have never been identified. I therefore investigated the possibility of the presence of $GABA_A$-ρ receptors with a selective antagonist, TPMPA (Ragozzino et al., 1996), at a concentration of 10 μM **(Figure 5.15).**

At **3 ms**, the PSPs of isolate animals were facilitated both during TPMPA and EtOH exposure, but had no strong response to washout **(Table 5.10)**. Communal PSPs had a similar trend, but it was extremely variable. At **5 ms**, the same trends were followed by both isolate and communal preparations.

At **10 ms**, as before, isolate preparations were again facilitated during TPMPA and EtOH exposure, and attenuated by washout. Communal preparations did not respond to TPMPA, but were relatively strongly facilitated by EtOH, which was partially reversible.

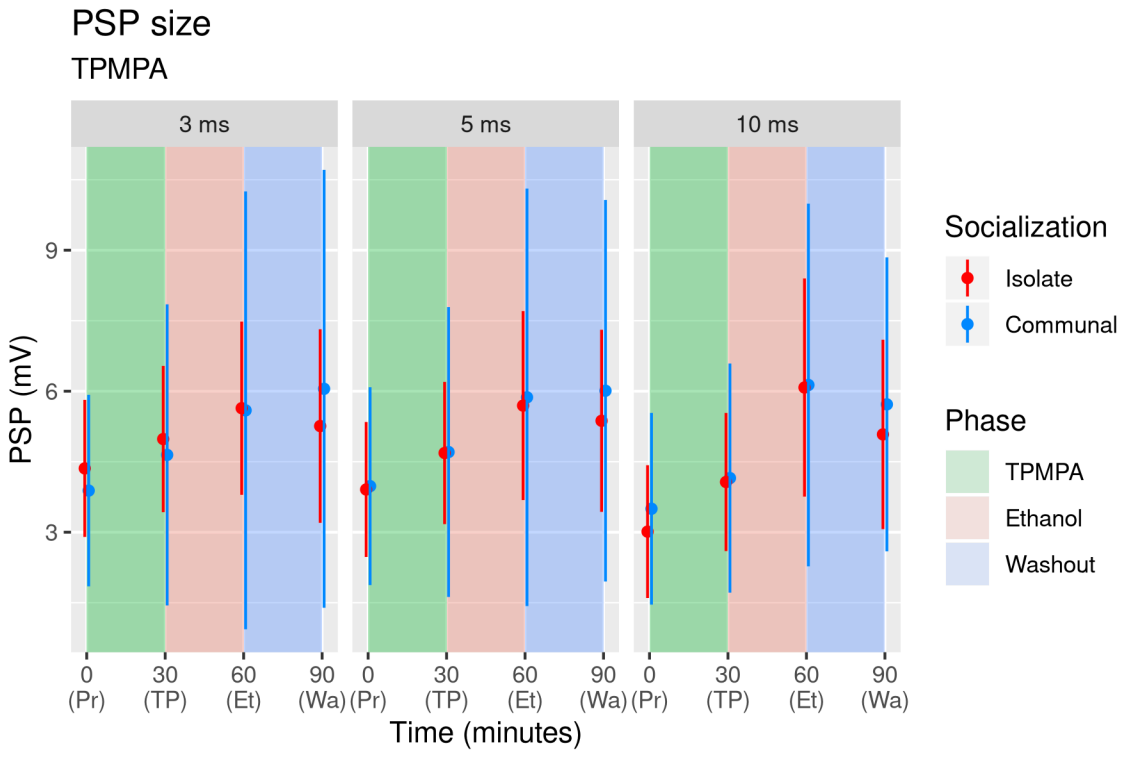

Figure 5.15. LG PSPs values at the end of each phase for TPMPA exposed preparations. Colored circles are means, and lines are means ± one standard deviation. The x-axis is color-coded based on the solution being superfused at each time. Time points correspond to the end of pretreatment (Pr), TPMPA (TP), EtOH (Et), and washout (Wa). PSPs of both social groups were facilitated by TPMPA and EtOH, but isolates underwent a slight washout effect, while communals only did at 10 ms. Communals had high variance, especially during EtOH exposure.

Table 5.10. Descriptive data for TPMPA condition. All units are millivolts.

Condition			3 ms		5 ms		10 ms	
Drug	Socialization	Phase	Mean	SD	Mean	SD	Mean	SD
TPMPA	Isolate	Pretreatment	4.36	1.46	3.91	1.44	3.01	1.41
TPMPA	Isolate	Drug	4.98	1.56	4.69	1.51	4.07	1.47
TPMPA	Isolate	Ethanol	5.64	1.84	5.69	2.01	6.08	2.32
TPMPA	Isolate	Washout	5.26	2.06	5.37	1.94	5.08	2.01
TPMPA	Communal	Pretreatment	3.89	2.04	3.98	2.10	3.50	2.04
TPMPA	Communal	Drug	4.65	3.20	4.71	3.08	4.15	2.44
TPMPA	Communal	Ethanol	5.59	4.66	5.87	4.44	6.13	3.86
TPMPA	Communal	Washout	6.05	4.66	6.01	4.06	5.72	3.13

TPMPA exposure did not have any particular effect, at any phase **(Figure 5.16, Table 5.11)**, measured at **3 ms**, **5 ms**, or **10 ms**, though there was some weak evidence that TPMPA attenuated EtOH's effects at 5 ms. The combined effects of EtOH and TPMPA were not notably different from EtOH after saline exposure at any time point *(3 ms: $p = 0.594$; 5 ms: $p = 0.070$; 10 ms: $p = 0.141$)*, though again, there was a weak possibility of an effect at 5 ms.

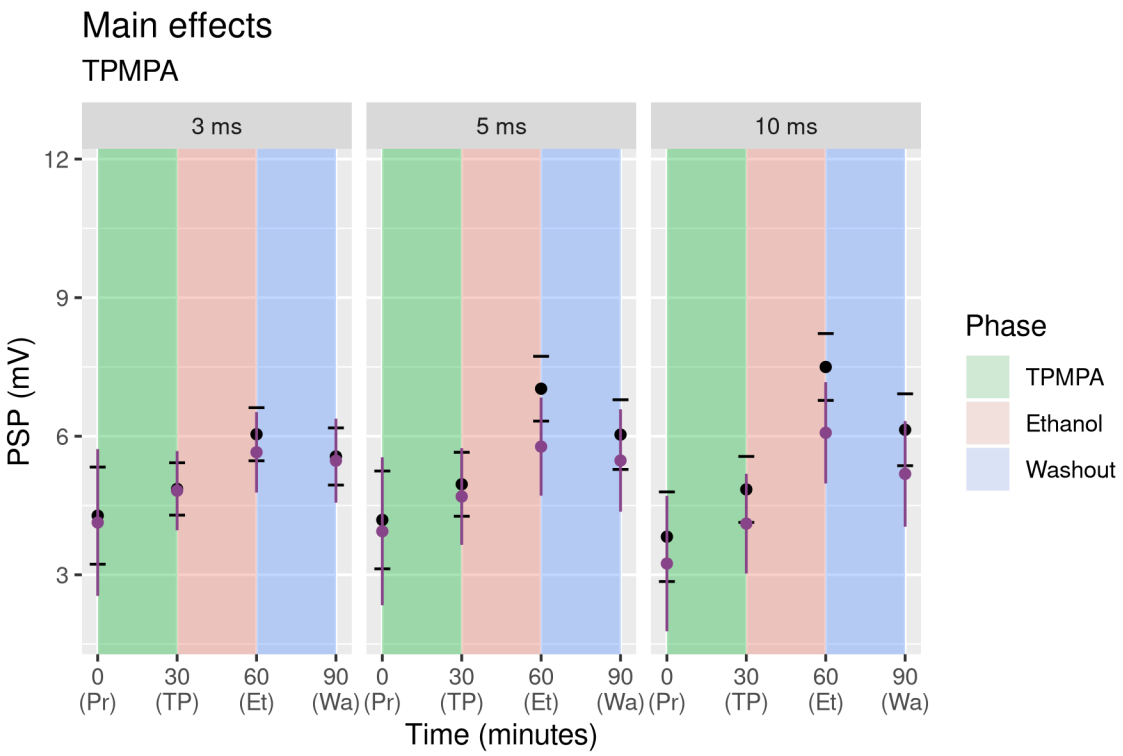

Figure 5.16. Main effects of TPMPA across phases for each measurement time. Colored circles are point estimates, and lines are 95% confidence intervals. Black circles are saline control estimates, shown here for comparison, with black bars for the control confidence interval. The x-axis is color-coded based on the solution being superfused at each time. Time points correspond to the end of pretreatment (Pr), TPMPA (TP), EtOH (Et), and washout (Wa). TPMPA generally did not appear to cause any changes compared to saline controls, though there was weak evidence that it may have interacted with EtOH at 5 ms.

Table 5.11. Main effects for TPMPA condition. Estimate and 95% confidence interval are in millivolts. P values are calculated between a given phase and the preceding one.

Condition			Statistic		
Drug	Phase	Time	Estimate	95% CI	P-value
TPMPA	Pretreatment	3 ms	4.13	[2.54, 5.72]	
TPMPA	Drug	3 ms	4.82	[3.96, 5.68]	0.805
TPMPA	Ethanol	3 ms	5.65	[4.78, 6.52]	0.437
TPMPA	Washout	3 ms	5.47	[4.56, 6.38]	0.531
TPMPA	Pretreatment	5 ms	3.94	[2.34, 5.54]	
TPMPA	Drug	5 ms	4.69	[3.65, 5.74]	0.972
TPMPA	Ethanol	5 ms	5.77	[4.71, 6.84]	0.075
TPMPA	Washout	5 ms	5.47	[4.37, 6.58]	0.234
TPMPA	Pretreatment	10 ms	3.24	[1.78, 4.71]	
TPMPA	Drug	10 ms	4.11	[3.03, 5.19]	0.776
TPMPA	Ethanol	10 ms	6.07	[4.98, 7.17]	0.232
TPMPA	Washout	10 ms	5.18	[4.04, 6.33]	0.434

TPMPA did not appear to interact with either socialization **(Figure 5.17, Table 5.12)** during **TPMPA** exposure, **EtOH**, or **washout**, though it should be noted that communals had (unexplained) high variance at all time points and phases.

In summary, TPMPA did not appear to have any effect on the LG neurons, which experienced the same facilitation as saline controls during pretreatment and EtOH phases as well as similar washout attenuation. It did not interact with socialization, either. These results suggest that $GABA_A$-ρ receptors are not critical to the sensory-evoked inhibition of the LG.

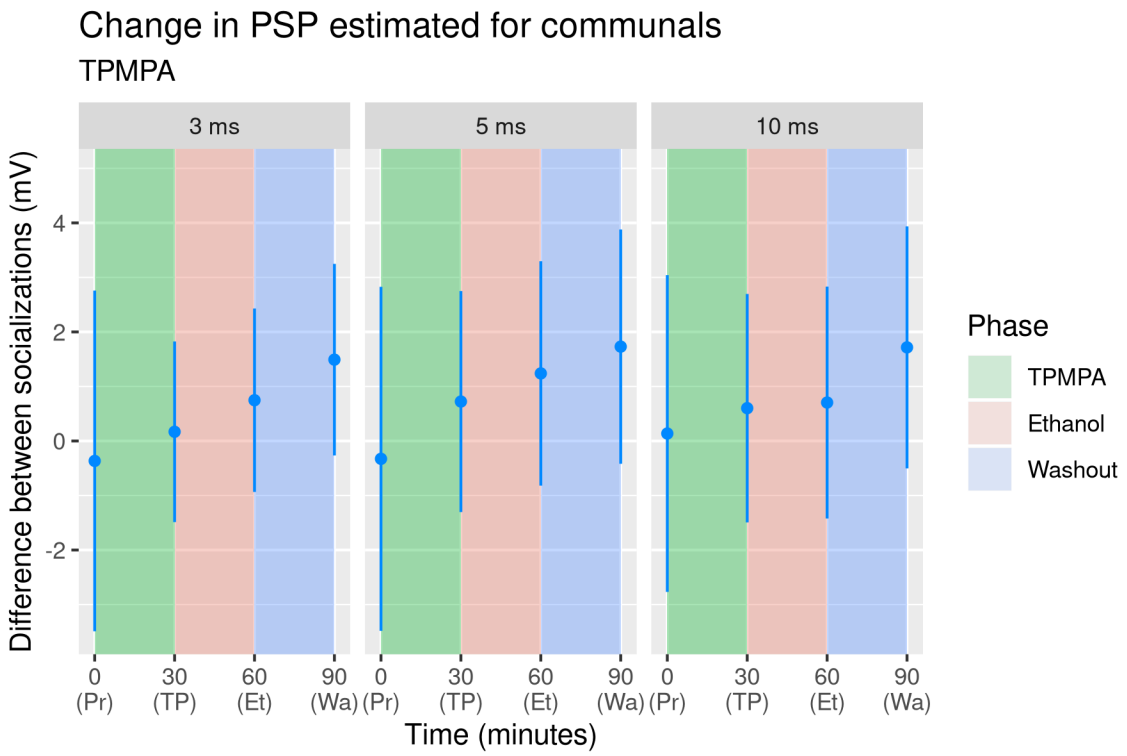

Figure 5.17. PSP difference observed between communals and isolates, controlling for the effects of TPMPA and EtOH. The circles represent point estimates of the effect that communalization has. Lines are 95% confidence intervals. The x-axis is color-coded based on the solution being superfused at each time. Time points correspond to the end of pretreatment (Pr), TPMPA (TP), EtOH (Et), and washout (Wa). At no point was there a clear difference between socializations.

Table 5.12. Social effects for TPMPA condition. Estimate and 95% confidence interval are in millivolts, and represent the difference in PSP magnitude caused by communalization when controlling for all other factors.

Condition			Statistic		
Drug	Phase	Time	Estimate	95% CI	P-value
TPMPA	Drug	3 ms	0.17	[-1.49, 1.83]	0.849
TPMPA	Ethanol	3 ms	0.75	[-0.93, 2.43]	0.407
TPMPA	Washout	3 ms	1.49	[-0.27, 3.25]	0.114
TPMPA	Drug	5 ms	0.72	[-1.30, 2.75]	0.505
TPMPA	Ethanol	5 ms	1.24	[-0.82, 3.30]	0.261
TPMPA	Washout	5 ms	1.73	[-0.42, 3.88]	0.133
TPMPA	Drug	10 ms	0.60	[-1.49, 2.70]	0.592
TPMPA	Ethanol	10 ms	0.70	[-1.42, 2.83]	0.536
TPMPA	Washout	10 ms	1.72	[-0.50, 3.94]	0.149

5.4.5. THIP - $GABA_A$-δ mediated inhibition

The LG's excitability is known to be regulated by tonic inhibition (Vu & Krasne, 1992; Vu & Krasne, 1993; Vu et al., 1993), and this tonic inhibition is thought to underlie some of the differences between communally housed and isolated crayfish when exposed to alcohol (Swierzbinski et al., 2017). Tonic inhibition is known to be largely mediated by extrasynaptic $GABA_A$-δ receptors, and it is also known that these receptors are responsive to physiological amounts of EtOH (Farrant & Nusser, 2005; Santhakumar et al., 2007). As tonic inhibition originates in the brain and is eliminated in the isolated nerve cord preparations used here, any tonic inhibitory receptors present on the LG should be available to bind relevant neurotransmitters. I therefore studied the possibility that these receptors are present on the LG using a selective agonist, THIP, at 10 μM (Stórustovu & Ebert, 2006) **(Figure 5.18).**

At **3 ms**, exposure to THIP resulted in neither isolates nor communals responding strongly at any phase **(Table 5.13)**. This was also observed at **5 ms**, in both isolates and communals, though both appear to have weak, somewhat inconsistent trends of facilitation. At **10 ms**, a facilitation during EtOH and attenuation during washout emerged for both isolates and communals.

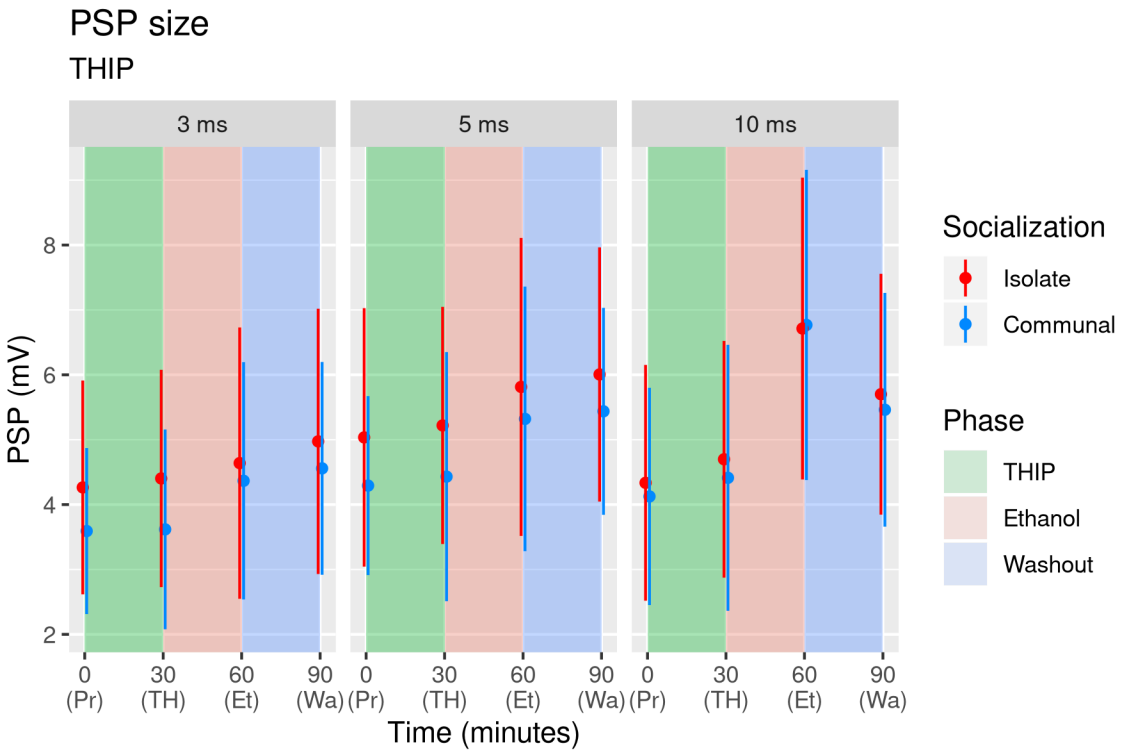

Figure 5.18. LG PSPs values at the end of each phase for THIP exposed preparations. Colored circles are means, and lines are means ± one standard deviation. The x-axis is color-coded based on the solution being superfused at each time. Time points correspond to the end of pretreatment (Pr), THIP (TH), EtOH (Et), and washout (Wa). Neither socialization displayed a strong response during any phase at 3 and 5 ms, though they were facilitated by EtOH at 10 ms.

Table 5.13. Descriptive data for THIP condition. All units are millivolts.

Condition			3 ms		5 ms		10 ms	
Drug	Socialization	Phase	Mean	SD	Mean	SD	Mean	SD
THIP	Isolate	Pretreatment	4.26	1.65	5.04	1.99	4.34	1.82
THIP	Isolate	Drug	4.40	1.67	5.22	1.83	4.70	1.82
THIP	Isolate	Ethanol	4.64	2.09	5.81	2.30	6.71	2.33
THIP	Isolate	Washout	4.97	2.04	6.01	1.96	5.70	1.86
THIP	Communal	Pretreatment	3.59	1.28	4.29	1.38	4.13	1.67
THIP	Communal	Drug	3.62	1.54	4.43	1.92	4.41	2.05
THIP	Communal	Ethanol	4.37	1.83	5.32	2.04	6.77	2.39
THIP	Communal	Washout	4.56	1.64	5.44	1.59	5.46	1.80

THIP itself did not appear to have a strong effect, but combined potently with EtOH (**Figure 5.19, Table 5.14**). At **3 ms**, THIP interfered with EtOH's facilitation to a

lesser degree. This effect was stronger at **5 ms**, where there was also weak evidence for a washout effect, though this may be in part mediated by its prevention of the facilitation of EtOH. THIP exposure did not produce major effects at **10 ms**.

The main effect of THIP was a substantial reduction of EtOH facilitation of the LG PSP at all time points when compared to EtOH exposure in controls *(3 ms: p = 0.004; 5 ms: p = 2e-4; 10 ms: p = 0.029)*. This effect was strongest at 3 ms and 5 ms.

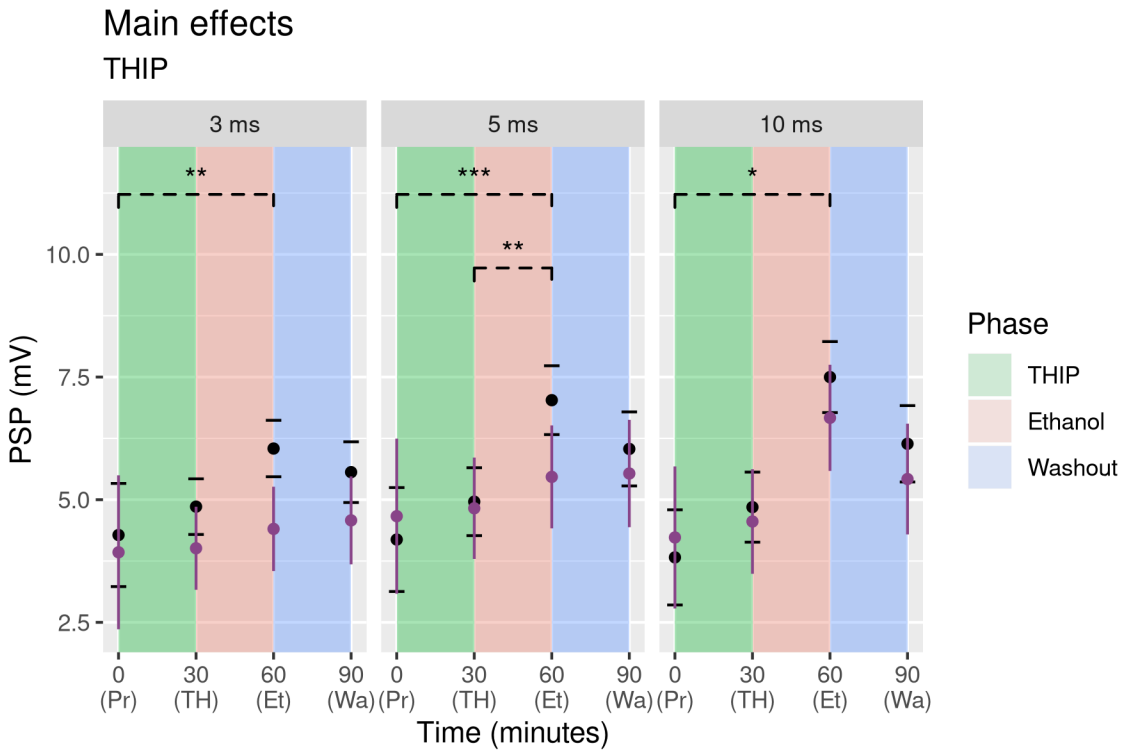

Figure 5.19. Main effects of THIP across phases for each measurement time. Colored circles are point estimates, and lines are 95% confidence intervals. Black circles are saline control estimates, shown here for comparison, with black bars for the control confidence interval. The x-axis is color-coded based on the solution being superfused at each time. Time points correspond to the end of pretreatment (Pr), THIP (TH), EtOH (Et), and washout (Wa). Brackets for p values are broken to signify that comparisons are between the differences between phases when exposed to THIP and the difference between phases when exposed to saline.

Table 5.14. Main effects for THIP condition. Estimate and 95% confidence interval are in millivolts. P values are calculated between a given phase and the preceding one.

Condition			Statistic		
Drug	Phase	Time	Estimate	95% CI	P-value
THIP	Pretreatment	3 ms	3.93	[2.36, 5.50]	
THIP	Drug	3 ms	4.01	[3.16, 4.86]	0.262
THIP	Ethanol	3 ms	4.40	[3.55, 5.26]	0.079
THIP	Washout	3 ms	4.58	[3.68, 5.48]	0.164
THIP	Pretreatment	5 ms	4.66	[3.08, 6.24]	
THIP	Drug	5 ms	4.83	[3.79, 5.86]	0.258
THIP	Ethanol	5 ms	5.47	[4.42, 6.51]	**0.009**
THIP	Washout	5 ms	5.53	[4.44, 6.63]	0.065
THIP	Pretreatment	10 ms	4.23	[2.78, 5.68]	
THIP	Drug	10 ms	4.56	[3.49, 5.62]	0.209
THIP	Ethanol	10 ms	6.67	[5.59, 7.75]	0.341
THIP	Washout	10 ms	5.42	[4.29, 6.55]	0.851

THIP's interaction with socialization was not appreciable at any time point **(Figure 5.20, Table 5.15)** during the **THIP**, **EtOH**, or **washout** phase.

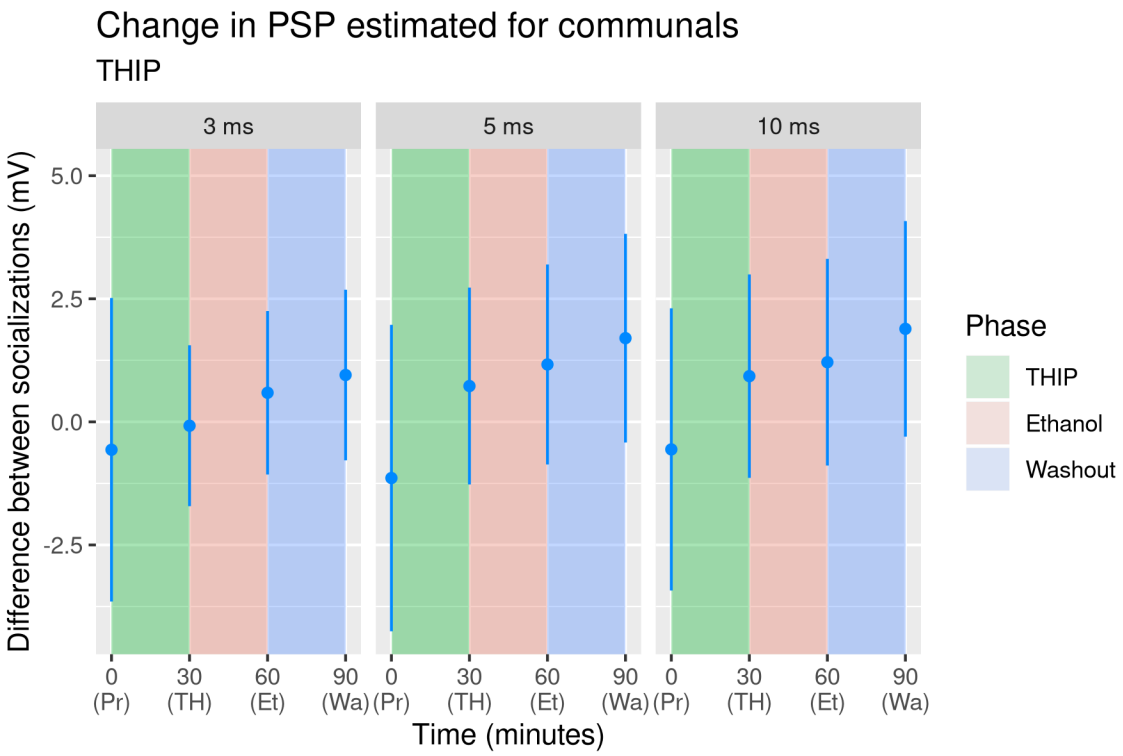

Figure 5.20. PSP difference observed between communals and isolates, controlling for the effects of THIP and EtOH. The circles represent point estimates of the effect that communalization has. Lines are 95% confidence intervals. The x-axis is color-coded based on the solution being superfused at each time. Time points correspond to the end of pretreatment (Pr), THIP (TH), EtOH (Et), and washout (Wa).

Table 5.15. Social effects for THIP condition. Estimate and 95% confidence interval are in millivolts, and represent the difference in PSP magnitude caused by communalization when controlling for all other factors.

Condition			Statistic		
Drug	Phase	Time	Estimate	95% CI	P-value
THIP	Drug	3 ms	-0.08	[-1.71, 1.56]	0.929
THIP	Ethanol	3 ms	0.59	[-1.07, 2.25]	0.506
THIP	Washout	3 ms	0.95	[-0.78, 2.68]	0.305
THIP	Drug	5 ms	0.73	[-1.27, 2.73]	0.497
THIP	Ethanol	5 ms	1.17	[-0.86, 3.20]	0.284
THIP	Washout	5 ms	1.70	[-0.42, 3.82]	0.135
THIP	Drug	10 ms	0.93	[-1.14, 2.99]	0.402
THIP	Ethanol	10 ms	1.21	[-0.89, 3.31]	0.281
THIP	Washout	10 ms	1.89	[-0.30, 4.08]	0.108

Overall, THIP exposure itself did not appear to have any effect on the LG PSP evoked with sensory afferent stimulation. However, THIP did interact with EtOH and caused a strong reduction in LG PSP when compared to EtOH effects following saline. Social status did not interact with THIP's effects.

5.4.6. Result Overview

Data were separated by socialization and linear models were run in order to generally summarize the interactions between drugs and EtOH. The effect of EtOH following drug exposure was compared to the effects of EtOH following saline exposure, and the differences graphed **(Figure 5.21)**. Overall, drug pretreatment did not strongly change the effects of EtOH. The only exception was THIP preexposure, which reduced EtOH's effects at 3 ms and 5 ms. There were no strong social differences in any conditions.

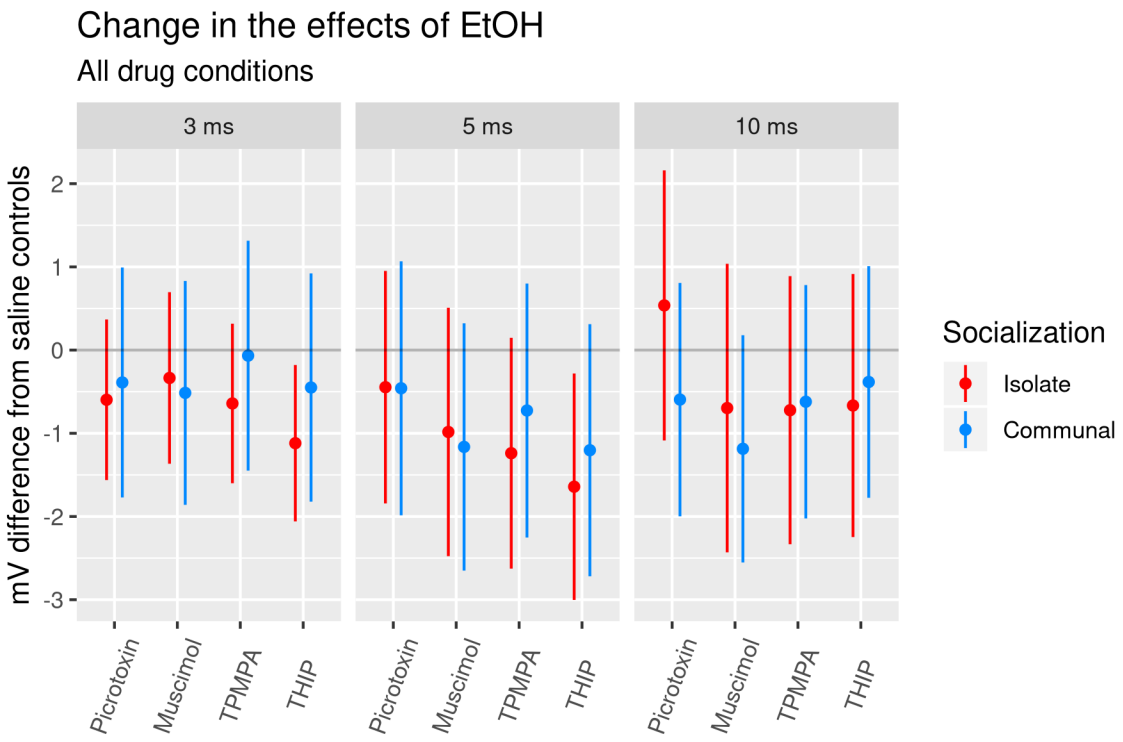

Figure 5.21. Change in the effects of EtOH after pretreatment with different drugs. Points are estimates, bars are 95% confidence intervals. Data represents the difference in EtOH's effects seen when preparations were pretreated with the drug in question, controlling for the effects of EtOH seen in the saline condition for that socialization. No clear differences due to socialization were seen. Drug pretreatment largely did not change the impact of EtOH, with the exception of THIP, which appears to have reduced the PSP facilitation caused by EtOH exposure.

5.5. Discussion of sensory-evoked inhibition

Saline exposure was used as a drug control, but caused a substantial potentiation of LG PSP by itself. This has been reported before, though it appears to be weakened in preparations without descending inhibition (Swierzbinski et al., 2017). While I did not see a clear difference in this facilitation based on social status, the estimate of the social effects on this saline-induced PSP facilitation showed the same pattern of higher increase in isolates that has been described previously in the presence of tonic inhibition

(Swierzbinski & Herberholz, 2018). Communal animals are likely to experience tactile input in the abdomen due to non-threatening stimuli (e.g., other crayfish in the group walking into them), while isolates are not. An increase in PSP (i.e., lowering the threshold for tail-flipping) in response to repeated stimulation makes adaptive sense for isolates, as unexpected stimulation when alone may represent a predator attack, while in a group it could represent a less dangerous signal such as a non-aggressive conspecific interaction. It is also possible that repeated stimuli modulate the LG's sensitivity in both socializations, but that the constant input that communals receive has already sensitized the LG sufficiently that it does not respond to further stimulation, while isolates have not undergone this sensitization.

EtOH exposure caused a facilitation of LG PSP in both isolates and communals. The finding that EtOH increases the excitability of the LG neuron is similar to what has been found in the LG before by Swierzbinski et al. (2017) and also in the PSP of the MG neuron in isolates by Swierzbinski and Herberholz (2018). Although they measured the MG PSP amplitude at slightly different time points (3 ms and 6 ms, while I measured the LG at 3 ms and 5 ms), we both found that, when exposed to EtOH for thirty minutes, the system under study had its PSP potentiated to about 150% of its initial level in both the early and late phase of its response to sensory inputs. Moreover, the subthreshold facilitation of the LG PSP when exposed to EtOH is congruent with previous work on the LG that looked at action potential generation (Swierzbinski et al., 2017), and parallels the effects that EtOH has on tail-flip behavior in freely behaving animals. It is notable that the effects are present even in completely isolated nerve cords, allowing the use of a

simple, reduced *ex vivo* preparation to study the cellular and molecular effects of EtOH on small neural circuits.

Swierzbinski et al. (2017) found that there are social differences in how the LG responds to low doses of EtOH in both freely behaving and semi-intact animals. This effect was not seen at high doses of EtOH. When the cord was cut, removing all tonic inhibition, the difference between communals and isolates disappeared, suggesting that communals' greater sensitivity to EtOH may be due to a higher level of tonic inhibition. In addition, cord transection also resulted in EtOH becoming less excitatory. I did not find evidence for a social difference in EtOH effects in the isolated abdominal nerve cord where all tonic inhibition is removed, which is in agreement with the previous work. Swierzbinski et al. (2017) suggested that $GABA_A$ receptor redistribution may underlie the socially-mediated difference in LG sensitivity to EtOH; this possibility will be discussed below with the results involving $GABA_A$ receptor agonists muscimol and THIP.

My work is the first to look at LG inhibition specifically between animals of different social histories. Despite the differential effect that alcohol has on crayfish behavior based on social status, and the fact that alcohol exerts a large proportion of its effects through interactions with inhibitory receptors in other animal models, I found little evidence of such interactions with most drugs that I tested. However, there was one important exception: picrotoxin produced a robust difference, and strongly increased LG PSP in communals while having relatively little effect in isolates. While previous work has found that social experience can change the LG's response to serotonin (Yeh et al., 1996; Yeh et al., 1997), this is the first demonstration that social experience modulates

inhibitory systems in crayfish. This result may suggest a new model for examining the interactions between social experience and inhibition. Picrotoxin is a non-specific chloride channel blocker, so while it is probable that it is interfering with GABAergic inhibition, further studies are needed to confirm that its actions are mediated through $GABA_A$ receptors, as glutamate-gated chloride channels are also sensitive to its effects (as discussed in section 4).

It is also interesting that this occurred in communals at the earliest measured time point of of the LG PSP (3 ms). Previous work, performed *in isolates only*, has suggested that there is no sensory-evoked LG inhibition three milliseconds following the stimulus (Vu et al., 1997). The proposed reason for the sensory-evoked inhibition is to prevent action potentials from being elicited by stimuli which are not sharp or strong enough to immediately recruit a threshold level of mechanoreceptors (Vu et al., 1997). My result is therefore surprising, since inhibition which occurs during the period that action potentials are generated does not match the theoretical purpose of this inhibition. The inhibition seen in my study likely adjusts the threshold of action potentials, much like tonic inhibition, which also seems to be socially mediated (Swierzbinski et al., 2017). However, the isolation of the abdominal section of the nerve cord removes the well-studied tonic inhibition which descends from the brain (Vu & Krasne, 1993), eliminating its antagonism as an explanation for this effect. The presence of this early inhibition suggests that either there is tonic inhibition that is local to the abdomen, or that there are short-latency inhibitory interneurons which are activated by afferent stimulation only in communals. It is known that GABA buildup can result in spillover from the synapse

when the afferents are stimulated repeatedly (Rossi & Hamann, 1998), and it is possible that these extrasynaptic receptors exist only in crayfish communals. This seems unlikely, however, in view of my results from THIP treatment, as THIP is selective for extrasynaptic receptors, yet was not more effective in modulating LG PSP of communals (see below).

Tonic inhibition shifts the threshold of action in response to immediate situations (Vu & Krasne, 1992; Vu & Krasne, 1993; Vu et al., 1993). Given the decentralized nature of the crayfish nervous system, it may be that descending tonic inhibition modulates escape in response to stimuli from the front of the animal (e.g., when feeding), and a local circuit modulates it in response to stimuli from the back. Communally housed animals are frequently approached from behind, backed into, or otherwise subject to stimuli which do not merit a sudden escape, while these unexpected interactions do not occur in isolation. Thus, these spurious abdominal stimulations may upregulate inhibition in communal animals.

Muscimol was effective at reducing the PSP compared to saline exposure alone, and my results suggest that it also interacts with EtOH to reduce the latter's facilitation. The combination of muscimol and EtOH was substantially different from that of EtOH alone, suggesting a synergistic effect on inhibition. Altogether, these results are consistent with muscimol having an inhibitory effect, along with a small interaction effect with EtOH, resulting in an overall strong level of inhibition. The simplest explanation is that muscimol is acting on inhibitory receptors, as it is expected to. EtOH causes less facilitation after muscimol, which suggests that the EtOH's potentiation of muscimol-

induced inhibition cancels out its excitatory effects. The LG PSP increased during washout, bringing it to the level seen in saline controls, though this effect, once again, was only observed in communals. Isolate preparations exposed to muscimol had lower PSPs after washout, compared to their saline controls. These results imply that muscimol does not wash out effectively in isolates, which is an effect seen with other drugs as well (Yeh et al., 1996; Swierzbinski et al., 2017).

While I found similar responses to EtOH in the LG PSP as those described by Swierzbinski and Herberholz (2018) for the MG PSP, different results were obtained when muscimol was involved: muscimol exposure did not cause a reduction in the MG's PSP size, but it did eliminate the effect of EtOH. As my experiments removed tonic inhibition, this could explain the difference between the studies. Removing tonic inhibition frees up its GABA receptors, and this allows muscimol to bind and create a stronger inhibitory effect, whereas if there is a consistent level of inhibition, muscimol must compete for receptors with the natural ligand GABA, which reduces its effect. Crayfish suppress their escape responses when they are restrained (Krasne & Wine, 1975), so it is probable that the preparations measuring the MG responses had a high level of tonic inhibition.

Swierzbinski and Herberholz (2018) attributed their findings in the MG neuron, after application of muscimol and EtOH, to the presence of $GABA_A$-ρ receptors. While the isolated LG responded to muscimol differently from the MG, suggesting that tonic inhibition may play a role in the MG's response, it does not rule out the possibility that the LG's sensory-evoked inhibition is partially mediated by $GABA_A$-ρ receptors.

However, the $GABA_A$-ρ antagonist TPMPA did not cause a dramatic change when compared to saline controls. There was tenuous evidence of an effect at 5 ms, during the later β component of the PSP, when the preparation was also exposed to EtOH. Given the lack of TPMPA effect during other phases and time points, and the weakness of the evidence, this possibility should be treated with skepticism. However, post-excitatory inhibition is beginning at 5 ms (Vu et al., 1997) and EtOH acts as an inhibitor of the $GABA_A$-ρ1 receptor (Mihic & Harris, 1996). If TPMPA and EtOH are competing for $GABA_A$-ρ receptors, and TPMPA is a weaker antagonist, then it may be that TPMPA is blocking EtOH from binding to the receptors, while allowing a higher level of GABAergic currents to flow than with EtOH alone. This would result in a higher level of net chloride conductance, causing slightly more inhibition and slightly reduced LG PSP. As TPMPA is an antagonist, its lack of strong effects observed in my experiments does not imply that this is also the case in an intact animal, as the absence of tonic inhibition in my preparations may have removed a source of input to TPMPA-sensitive receptors.

$GABA_A$-δ receptors present a major target of EtOH (Santhakumar et al., 2007), making them an important receptor subtype to study when attempting to understand EtOH's effects. I used the selective $GABA_A$-δ agonist THIP to test whether or not they are present in crayfish, and, if so, whether they are targeted by EtOH. THIP had no strong effect on its own. However, it is clear that preexposure to THIP caused a reduction in the excitatory effect of EtOH. Given EtOH's strong potentiation at $GABA_A$-δ receptors (and THIP's weak activity at receptors lacking a δ subunit), it can be suggested that EtOH and THIP are acting synergistically on $GABA_A$-δ receptors in the crayfish LG circuit.

This is the first clear demonstration that $GABA_A$-δ-like receptors exist in the crayfish LG circuit, and are targeted by EtOH. $GABA_A$-δ receptors are extrasynaptic receptors generally involved in tonic inhibition (reviewed by Farrant & Nusser, 2005), and thus may underlie the well-described descending tonic inhibition in crayfish (Vu & Krasne, 1992; Vu & Krasne, 1993; Vu et al., 1993), which may interact with the effects of alcohol (Swierzbinski et al., 2017). As tonic inhibition is absent in the preparations used in my work, the receptors responsible for it should be free for ligands to bind. The strong effects of 10 μM THIP, when preparations were subsequently exposed to EtOH, is particularly interesting given that previous work in the crayfish stretch receptor found that THIP showed no effect at much higher concentrations (Krause et al., 1981; Deisz & Dose, 1983). While those studies did not test the combined effects of THIP and alcohol, and I did not see clear inhibition of the LG PSP from THIP alone, this result is certainly intriguing. It may suggest that crayfish have $GABA_A$-δ receptors which mediate tonic inhibition and are present in the LG circuit, but not in other parts of the crayfish nervous system. In the future, additional measures, such as conductance changes in LG, would likely be needed to better understand the effects of THIP.

Swierzbinski et al. (2017) suggested that social isolation may result in a redistribution of the receptors involved in tonic inhibition, and that this may underlie the social difference in EtOH sensitivity. My results suggest that this might not be the case. Rather, it is likely a difference in the *release* of GABA, via descending inputs, that drives the social differences in sensitivity to EtOH. This possibility could not be directly tested in my preparations, due to the lack of descending inhibition in the isolated nerve cord.

However, several of my findings make it unlikely that tonic receptor redistribution plays a large role in this difference: I did not find evidence of a socialization effect on EtOH sensitivity, and I did not find a social difference in the response to muscimol or THIP, two drugs which would presumably be more effective if the distribution of tonic receptors was increased. However, there are a few caveats to my findings. Firstly, it is possible that the concentrations of muscimol and THIP used in my study were too high. Both muscimol and THIP were effective in reducing the LG PSP size in the EtOH phase. Both THIP and muscimol are more effective than GABA at stimulating $GABA_A$-δ receptors (Stórustovu & Ebert, 2006), and EtOH potentiates the effect of GABA at $GABA_A$-δ receptors (Sundstrom-Poromaa et al., 2002; Hanchar et al., 2005). Together this could mask excitation strongly enough to obscure social differences. It should also be noted that there are important differences between my experiments and those performed by Swierzbinski et al. (2017). My experiments were performed in adult animals, rather than in juveniles. Additionally, the concentration of EtOH I used was higher than the concentration used by Swierzbinski et al. (2017), although my concentration was within the physiologically relevant range, and the need for a higher concentration in adults reflects a behavioral insensitivity compared to juveniles (Herberholz lab, unpublished results). Finally, my quantification of excitation was based on PSP changes, as this allows me to explore the more subtle changes in inhibition that would not be discernible via analysis of spikes, the method used by Swierzbinski et al. (2017).

Overall, my results suggest that the socially-mediated differences in response to EtOH exposure are at least in part due to descending inputs from the brain and are

therefore eliminated in isolated nerve cords. Communals do not appear to have a higher quantity of tonic receptors (although the picrotoxin experiments suggest that they may have a higher overall number of GABA receptors) but they may have a higher level of descending tonic GABA release.

I found that THIP displayed a similar pharmacological profile to the effects of muscimol, both in my experiments and in those performed by Swierzbinski and Herberholz in the MG (2018). Muscimol, like THIP, is a strong agonist at $GABA_A$-δ receptors (Stórustovu & Ebert, 2006), which, as already discussed, EtOH potentiates. Muscimol's attenuation of EtOH's effect, then, may be partially due to the same mechanisms proposed for THIP's attenuation of EtOH. Both drugs could strongly activate $GABA_A$-δ currents, which would then be potentiated by EtOH, resulting in a strong inhibition which counters the excitatory effects that EtOH generally exerts. This effect would likely be stronger in the isolated LG than in the MG because tonic inhibition is still present in MG preparations, so muscimol must compete for receptors. It also seems reasonable that muscimol has a stronger effect on the LG compared to THIP when either one is applied alone, as muscimol has activity at other $GABA_A$ receptor subtypes, while THIP is more selective.

In summary, my results suggest that there are social differences in inhibition of the LG neuron. This inhibition is sensitive to picrotoxin, which is more effective in communals, though further work is necessary to show that its actions are not through effects on glutamatergic receptors. Additionally, my results suggest that the social differences in sensitivity to EtOH in the LG is mediated by descending inputs, rather than

local changes to the neuron's receptors. I have also discovered that crayfish appear to possess something akin to the mammalian $GABA_A\delta$ receptor, which displays relevant pharmacological properties similar to that of human receptors, including an interaction with EtOH, and which may mediate tonic inhibition.

6. Future directions

My dissertation work explores several facets of inhibition: the cause of the mysterious depolarization that inhibits the LG following an action potential, and the qualities of the sensory-evoked inhibition which make up a portion of the LG's PSP, as well as identifying a receptor subtype which may be involved in tonic inhibition. Though I did not conclusively identify all the mechanisms underlying autoinhibition, my work makes important contributions to the limited body of knowledge on this phenomenon. I have shown that the dIPSP is affected by bath applications of both GABA and glutamate, and that the LG *axon* is sensitive to both of these compounds. I have shown that the glutamatergic response can be eliminated by picrotoxin, suggesting an inhibitory role involving glutamate-gated chloride channels. I have also found that the LG autoinhibition appears to be calcium-dependent, suggesting a vesicular neurotransmitter release that is likely local and monosynaptic. A further understanding of autoinhibition may thus help inform studies in mammals, who have also been shown to modulate neural activity through axonal $GABA_A$ receptors (Trigo et al., 2008).

In addition, the work presented here sheds further light on the inhibition used by crayfish when responding to stimuli that evoke a tail-flip. I have discovered that the $GABA_A$-δ agonist THIP is a potent blocker of the excitatory effects of EtOH. Combined with the knowledge that work in the stretch receptor found THIP ineffective (Krause et al., 1981; Deisz & Dose, 1983), this provides some evidence that these receptors may

play a role in the tonic inhibition of the LG. In mammals, including humans, EtOH strongly modulates these receptors (Santhakumar et al., 2007; Lobo & Harris, 2008; Kumar et al., 2009), suggesting that experiments on crayfish involving the interplay between EtOH and tonic inhibition are likely to generalize. I have also discovered that picrotoxin has an effect on the early β phase of the PSP in communally housed animals, suggesting that inhibition in the LG circuit is shaped by social experience. Finally, the lack of social differences that I found in response to EtOH suggests that tonic descending inhibition is critical for EtOH's behavioral effects. These discoveries provide fertile ground for further studies on the interplay between inhibition and alcohol intoxication.

6.1. Autoinhibition

Though I did not find the interneurons that mediate the LG's autoinhibition, I have provided evidence that may guide future experiments. We now know that the LG is reactive to glutamate, and that the mechanism requires calcium. It seems probable that glutamate is released onto the LG axon at various locations which are spatially dispersed. Occasional synapses containing GABA-like vesicles have been reported on the LG axon (Lee & Krasne, 1993). It may be difficult to locate these by transaxial sectioning, but it is possible that coronal or sagittal sections through the axolemma would provide a better approach. Another strategy would be to fill the LG with intracellular dyes, and stimulate it to allow the dye to pass through rectifying electrical junctions, as the dIPSP's speed suggests that only electrical synapses are involved between the LG and its inhibitor.

6.2. Sensory-evoked inhibition

While the giant fibers of the crayfish have been studied for a long time, some of the results here raise new questions. I have found that the sensory-evoked inhibition, which crayfish use to selectively respond to phasic stimuli, has socially-mediated differences, which became apparent upon exposure to picrotoxin. It has previously been shown that the LG's response to serotonin is affected by social history (Yeh et al., 1996; Yeh et al., 1997), and I have now presented results suggesting the inhibitory system of crayfish is also changed by social experience. In addition, this change is visible at the level of a single cell, *and* it remains in isolated nerve cords, implying that there is either a redistribution of receptors or a local change in synaptic weights or neuronal connectivity involved. Further studies could investigate the social differences seen in both the tonic and sensory-evoked inhibitory systems, and discern the different roles that these modulations likely play in social behavior.

6.3. Tonic inhibition

Tonic inhibition is well studied in the lateral giant, and is used to control the threshold of tail-flip behavior (Vu & Krasne, 1992; Vu & Krasne, 1993; Vu et al., 1993). I have found evidence that the LG circuit has $GABA_A$-δ-like receptors, which are implicated in mediating tonic inhibition in other organisms, including humans.

Crayfish approaching a food reward respond to shadows simulating a predator attack by either tail-flipping away or freezing in place; this economic decision is made

based on the value of the food reward, the degree of threat represented by the shadow, and the internal state of the animal (Liden & Herberholz, 2008; Liden et al., 2010; Schadegg & Herberholz 2017). The tail-flips in response to shadows are produced by the MGs, which receive their inputs in the brain. The MG is affected by GABAergic drugs like picrotoxin, as the LG is (Swierzbinski, 2016; Swierzbinski & Herberholz, 2018), and its threshold is likely modulated by tonic inhibition. Usage of THIP in these experiments will allow a better understanding of how crayfish make these economic decisions, and how they evaluate risk and reward in a dangerous situation. Thus, THIP is an excellent candidate with which to further study tonic inhibition in crayfish neural circuits, including the MG neuron, and uncover the relationship between tonic inhibition and decision-making. Inhibition is critical for making choices even in humans (Jocham et al., 2012), indicating how general the behavioral importance of inhibition is. The knowledge gained from further studies on decision making in crayfish, through the lens of tonic inhibition, will provide a framework which can guide research in other animals.

In addition, the MG is responsive to EtOH, as the LG is (Swierzbinksi, 2016; Swierzbinski & Herberholz, 2018). These circuits are both useful in separate ways, as the LG is relatively simple and easily accessible, while the MG can be observed both through intracellular recordings and non-invasively in freely behaving animals. These factors, along with the ease of studying alcohol in crayfish, make crayfish a highly suitable model in which to study the basic effects of alcohol. Given alcohol's strong action at $GABA_A$-δ receptors in mammals (Santhakumar et al., 2007), and the strong interaction between alcohol and THIP that I have now demonstrated in crayfish, THIP may prove a useful

tool to better understand the cellular and neurochemical processes of alcohol intoxication and addiction in the future.

Appendix

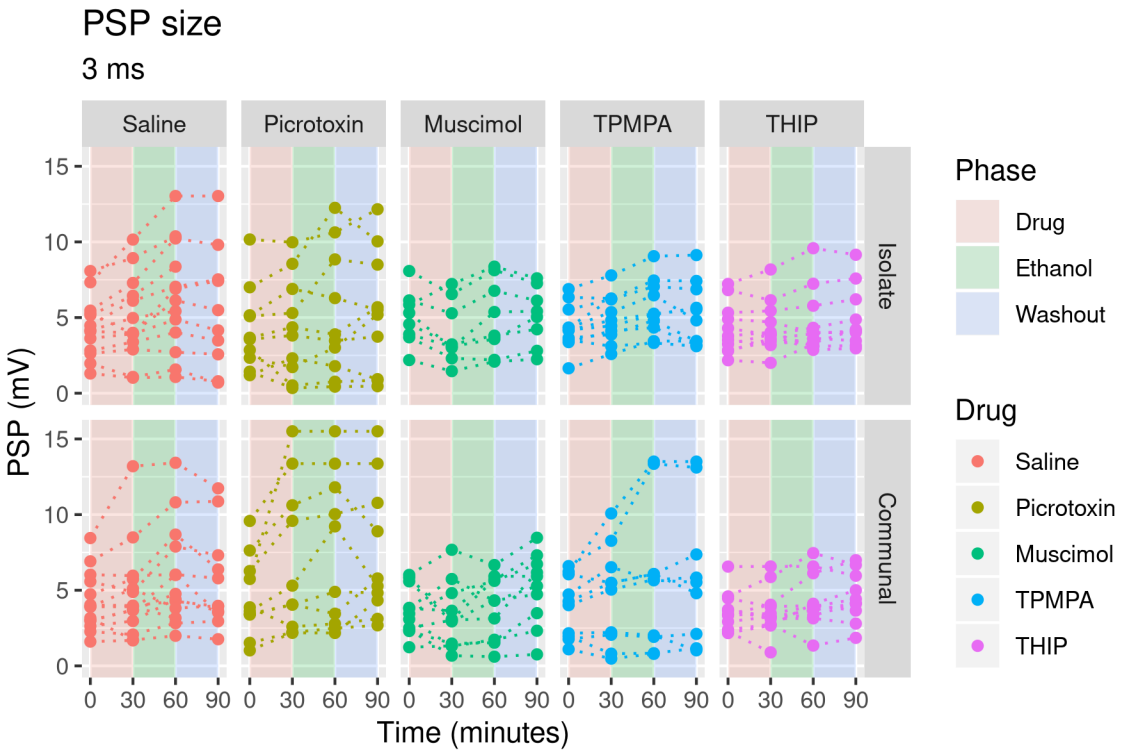

Figure. PSP size as a function of phase, measured at 3 ms. Each data point is plotted as a filled circle. Dotted lines represent the same preparation. The x-axis is color-coded based on the phase of the experiment. Time points correspond to the end of pretreatment (0), drug (30), EtOH (60), and washout (90).

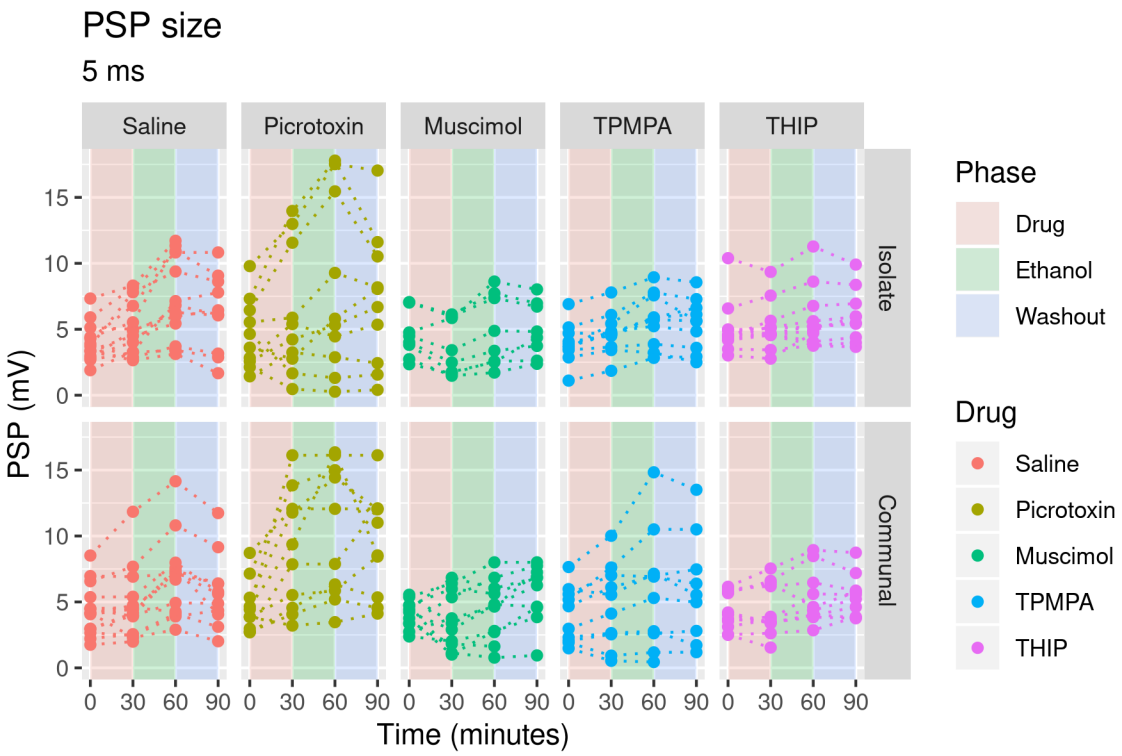

Figure. PSP size as a function of phase, measured at 5 ms. Each data point is plotted as a filled circle. Dotted lines represent the same preparation. The x-axis is color-coded based on the phase of the experiment. Time points correspond to the end of pretreatment (0), drug (30), EtOH (60), and washout (90).

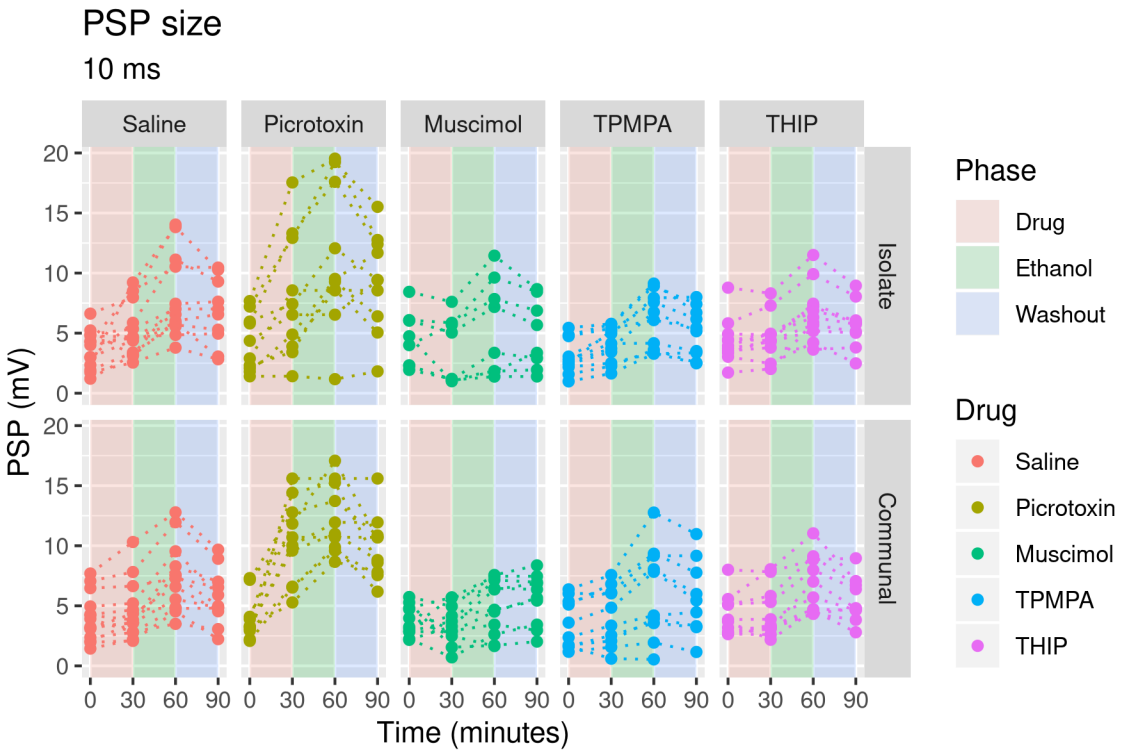

Figure. PSP size as a function of phase, measured at 10 ms. Each data point is plotted. Each data point is plotted as a filled circle. Dotted lines represent the same preparation. The x-axis is color-coded based on the phase of the experiment. Time points correspond to the end of pretreatment (0), drug (30), EtOH (60), and washout (90).

Drug	Socialization	Pretreatment	Drug	Ethanol	Washout
Saline	Communal	14	14	13	11
Picrotoxin	Communal	10	10	10	10
Muscimol	Communal	11	11	11	10
TPMPA	Communal	10	10	10	9
THIP	Communal	11	11	10	10
Saline	Isolate	13	13	13	10
Picrotoxin	Isolate	10	10	10	10
Muscimol	Isolate	8	8	8	8
TPMPA	Isolate	11	11	10	10
THIP	Isolate	11	11	11	10

Table. Sample sizes for ethanol experiments.

References

Ahlmann-Eltze, C. (2019). ggsignif: Significance Brackets for 'ggplot2'. *R package*, version 0.6.0.

Algarin, J. M., Ramaswamy, B., Venuti, L., Swierzbinski, M. E., Baker-McKee, J., Weinberg, I. N., Chen, Y. J., Krivorotov, I. N., Katine, J. A., Herberholz, J., & Araneda, R. C. (2019). Activation of Microwave Signals in Nanoscale Magnetic Tunnel Junctions by Neuronal Action Potentials. *IEEE Magnetics Letters*, *10*, 1-5.

Antonsen, B. L., & Edwards, D. H. (2003). Differential dye coupling reveals lateral giant escape circuit in crayfish. *Journal of Comparative Neurology*, *466*(1), 1-13.

Arnau, J., Bendayan, R., Blanca, M. J., & Bono, R. (2013). The effect of skewness and kurtosis on the robustness of linear mixed models. *Behavior research methods*, *45*(3), 873-879.

Attwell, D., Barbour, B., & Szatkowski, M. (1993). Nonvesicular release of neurotransmitter. *Neuron, 11(3),* 401–407. https://doi.org/10.1016/0896-6273(93)90145-H

Bagnato, S., Boccagni, C., Sant'Angelo, A., Prestandrea, C., Rizzo, S., & Galardi, G. (2012). Patients in a vegetative state following traumatic brain injury display

a reduced intracortical modulation. *Clinical neurophysiology*, *123*(10), 1937-1941.

Bates, D., Mächler, M., Bolker, B., & Walker, S. (2015). Fitting linear mixed-effects models using lme4. *Journal of Statistical Software, 67*(1), 1-48.

Pinheiro, J., Bates, D., DebRoy, S., & Sarkar, D. (2016). R Core Team (2015) nlme: linear and nonlinear mixed effects models. *R package,* version 3.1–140.

Baulac, S., Huberfeld, G., Gourfinkel-An, I., Mitropoulou, G., Beranger, A., Prud'homme, J. F., Baulac, M., Brice, A., Bruzzone, R. and LeGuern, E. (2001). First genetic evidence of GABA A receptor dysfunction in epilepsy: a mutation in the γ2-subunit gene. *Nature genetics*, *28*(1), 46.

Blednov, Y. A., Borghese, C. M., Ruiz, C. I., Cullins, M. A., Da Costa, A., Osterndorff-Kahanek, E. A., Homanics, G. E. and Harris, R. A. (2017). Mutation of the inhibitory ethanol site in GABAAρ1 receptors promotes tolerance to ethanol-induced motor incoordination. *Neuropharmacology*, *123*, 201–209. https://doi.org/10.1016/j.neuropharm.2017.06.013

Blundon, J. a, & Bittner, G. D. (1992). Effects of ethanol and other drugs on excitatory and inhibitory neurotransmission in the crayfish. *Journal of Neurophysiology*, *67*(3), 576–87.

Bovbjerg, R. V. (1953). Dominance order in the crayfish Orconectes virilis (Hagen). *Physiological Zoology*, *26*(2), 173-178.

Bryan, J. S., & Krasne, F. B. (1977). Presynaptic inhibition: the mechanism of protection from habituation of the crayfish lateral giant fibre escape response. *The Journal of physiology*, *271*(2), 369-390.

Calabrese, R. L. (1976). Crayfish mechanoreceptive interneurons. *Journal of comparative physiology*, *105*(1), 103-114.

Cleland, T. A. (1996). Inhibitory glutamate receptor channels. *Molecular neurobiology*, *13*(2), 97-136.

Cully, D. F., Paress, P. S., Liu, K. K., Schaeffer, J. M., & Arena, J. P. (1996). Identification of a Drosophila melanogaster glutamate-gated chloride channel sensitive to the antiparasitic agent avermectin. *Journal of Biological Chemistry*, *271*(33), 20187–20191. https://doi.org/10.1074/jbc.271.33.20187

Deisz, R. A., & Dose, M. (1983). Comparison of GABA analogues at the crayfish stretch receptor neurone. *Brain research bulletin*, *11*(3), 283-288.

Dimitriadou, E., Hornik, K., Leisch, F., Meyer, D., & Weingessel, A. (2019). e1071: Misc functions of the Department of Statistics, Probability Theory Group (e1071), TU Wien. *R package*, version 1.7-3

Eckert, R. O. (1961). Reflex relationships of the abdominal stretch receptors of the crayfish. II. Stretch receptor involvement during the swimming reflex. *Journal of cellular and comparative physiology*, *57*(3), 163-174.

Edwards, D. (1990). Mechanisms of depolarizing inhibition at the crayfish giant motor synapse. I. Electrophysiology. *Journal of Neurophysiology*, *64*(2).

Edwards, D. H., Heitler, W. J., & Krasne, F. B. (1999). Fifty years of a command neuron: the neurobiology of escape behavior in the crayfish. *Trends in Neurosciences*, *22*(4), 153–61.

Fairman, W. A., Vandenberg, R. J., Arrriza, J. L., Kavanaugh, M. P., & Amara, S. G. (1995). An excitatory amino-acid transporter with properties of a ligand-gated chloride channel. *Nature*, *375*(6532), 599.

Farrant, M., & Nusser, Z. (2005). Variations on an inhibitory theme: phasic and tonic activation of GABA A receptors. *Nature Reviews Neuroscience*, *6*(3), 215.

Fatt, P., & Katz, B. (1952). Spontaneous subthreshold activity at motor nerve endings. *The Journal of physiology*, *117*(1), 109-128.

Florey, E. (1954). An inhibitory and an excitatory factor of mammalian central nervous system, and their action on a single sensory neuron. *Archives of Physiology and Biochemistry, 62(1),* 33–53. https://doi.org/10.3109/13813455409145367

Franke, C., Hatt, H., & Dudel, J. (1986). The inhibitory chloride channel activated by glutamate as well as γ-amino-butyric acid (GABA) - Single channel recordings from crayfish muscle. *Journal of Comparative Physiology A, 159(5),* 591–609. https://doi.org/10.1007/BF00612033

Friedman, R. N., Bittner, G. D., & Blundon, J. a. (1988). Electrophysiological and behavioral effects of ethanol on crayfish. *The Journal of Pharmacology and Experimental Therapeutics, 246(1),* 125–131.

Froemke, R. C. (2015). Plasticity of Cortical Excitatory-Inhibitory Balance. *Annual Review of Neuroscience*, *38*(1), 195–219. https://doi.org/10.1146/annurev-neuro-071714-034002

Foss-Feig, J. H., Adkinson, B. D., Ji, J. L., Yang, G., Srihari, V. H., McPartland, J. C., Krystal, J. H., Murray, J. D. and Anticevic, A. (2017). Searching for Cross-Diagnostic Convergence: Neural Mechanisms Governing Excitation and Inhibition Balance in Schizophrenia and Autism Spectrum Disorders. *Biological Psychiatry, 81(10),* 848–861. https://doi.org/10.1016/j.biopsych.2017.03.005

Furshpan, E., & Potter, D. (1959). Transmission at the giant motor synapses of the crayfish. *The Journal of Physiology*, 289–325.

Furutani, S., Nakatani, Y., Miura, Y., Ihara, M., Kai, K., Hayashi, H., & Matsuda, K. (2015). GluCl a target of indole alkaloid okaramines: a 25 year enigma solved. *Scientific Reports*, *4*(1), 6190. https://doi.org/10.1038/srep06190

Gafurov, B., Urazaev, A. K., Grossfeld, R. M. and Lieberman, E. M. (2001). N-Acetylaspartylglutamate (NAAG) is the probable mediator of axon-to-glia signaling in the crayfish medial giant nerve fiber. *Neuroscience*. https://doi.org/10.1016/S0306-4522(01)00271-8

Gafurov, B. S., Urazaev, A. K., Grossfeld, R. M., & Lieberman, E. M. (2002). Mechanism of NMDA receptor contribution to axon-to-glia signaling in the crayfish medial giant nerve fiber. *Glia, 38(1),* 80–86. https://doi.org/10.1002/glia.10042

Graham, M. E., & Herberholz, J. (2009). Stability of dominance relationships in crayfish depends on social context. *Animal Behaviour*, 77(1), 195-199.

Hama, K. (1961). Some observations on the fine structure of the giant fibers of the crayfishes (Cambarus virilus and Cambarus clarkii) with special reference to the submicroscopic organization of the synapses. *The Anatomical Record*, *141*(4), 275-293.

Hanchar, H. Jacob, et al. "Alcohol-induced motor impairment caused by increased extrasynaptic GABA A receptor activity." *Nature neuroscience* 8.3 (2005): 339.

Heilig, M., Epstein, D. H., Nader, M. A., & Shaham, Y. (2016). Time to connect: bringing social context into addiction neuroscience. *Nature Reviews Neuroscience*, *17*(9), 592.

Heitler, W., Watson, A., Falconer, S., & Powell, B. (2001). Glutamate is a transmitter that mediates inhibition at the rectifying electrical motor giant synapse in the crayfish. *Journal of Comparative Neurology*, *26*(September 2000), 12–26.

Herberholz, J., Antonsen, B. L., & Edwards, D. H. (2002). A lateral excitatory network in the escape circuit of crayfish. *The Journal of Neuroscience: The Official Journal of the Society for Neuroscience*, 22(20), 9078–85.

Herberholz, J., Sen, M., & Edwards, D. (2004). Escape behavior and escape circuit activation in juvenile crayfish during prey-predator interactions. *Journal of Experimental Biology*, *207*(11), 1855–1863. https://doi.org/10.1242/jeb.00992

Herberholz, J., Issa, F. A., & Edwards, D. H. (2001). Patterns of neural circuit activation and behavior during dominance hierarchy formation in freely behaving crayfish. *Journal of Neuroscience*, 21(8), 2759-2767.

Herberholz, J., Swierzbinski, M. E., & Birke, J. M. (2016). Effects of different social and environmental conditions on established dominance relationships in crayfish. *The Biological Bulletin*, 230(2), 152-164.

Herberholz, J., McCurdy, C., & Edwards, D. H. (2007). Direct benefits of social dominance in juvenile crayfish. *The Biological Bulletin*, 213(1), 21-27.

Hultborn, H., Jankowska, E., & Lindström, S. (1971). Recurrent inhibition of interneurones monosynaptically activated from group Ia afferents. *Journal of Physiology*, 215, 613–636.

Huxley T. H. (1879) The Crayfish: an Introduction to the Study of Zoology. C. Kegan Paul & Co., London.

Ikeda, T., Zhao, X., Kono, Y., Yeh, J. Z., & Narahashi, T. (2003). Fipronil Modulation of Glutamate-Induced Chloride Currents in Cockroach Thoracic Ganglion Neurons. *NeuroToxicology*, *24*(6), 807–815. https://doi.org/10.1016/S0161-813X(03)00041-X

Imeh-Nathaniel, A., Okon, M., Huber, R., & Nathaniel, T. I. (2014). Exploratory behavior and withdrawal signs in Crayfish : Chronic central morphine injections and termination effects. *Behavioural Brain Research*, *264*, 181–187. https://doi.org/10.1016/j.bbr.2014.01.026

Jocham, G., Hunt, L. T., Near, J., & Behrens, T. E. J. (2012). A mechanism for value-guided choice based on the excitation-inhibition balance in prefrontal cortex. *Nature Neuroscience*, *15*(7), 960–961. https://doi.org/10.1038/nn.3140

Johnson, G. E. (1924). Giant Nerve Fibers In Crustaceans With Special Reference To Cambarus And Palaemonetes. *The Journal of Comparative Neurology*, *36*(4), 323–373.

Jones, S. M., & Palmer, M. J. (2009). Activation of the tonic GABAC receptor current in retinal bipolar cell terminals by nonvesicular GABA release. *Journal of neurophysiology*, *102*(2), 691-699.

Kane, N. S., Hirschberg, B., Qian, S., Hunt, D., Thomas, B., Brochu, R., … Cully, D. F. (2000). Drug-resistant Drosophila indicate glutamate-gated chloride channels are targets for the antiparasitics nodulisporic acid and ivermectin. *Proceedings of the National Academy of Sciences*, *97*(25), 13949–13954. https://doi.org/10.1073/pnas.240464697

Kane, L. S., Buttram Jr, J. G., Urazaev, A. K., Lieberman, E. M., & Grossfeld, R. M. (2000). Uptake and metabolism of glutamate at non-synaptic regions of crayfish central nerve fibers: implications for axon–glia signaling. *Neuroscience*, *97*(3), 601-609.

Kanner, B. I., & Sharon, I. (1978). Active Transport of L-Glutamate by Membrane Vesicles Isolated from Rat Brain. *Biochemistry, 17(19),* 3949–3953. https://doi.org/10.1021/bi00612a011

Kanner, B. I. (1978). Active transport of γ-aminobutyric acid by membrane vesicles isolated from rat brain. *Biochemistry*, *17*(7), 1207-1211.

Kao, C. Y. (1960). Postsynaptic electrogenesis in septate giant axons. II. Comparison of medial and lateral giant axons of crayfish. *Journal of neurophysiology*, *23*(6), 618-635.

Kennedy, D., McVittie, J., Calabrese, R., Fricke, R. A., Craelius, W., & Chiapella, P. (1980). Inhibition of mechanosensory interneurons in the crayfish. I. Presynaptic inhibition from giant fibers. *Journal of Neurophysiology*, *43*(6), 1495-1509.

Kennedy, D., Calabrese, R. L., & Wine, J. J. (1974). Presynaptic inhibition: primary afferent depolarization in crayfish neurons. *Science*, *186*(4162), 451-454.

Kirk, M. D. (1985). Presynaptic inhibition in the crayfish CNS: pathways and synaptic mechanisms. Journal of Neurophysiology, 54(5), 1305?25.

Kramer, A. P., & Krasne, F. B. (1984). Crayfish escape behavior: production of tailflips without giant fiber activity. *Journal of neurophysiology*, *52*(2), 189-211.

Krasne, F. B., & Stirling, C. A. (1972). Synapses of crayfish abdominal ganglia with special attention to afferent and efferent connections of the lateral giant fibers. *Zeitschrift für Zellforschung und mikroskopische Anatomie*, *127*(4), 526-544.

Krasne, F. B. (1969). Excitation and habituation of the crayfish escape reflex: the depolarizing response in lateral giant fibres of the isolated abdomen. *Journal of Experimental Biology*, *50*(1), 29-46.

Krasne, F. B., & Wine, J. J. (1975). Extrinsic modulation of crayfish escape behaviour. *Journal of Experimental Biology*, *63*(2), 433-450.

Krause, D. N., Ikeda, K., & Roberts, E. (1981). Dose-conductance relationships for GABA agonists and the effect of uptake inhibitors in crayfish stretch receptor neurons. *Brain research*, *225*(2), 319-332.

Kumar, S., Porcu, P., Werner, D. F., Matthews, D. B., Diaz-Granados, J. L., Helfand, R. S., & Morrow, A. L. (2009). The role of GABA(A) receptors in the acute and chronic effects of ethanol: a decade of progress. *Psychopharmacology (Berl)*, *205*(4), 529–564. https://doi.org/10.1007/s00213-009-1562-z

Kusano, K., & Grundfest, H. (1965). Circus reexcitation as a cause of repetitive activity in crayfish lateral giant axons. *Journal of Cellular and Comparative Physiology*, *65*(3), 325-336.

Kuznetsova, A., Brockhoff, P. B., & Christensen, R. H. B. (2017). lmerTest package: tests in linear mixed effects models. *Journal of Statistical Software*, *82*(13), 1-26.

Langosch, D., Becker, C. M., & Betz, H. (1990). The inhibitory glycine receptor: A ligand gated chloride channel of the central nervous system. *Eur. J. Biochem.*, *194*, 1–8.

Lee, S. C., & Krasne, F. B. (1993). Ultrastructure of the circuit providing input to the crayfish lateral giant neurons. *The Journal of comparative neurology*, *327*(2), 271-288.

Leitch, B., Heitler, W. J., Cobb, J. L. S., & Pitman, R. M. (1990). Anti-GABA antibodies label a subpopulation of chemical synapses which modulate an electrical synapse in crayfish. *Journal of neurocytology*, *19*(6), 929-936.

Leon, A. C., & Heo, M. (2009). Sample sizes required to detect interactions between two binary fixed-effects in a mixed-effects linear regression model. *Computational statistics & data analysis*, *53*(3), 603-608.

Liden, W. H., & Herberholz, J. (2008). Behavioral and neural responses of juvenile crayfish to moving shadows. *Journal of Experimental Biology*, *211*(9), 1355-1361.

Liden, W. H., Phillips, M. L., & Herberholz, J. (2010). Neural control of behavioural choice in juvenile crayfish. *Proceedings. Biological Sciences / The Royal Society*, *277*(1699), 3493–3500. https://doi.org/10.1098/rspb.2010.1000

Lieberman, E. M., Hargittai, P. T., & Grossfeld, R. M. (1994). Electrophysiological and metabolic interactions between axons and glia in crayfish and squid. *Progress in neurobiology*, *44*(4), 333-376.

Lobo, I. A., & Harris, R. A. (2008). GABAA receptors and alcohol. *Pharmacology Biochemistry and Behavior.* https://doi.org/10.1016/j.pbb.2008.03.006

Lovinger, D. M. (1999). 5-HT3 receptors and the neural actions of alcohols: An increasingly exciting topic. *Neurochemistry International*. https://doi.org/10.1016/S0197-0186(99)00054-6

Marder, E., & Paupardin-Tritsch, D. (1978). The pharmacological properties of some crustacean neuronal acetylcholine, gamma-aminobutyric acid, and L-

glutamate responses. *The Journal of Physiology*, *280*(1), 213–236. https://doi.org/10.1113/jphysiol.1978.sp012381

Melcangic, M., & Bowery, N. G. (1996). GABA and its receptors in the spinal cord. *Trends in pharmacological sciences*, *17*(12), 457-462.

Mihic, S. J., & Harris, R. A. (1996). Inhibition of rho1 receptor GABAergic currents by alcohols and volatile anesthetics. *Journal of Pharmacology and Experimental Therapeutics*, *277*(1), 411-416.

Mihic, S. J., Ye, Q., Wick, M. J., Koltchine, V. V, Krasowski, M. D., Finn, S. E., … Harrison, N. L. (1997). Sites of alcohol and volatile anaesthetic action on GABA(A) and glycine receptors. *Nature*, *389*(6649), 385–389. https://doi.org/10.1038/38738

Miller, M. W., Vu, E. T., & Krasne, F. B. (1992). Cholinergic transmission at the first synapse of the circuit mediating the crayfish lateral giant escape reaction. *Journal of neurophysiology*, *68*(6), 2174-2184.

Mulloney, B., & Hall, W. M. (1990). GABA-ergic neurons in the crayfish nervous system: An immunocytochemical census of the segmental ganglia and stomatogastric system. *Journal of Comparative Neurology*, *291*(3), 383-394.

Nagayama, T., Kimura, K. I., Araki, M., Aonuma, H., & Newland, P. L. (2004). Distribution of glutamatergic immunoreactive neurons in the terminal abdominal ganglion of the crayfish. *Journal of Comparative Neurology*, *474*(1), 123-135.

Nagayama, T. (2005). GABAergic and glutamatergic inhibition of nonspiking local interneurons in the terminal abdominal ganglion of the crayfish. *Journal of Experimental Zoology Part A: Comparative Experimental Biology*, *303*(1), 66-75.

Olsen, R. W., & Sieghart, W. (2009). $GABA_A$ receptors: subtypes provide diversity of function and pharmacology. *Neuropharmacology*, *56*(1), 141-148.

Otsuka, M., Iversen, L. L., Hall, Z. W., & Kravitz, E. A. (1966). Release of gamma-aminobutyric acid from inhibitory nerves of lobster. *Proceedings of the National Academy of Sciences of the United States of America*, *56*(4), 1110.

Owens, D. F., & Kriegstein, A. R. (2002). Is there more to GABA than synaptic inhibition? *Nature Reviews. Neuroscience, 3(9),* 715–727. https://doi.org/10.1038/nrn919

Panksepp, J. B., & Huber, R. (2004). Ethological analyses of crayfish behavior: A new invertebrate system for measuring the rewarding properties of psychostimulants. *Behavioural Brain Research*, *153*(1), 171–180. https://doi.org/10.1016/j.bbr.2003.11.014

Peacock, A., Leung, J., Larney, S., Colledge, S., Hickman, M., Rehm, J., Giovino, G. A., West, R., Hall, W., Griffiths, P. and Ali, R. (2018). Global statistics on alcohol, tobacco and illicit drug use: 2017 status report. *Addiction*, *113*(10), 1905-1926.

Pearlstein, E., Clarac, F., & Cattaert, D. (1998). Neuromodulation of reciprocal glutamatergic inhibition between antagonistic motoneurons by 5-

hydroxytryptamine (5-HT) in crayfish walking system. *Neuroscience Letters*, *241*(1), 37–40.

Pearlstein, E., Watson, a. H. D., Bévengut, M., & Cattaert, D. (1998). Inhibitory connections between antagonistic motor neurones of the crayfish walking legs. *Journal of Comparative Neurology*, *399*(2), 241–254. https://doi.org/10.1002/(SICI)1096-9861(19980921)399:2<241::AID-CNE7>3.0.CO;2-0

Pearson, K. G. (1998). Vertebrates and Invertebrates. *Science*, *279*(5354), 1113a–1117. https://doi.org/10.1126/science.279.5354.1113a

Peoples, R. W., & Weight, F. F. (1995). Cutoff in potency implicates alcohol inhibition of N-methyl-D-aspartate receptors in alcohol intoxication. *Proceedings of the National Academy of Sciences, 92(7),* 2825–2829. https://doi.org/10.1073/pnas.92.7.2825

R core team (2019). R: A language and environment for statistical computing. Vienna, Austria.

Ragozzino, D., Woodward, R. M., Murata, Y., Eusebi, F., Overman, L. E., & Miledi, R. (1996). Design and in vitro pharmacology of a selective γ-aminobutyric acid$_C$ receptor antagonist. *Molecular Pharmacology*, *50*(4), 1024-1030.

Raymond, V., Sattelle, D. B., & Lapied, B. (2000). Co-existence in DUM neurones of two GluCl channels that differ in their picrotoxin sensitivity. *NeuroReport, 11(12),* 2695–2701. https://doi.org/10.1097/00001756-200008210-00018

Rehm, J., & Shield, K. D. (2013). Global alcohol-attributable deaths from cancer, liver cirrhosis, and injury in 2010. *Alcohol research: current reviews*, *35*(2), 174-183.

Roberts, A. (1968). Recurrent inhibition in the giant-fibre system of the crayfish and its effect on the excitability of the escape response. Journal of Experimental Biology, 48(3), 545–67.

Roberts, A., Krasne, F. B., Hagiwara, G., Wine, J. J., & Kramer, A. P. (1982). Segmental giant: evidence for a driver neuron interposed between command and motor neurons in the crayfish escape system. *Journal of neurophysiology*, *47*(5), 761-781.

Robinson, D., & Hayes, A. (2019). Broom: Convert statistical analysis objects into tidy tibbles. *R package,* version 0.5.2.

Rossi, D. J., & Hamann, M. (1998). Spillover-mediated transmission at inhibitory synapses promoted by high affinity α6 subunit GABAA receptors and glomerular geometry. *Neuron*, *20*(4), 783-795.

Santhakumar, V., Wallner, M., & Otis, T. S. (2007). Ethanol acts directly on extrasynaptic subtypes of GABAA receptors to increase tonic inhibition. *Alcohol*, *41*(3), 211–221. https://doi.org/10.1016/j.alcohol.2007.04.011

Sattelle, D. B., & Buckingham, S. D. (2006). Invertebrate studies and their ongoing contributions to neuroscience. *Invertebrate Neuroscience*, *6*(1), 1–3. https://doi.org/10.1007/s10158-005-0014-7

Schadegg, A. C., & Herberholz, J. (2017). Satiation level affects anti-predatory decisions in foraging juvenile crayfish. *Journal of Comparative Physiology A*, *203*(3), 223-232.

Sellström, Å., & Hamberger, A. (1977). Potassium-stimulated γ-aminobutyric acid release from neurons and glia. *Brain Research*, *119*(1), 189-198.

Shrager, P., Starkus, J. C., Lo, M. V., & Peracchia, C. (1983). The periaxonal space of crayfish giant axons. *The Journal of general physiology*, *82*(2), 221-244.

Smith, S. S., & Gong, Q. H. (2007). Ethanol effects on GABA-gated current in a model of increased α4βδ GABAAreceptor expression depend on time course and preexposure to low concentrations of the drug. *Alcohol*. https://doi.org/10.1016/j.alcohol.2007.04.007

Stahre, M., Roeber, J., Kanny, D., Brewer, R. D., & Zhang, X. (2014). Peer reviewed: Contribution of excessive alcohol consumption to deaths and years of potential life lost in the United States. *Preventing chronic disease*, *11*.

Stirling, C. A. (1972). The ultrastructure of giant fibre and serial synapses in crayfish. *Zeitschrift für Zellforschung und mikroskopische Anatomie*, *131*(1), 31-45.

í Stórustovu, S., & Ebert, B. (2006). Pharmacological characterization of agonists at δ-containing $GABA_A$ receptors: functional selectivity for extrasynaptic receptors is dependent on the absence of γ2. *Journal of Pharmacology and Experimental Therapeutics*, *316*(3), 1351-1359.

Sundstrom-Poromaa, I., Smith, D. H., Gong, Q. H., Sabado, T. N., Li, X., Light, A., Wiedmann, M., Williams, K. and Smith, S. S. (2002). Hormonally regulated α 4 β 2 δ GABA A receptors are a target for alcohol. *Nature neuroscience*, *5*(8), 721.

Swierzbinski, M. E., Lazarchik, A. R., & Herberholz, J. (2017). Prior social experience affects the behavioral and neural responses to acute alcohol in juvenile crayfish. *The Journal of Experimental Biology*, *220*(8), 1516–1523. https://doi.org/10.1242/jeb.154419

Swierzbinski, M. E., & Herberholz, J. (2018). Effects of ethanol on sensory inputs to the medial giant interneurons of crayfish. *Frontiers in Physiology*, *9*, 448.

Szatkowski, M., Barbour, B., & Attwell, D. (1990). Non-vesicular release of glutamate from glial cells by reversed electrogenic glutamate uptake. *Nature*, *348*(6300), 443-446.

Tatti, R., Haley, M. S., Swanson, O. K., Tselha, T., & Maffei, A. (2017). Neurophysiology and Regulation of the Balance Between Excitation and Inhibition in Neocortical Circuits. *Biological Psychiatry, 81(10),* 821–831. https://doi.org/10.1016/j.biopsych.2016.09.017

Teshiba, T., Shamsian, a, Yashar, B., Yeh, S. R., Edwards, D. H., & Krasne, F. B. (2001). Dual and opposing modulatory effects of serotonin on crayfish lateral giant escape command neurons. *The Journal of Neuroscience : The Official Journal of the Society for Neuroscience*, *21*(12), 4523–9.

Trigo, F. F., Marty, A., & Stell, B. M. (2008). Axonal GABAA receptors. *European Journal of Neuroscience*, *28*(5), 841-848.

Urazaev, A. K., Buttram, J. G., Deen, J. P., Gafurov, B. S., Slusher, B. S., Grossfeld, R. M., & Lieberman, E. M. (2001). Mechanisms for clearance of released N-acetylaspartylglutamate in crayfish nerve fibers: Implications for axon-glia signaling. *Neuroscience*, *107*(4), 697–703. https://doi.org/10.1016/S0306-4522(01)00393-1

Urazaev, A. K., Grossfeld, R. M., & Lieberman, E. M. (2005). Regulation of glutamate carboxypeptidase II hydrolysis of N-acetylaspartylglutamate (NAAG) in crayfish nervous tissue is mediated by glial glutamate and acetylcholine receptors. *Journal of Neurochemistry*, *93*(3), 605–610. https://doi.org/10.1111/j.1471-4159.2005.03041.x

Urazaev, A. K., Grossfeld, R. M., Fletcher, P. L., Speno, H., Gafurov, B. S., Buttram, J. G., & Lieberman, E. M. (2001). Synthesis and release of N-acetylaspartylglutamate (NAAG) by crayfish nerve fibers: implications for axon-glia signaling. *Neuroscience*, *106*(1), 237–47.

Valenzuela, C. F., & Jotty, K. (2015). Mini-review: Effects of ethanol on GABAAreceptor-mediated neurotransmission in the cerebellar cortex—recent advances. *Cerebellum*, *14*(4), 438–446. https://doi.org/10.1007/s12311-014-0639-3

Van Harreveld, A. (1936). A physiological solution for freshwater crustaceans. *Proceedings of the Society for Experimental Biology and Medicine*, *34*(4), 428-432.

Viancour, T. A., Seshan, K. R., Bittner, G. D., & Sheller, R. A. (1987). Organization of axoplasm in crayfish giant axons. *Journal of neurocytology*, *16*(4), 557-566.

Villegas, J. (1984). Axon-Schwann cell relationship. In *Current Topics in Membranes and Transport* (Vol. 22, pp. 547-571). Academic Press.

Vu, E. T., & Krasne, F. B. (1992). Evidence for a computational distinction between proximal and distal neuronal inhibition. *Science*, *255*(5052), 1710-1712.

Vu, E. T., Lee, S. C., & Krasne, F. B. (1993). The mechanism of tonic inhibition of crayfish escape behavior: distal inhibition and its functional significance. *The Journal of Neuroscience : The Official Journal of the Society for Neuroscience*, *13*(10), 4379–93.

Vu, E. T., & Krasne, F. B. (1993). Crayfish tonic inhibition: prolonged modulation of behavioral excitability by classical GABAergic inhibition. *Journal of Neuroscience*, *13*(10), 4394-4402.

Vu, E. T., Berkowitz, A., & Krasne, F. B. (1997). Postexcitatory inhibition of the crayfish lateral giant neuron: a mechanism for sensory temporal filtering. *Journal of Neuroscience*, *17*(22), 8867-8879.

Watanabe, A., & Grundfest, H. (1961). Impulse Propagation at the Septal and Commissural Junctions of Crayfish Lateral Giant Axons. *The Journal of General Physiology*, *45*(48), 267–308.

Wick, M. J., Mihic, S. J., Ueno, S., Mascia, M. P., Trudell, J. R., Brozowski, S. J., … Harris, R. a. (1998). Mutations of -aminobutyric acid and glycine receptors change alcohol cutoff: Evidence for an alcohol receptor? *Proceedings of the National Academy of Sciences*, *95*(11), 6504–6509. https://doi.org/10.1073/pnas.95.11.6504

Wickham, H. (2011). The Split-Apply-Combine Strategy for Data Analysis. *Journal of Statistical Software*, *40*(1), 1-29.

Wickham, H. (2016). ggplot2: elegant graphics for data analysis. Springer.

Wine, J. J. (1984). The structural basis of an innate behavioural pattern. *Journal of Experimental Biology*, 319, 283–319.

Wine, J. J., & Krasne, F. B. (1982). The cellular organization of crayfish escape behavior. *The biology of Crustacea*, *4*, 241-292.

Wine, J. J., & Krasne, F. B. (1972). The organization of escape behaviour in the crayfish. *The Journal of Experimental Biology*, *56*(1), 1–18.

Wolf, F. W., & Heberlein, U. (2003). Invertebrate models of drug abuse. *Journal of Neurobiology*, *54*(1), 161–178. https://doi.org/10.1002/neu.10166

Wolstenholme, A. J. (2012). Glutamate-gated chloride channels. *Journal of Biological Chemistry*. https://doi.org/10.1074/jbc.R112.406280

Wolstenholme, A. J., & Rogers, A. T. (2006). Glutamate-gated chloride channels and the mode of action of the avermectin/milbemycin anthelmintics. *Parasitology*, *131*(S1), S85. https://doi.org/10.1017/S0031182005008218

Yamakura, T., & Harris, R. A. (2000). Effects of gaseous anesthetics nitrous oxide and xenon on ligand-gated ion channels: Comparison with isoflurane and ethanol. *Anesthesiology*, *93*(4), 1095–1101. https://doi.org/10.1097/00000542-200010000-00034

Yeh, S. R., Fricke, R. A., & Edwards, D. H. (1996). The effect of social experience on serotonergic modulation of the escape circuit of crayfish. *Science*, *271*(5247), 366-369.

Yeh, S. R., Musolf, B. E., & Edwards, D. H. (1997). Neuronal adaptations to changes in the social dominance status of crayfish. *Journal of Neuroscience*, *17*(2), 697-708.

Zhang, D., Pan, Z. H., Awobuluyi, M., & Lipton, S. A. (2001). Structure and function of GABAC receptors: a comparison of native versus recombinant receptors. *Trends in Pharmacological Sciences*, *22*(3), 121-132.

Zhao, X., & Salgado, V. L. (2010). The role of GABA and glutamate receptors in susceptibility and resistance to chloride channel blocker insecticides. *Pesticide Biochemistry and Physiology*, *97*(2), 153–160. https://doi.org/10.1016/j.pestbp.2009.10.002

Zhao, X., Salgado, V. L., Yeh, J. Z., & Narahashi, T. (2004). Kinetic and pharmacological characterization of desensitizing and non-desensitizing glutamate-gated chloride channels in cockroach neurons. *NeuroToxicology*, *25*(6), 967–980. https://doi.org/10.1016/j.neuro.2004.04.004

Zucker, R. S. (1972). Crayfish escape behavior and central synapses. I. Neural circuit exciting lateral giant fiber. *Journal of Neurophysiology*, *35*(5), 599-620.

Zucker, R. S. (1974). Excitability changes in crayfish motor neurone terminals. *The Journal of physiology*, *241*(1), 111-126.